A STUDY OF THE EFFECTS OF PARAMETER VARIATION ON THE FLYING QUALITIES OF THE XV-4B V/STOL AIRCRAFT

ARTHUR G. JONES

FLIGHT DYNAMICS LABORATORY

FOREWORD

This report provides the results of an in-house program conducted by the Control Criteria Branch with support from the Systems Dynamics Branch's Engineering Flight Simulation Group. These organizations are elements of the Air Force Flight Dynamics Laboratory, Wright-Patterson Air Force Base, Ohio. The work was performed under Project 8219, "Stability and Control Investigation" Work Unit 821907012, "XV-4B Stability and Control". Acknowledgement is given to Mr. Ray Haas, Lt Fred Unfried of the Engineering Flight Simulation Group for their assistance on the Flight Control Division Simulator and to Messrs. Fred Thomas, David Mayhew, Robert Nicholson, and Evard Flinn of the Control Criteria Branch, for their assistance in initial data preparation and final data reduction. The Project Engineer was Arthur G. Jones, AFFDL/FGC, Wright-Patterson Air Force Base, Ohio. The work reported herein was accomplished between October 1967 and October 1969 with the report submitted March 1971.

This technical report has been reviewed and is approved.

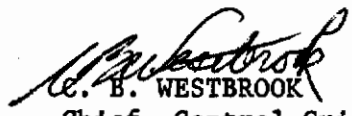

C. B. WESTBROOK
Chief, Control Criteria Branch
Aeronautical Systems Division
Air Force Flight Dynamics Laboratory

ABSTRACT

The dominating influence of the propulsion system on the dynamic motion of a V/STOL aircraft operating in the hover or low-velocity flight modes has greatly increased the difficulty of developing such an aircraft to be stable and controllable during these modes. Small variations in stability derivatives caused by either changes in the propulsive system or errors in measurement or analytical prediction programs have been shown to cause significant changes in the dynamic characteristics of such aircraft. To better understand relationships, a program was performed using the Lockheed XV-4B jet-lift aircraft as a subject configuration. During this program, the magnitudes of ten of the stability derivatives used to describe the aircraft were varied individually, and the change in the roots of the linearized, uncoupled equations of motion noted. Results include data depicting:

1. The relationship between the propulsively induced component of each derivative to the aerodynamically and interference induced components.

2. The variation of both the components and the total derivatives with flight velocity.

3. The change in the motion characteristics of the aircraft with changes from a basic value of the chosen stability derivatives.

The derivatives found to have the greatest influence on the dynamic characteristics of the XV-4B at hover and low transition velocities were M_u in the longitudinal mode and L_v in the lateral-directional mode.

TABLE OF CONTENTS

INDEX OF FIGURES

INDEX OF FIGURES (Cont.)

INDEX OF FIGURE (Cont.)

SYMBOLS

u,v,w	Perturbations along x,y,z axis	Ft/Sec
p,q,r	Pitch, Roll, Yaw Rates about the x,y,z axis	Rad/Sec
α	Angle of Attack	Deg
β	Angle of Sideslip	Deg
g	Acceleration Due to Gravity	Ft/Sec^2
I_x, I_y, I_z	Moment of Inertia About the x,y,z axis	Slug Ft^2
I_{xz}	Product of Inertia	Slug Ft^2
W	Weight of Aircraft	Lbs
m	Mass of Aircraft W/g	Slugs
N	Yawing Moment	Ft Lb
M	Pitching Moment	Ft Lb
L	Rolling Moment	Ft Lb
X	X Force	Lb
Y	Y Force	Lb
Z	Z Force	Lb
ω_n	Undamped Natural Frequency	Rad/Sec
σ	Real Part of Root(s)	Rad/Sec
δ	Damping Ratio	
$j\omega$	Imaginary Part of Root(s)	
s	Laplace Operator $s = \sigma + j\omega$	
γ_v	Nozzle Deflection (average of 6 or 4 engines) measured from a 10° aft position	Deg

SYMBOLS (Cont.)

δ_e	Elevator Deflection, positive trailing edge on	Deg
δ_a	Aileron Deflection, positive, right aileron down	Deg
δ_r	Rudder deflection positive trailing edge left	Deg
C-RPM	RPM% Cruise Engines (2)	%
L-RPM	RPM% Lift Engines (4)	%
θ	Pitch Attitude	Deg
δ_F	Flap Deflection	Deg
δ_{TL}	Change in Lift Engine Thrust (4)	Lbs
δ_{TC}	Change in Cruise Engine Thrust (2)	Lbs
δ_{TA}	Change in Vertical Thrust of all Engines	Lbs

Derivatives

$M_w = \frac{1}{I_y} \frac{\partial M}{\partial w}$	1/Ft-Sec
$Z_w = \frac{1}{m} \frac{\partial Z}{\partial w}$	1/Sec
$X_w = \frac{1}{m} \frac{\partial X}{\partial w}$	1/Sec
$M_u = \frac{1}{I_y} \frac{\partial M}{\partial u}$	1/Ft-Sec
$Z_u = \frac{1}{m} \frac{\partial Z}{\partial u}$	1/Sec
$X_u = \frac{1}{m} \frac{\partial X}{\partial u}$	1/Sec
$M_q = \frac{1}{I_y} \frac{\partial M}{\partial q}$	1/Sec-Rad

SYMBOLS (Cont.)

$Z_q = \frac{1}{m} \frac{\partial Z}{\partial q}$	Ft/Sec-Rad
$X_q = \frac{1}{m} \frac{\partial X}{\partial q}$	Ft/Sec-Rad
$n_{z_\alpha} = \frac{\partial n_z}{\partial \alpha}$	1/Rad
$M_{\delta_e} = \frac{1}{I_y} \frac{\partial M}{\partial \delta e}$	$1/Sec^2$ - Rad
$Z_{\delta_e} = \frac{1}{m} \frac{\partial Z}{\partial \delta e}$	Ft/Sec^2 - Rad
$X_{\delta_e} = \frac{1}{m} \frac{\partial X}{\partial \delta_e}$	Ft/Sec^2 - Rad
$M_{\gamma_v} = \frac{1}{I_y} \frac{\partial M}{\partial \gamma_v}$	$1/Sec^2$ - Rad
$X_{\gamma_v} = \frac{1}{m} \frac{\partial X}{\partial \gamma_v}$	Ft/Sec^2 - Rad
$Z_{\gamma_v} = \frac{1}{m} \frac{\partial Z}{\partial \gamma_v}$	Ft/Sec^2 - Rad
$M_{\delta_{TL}} = \frac{1}{I_y} \frac{\partial M}{\partial \delta_{TL}}$	$1/Sec^2$ - Lb
$X_{\delta_{TL}} = \frac{1}{m} \frac{\partial X}{\partial \delta_{TL}}$	Ft/Sec^2 - Lb
$Z_{\delta_{TL}} = \frac{1}{m} \frac{\partial Z}{\partial \delta_{TL}}$	Ft/Sec^2 - Lb
$M_{\delta_{TC}} = \frac{1}{I_y} \frac{\partial M}{\partial \delta_{TC}}$	$1/Sec^2$ - Lb
$X_{\delta_{TC}} = \frac{1}{m} \frac{\partial X}{\partial \delta_{TC}}$	Ft/Sec^2 - Lb
$Z_{\delta_{TC}} = \frac{1}{m} \frac{\partial Z}{\partial \delta_{TC}}$	Ft/Sec^2 - Lb

SYMBOLS (Cont.)

$M_{\delta_{TA}} = \frac{1}{I_y} \frac{\partial M}{\partial \delta_{TA}}$	$1/Sec^2$ - Lb
$X_{\delta_{TA}} = \frac{1}{m} \frac{\partial X}{\partial \delta_{TA}}$	Ft/Sec^2 - Lb
$Z_{\delta_{TA}} = \frac{1}{m} \frac{\partial Z}{\partial \delta_{TA}}$	Ft/Sec^2 - Lb
$N_v = \frac{1}{I_z} \frac{\partial N}{\partial v}$	1/Ft - Sec
$L_v = \frac{1}{I_x} \frac{\partial L}{\partial v}$	1/Ft - Sec
$Y_v = \frac{1}{m} \frac{\partial Y}{\partial v}$	1/Sec - Rad
$N_r = \frac{1}{I_z} \frac{\partial N}{\partial r}$	1/Sec - Rad
$L_r = \frac{1}{I_x} \frac{\partial L}{\partial r}$	1/Sec - Rad
$Y_r = \frac{1}{m} \frac{\partial Y}{\partial r}$	Ft/Sec - Rad
$N_{\delta_r} = \frac{1}{I_z} \frac{\partial N}{\partial \delta r}$	$1/Sec^2$ - Rad
$L_{\delta_r} = \frac{1}{I_x} \frac{\partial L}{\partial \delta r}$	$1/Sec^2$ - Rad
$Y_{\delta_r} = \frac{1}{m} \frac{\partial Y}{\partial \delta_r}$	$1/Sec^2$ - Rad
$N_{\delta_a} = \frac{1}{I_z} \frac{\partial N}{\partial \delta_a}$	$1/Sec^2$ - Rad
$L_{\delta_a} = \frac{1}{I_x} \frac{\partial L}{\partial \delta_a}$	$1/Sec^2$ - Rad
$Y_{\delta_a} = \frac{1}{m} \frac{\partial Y}{\partial \delta_a}$	Ft/Sec^2 - Rad

SYMBOLS (Cont.)

$Y_p = \frac{1}{m} \frac{\partial Y}{\partial p}$	Ft/Sec - Rad
$L_p = \frac{1}{I_x} \frac{\partial L}{\partial p}$	1/Sec - Rad
$N_p = \frac{1}{I_z} \frac{\partial N}{\partial p}$	1/Sec - Rad

SECTION I

INTRODUCTION

During the development of heavier-than-air aircraft from the first to present day vehicles, there have been parallel efforts to develop techniques for defining the flight characteristics of each new vehicle in advance. These efforts have resulted in many approaches, varying from scale model testing to purely mathematical analysis, to a mixture of both. Although the quality of each approach has improved over the years, it has never reached a level where any particular technique can be said to perfectly predict the performance or dynamic behavior of each new vehicle. The quality, however, has generally been adequate for design.

With the advent of V/STOL aircraft concepts, however, the techniques that have been developed for conventional aircraft fall far short of being adequate for predicting the dynamic behavior of these aircraft for design purposes. One reason for this is the increased influence of propulsive lift and very low speeds on the dynamic behavior of the V/STOL aircraft. There is also a wide variation possible in the airframe-propulsion system geometric relationship, which further makes the task of predicting the dynamic characteristics of the V/STOL aircraft difficult.[3,5,6,7] In fact, the dynamic characteristics of V/STOL aircraft have been shown to be significantly configuration oriented.

In recognition of the difficulty in predicting the aerodynamic stability derivatives of the V/STOL aircraft, this study was performed to evaluate the effect of variations in the value of these derivatives on the dynamic behavior of the aircraft. Also, since propulsive lift is an important part of the V/STOL aircraft lifting system, the contribution of propulsive lift to the dominant stability derivatives was examined. These studies were performed for only the hover or near-hover and transition phases of V/STOL flight. Both of these phases depend significantly on propulsive lift and, therefore, constitute the greatest departure from conventional aircraft flight. In keeping with nomenclature adopted by Lockheed Aircraft for the XV-4B aircraft,[2,4] the hover or

near-hover phase is called Phase I and the transition phase, Phase II.

During the process of preparing data for simulating the Lockheed XV-4B jet-lift aircraft (Figure 1)[2,3,4], it was decided to perform this study by using the simulator as a source for the open loop stability derivatives for a limited number of specific flight conditions. This was done by changing the independent variable a small amount from trim and noting the difference in the dependent variable. The data for the XV-4B simulation were obtained in two ways:

1) from powered model tests in the NASA/Langley V/STOL wind tunnel for static characteristics and

2) from hand calculations using standard empirical formulas for the dynamic characteristics.

The propulsion-aerodynamic interference values were obtained by taking the difference between power-on and power-off-plus-thrust wind tunnel data. All derivatives were determined from the simulator for an airplane gross weight of 11,000 pounds, cg located at 10 percent of the mac, and seven flight velocities. Since insufficient ground effects data existed, an arbitrary altitude of 1000 feet was chosen for all study data. The aircraft configuration for Phase I, the hover phase, was with all six engines lifting and wheels and flaps fully extended. The configuration for Phase II, transition, had four engines lifting and two converted for forward flight thrust, gear and flaps still fully extended. The seven velocities studied varied from one fps to 100 knots in Phase I and from 70 knots to 150 knots in Phase II, providing a velocity overlap from 70 to 100 knots.

The basic stability derivatives for these geometric and operational conditions as determined from the simulator were then used as input data for a digital computer program[8] that extracts the roots of the longitudinal and lateral characteristic equations. The resulting output from this program describes the dynamic behavior of the aircraft represented by the input. Of 19 input stick-fixed derivatives, only 10 were considered for variation; these being chosen on the basis of past experience as being most important. The magnitudes of these 10 derivatives were then varied by as much as ±100 percent and the roots of the characteristic equations computed. The results are data that indicate the change in

stick-fixed dynamic stability characteristics of the XV-4B with one of the 10 derivatives varied while all of the remaining derivatives (19) are held constant.

Section II presents the results of an examination of the 10 stability derivatives to determine the relationship among the components that make up the derivatives and the variation of these components with aircraft velocity. The dominant components in general are due to the propulsion system, the airplane aerodynamics, and the interference between the two. These data are presented for Phase I only. Section III presents data that show the influence of derivative magnitude variation on the roots of the longitudinal aircraft dynamic characteristic equation, and Section IV shows the influence of derivative magnitude variation on the roots of the lateral-directional characteristic equation.

Appendix I summarizes the basic values of the 19 stability derivatives and the thrust and control derivatives used as a foundation for this study for both Phase I and Phase II flight. These basic values were determined by the XV-4B simulation procedure described above. Appendix II summarizes the changes in magnitude for each stability derivative that was studied along with the resulting values of all the roots. Appendix III presents the variation of the XV-4B inertial characteristics with airplane weight at constant center of gravity location.

SECTION II

FACTORS THAT CONTRIBUTE TO THE TEN STUDY DERIVATIVES

In this section, each of the ten stability derivatives that were varied during the study is examined to determine the variation of its dominant components with aircraft flight velocity. These stability derivatives are all dimensional and consist of M_q, X_u, M_u, Z_w, M_w, L_p, Y_v, N_v, and N_r. A stability axis system was used for all derivatives. The dominant components of each derivative were considered to be induced by propulsion, aerodynamics, and interference between the propulsive system flow field and the airframe flow field. Each of these components is considered to be independent of the others such that the derivative value is the simple sum of all components. Only the Phase I velocity range is considered since the primary purpose for this section is to show trends of the data only. The Phase II data will exhibit trends that are very similar to the trends shown by the Phase I data. All derivative values are included in Appendix I.

Each derivative is discussed in the above noted sequence in the paragraphs below. These discussions consist primarily of an explanation of the dominant contributing factors, both operational and geometric, to the derivative variation shown.

M_q (Figure 2)

This derivative indicates the change in pitching moment due to pitch rate. The largest component of M_q is induced aerodynamically by tail lift. The pitch rate of the aircraft causes a significant increase in horizontal tail angle of attack which yields a tail lift induced nose-down pitching moment. M_q values used during the simulation (which yielded the open-loop derivative values for the specific study operating conditions) were determined empirically and include the effect of other parts of the aircraft besides the horizontal tail. The calculation did not, however, include the effect of pitch rate on the moment contribution caused by internal engine air mass flow.

The second contribution, based on ram drag, results from a change in the angle of attack of the inlets of the

engines with pitch rate. At hover, this component becomes the derivative.

X_u (Figure 3)

This derivative indicates the change in longitudinal aircraft force with a change in forward velocity. The largest contributing factor to X_u is the engine inlet ram drag, which changes very little with velocity because a near-constant thrust level on the lift engines was used for trim throughout the velocity range considered. Second largest is the effect due to interference, which is caused by the high-pressure area in front and low-pressure area behind the six engine jets as they exit from the fuselage. The smallest contributing factor is aircraft aerodynamic drag.

M_u (Figure 4)

This derivative represents the change in pitching moment with a change in forward velocity. The product of engine inlet ram drag as noted above and the moment arm to each inlet contributed a relatively constant nose-up value. The interference component is caused by the drag and lift effects produced by pressure changes in front of and behind the engine jet. The total effect of the product of these forces and their moment arm is a nose-down pitching moment at very low velocities and a nose-up moment as velocity increases. This change results from the jet nozzle being deflected rearward to increase trim velocity. The change in the aerodynamic component with velocity results from the sum of the overall aerodynamic characteristics of the vehicle and the effect of trim elevator settings on these characteristics.

Z_w (Figure 5)

This derivative indicates vertical force change with a change in vertical velocity. The predominate component, the aerodynamic one, results from the change in aircraft lift and drag caused by the change in angle of attack of the wing and tail surfaces due to vertical velocity. Changes in the Z-force component of ram drag and interference drag resulting from this change in angle of attack, although small at higher velocities, become predominant near hover. The interference force results from changes in pressure on the bottom of the aircraft due to jet entrainment and on the top

of the wing/fuselage due to inlet flow. Data from another program[3] on the XV-4B indicate that of the total interference forces acting on the aircraft, about 10% are produced by pressures on the top surface of the aircraft and the other 90% by a reduction of pressure on the bottom of the aircraft.

M_w (Figure 6)

The change in pitching moment with a change in vertical velocity is represented by this derivative. Above 40 knots this derivative is predominantly aerodynamic in nature, produced by a change in horizontal tail angle of attack with a change in vertical velocity. The momentum component is produced by the vertical-velocity-induced change in angle of attack at the engine inlets, with all six engines contributing to the total effect. The momentum component results from a change in engine inlet ram drag, with the magnitude of the moment increasing slightly with velocity. The interference component results from the same change in wing-fuselage pressures that causes the Z_w derivative, acting through the moment arms from the appropriate centers of pressure.

L_p (Figure 7)

This derivative indicates the rolling moment resulting from roll rate. The only value of significance is the aerodynamic contribution, which results primarily from the differential lift generated on the wing panels due to the asymmetrical panel angles of attack caused by the rolling velocity.

Y_v (Figure 8)

This derivative represents aircraft side force due to side velocity. The interference component is dominant, depending on the magnitudes of engine thrust and sideslip. This component is primarily a function of the build-up of positive and negative side pressures on the wing/fuselage combination due to flow into the engine inlets and out of the jet exhaust.

The aerodynamic component, which is next strongest, comes from pure aerodynamic differential pressure across the fuselage and vertical tail during sideslip. The smallest component results from the sideward component of ram air

momentum force on all engine inlets during a sideslip.

L_v (Figure 9)

This derivative indicates rolling moment variation with changes in side velocity. The largest component, that due to interference, is a function of the asymmetrical pressures on the upper and lower surfaces of the body, wing, and vertical tail caused by the inflow of air at the engine inlet and outflow of the jet exhaust at the engine exit. The aerodynamic component results from the well-known dihedral effect produced mainly by a differential in lift on the wing panels due to sideslip. The momentum component results from the side ram air force components at the engine inlets multiplied by the moment arm to each inlet; the top inlets being the main contributors.

N_v (Figure 10)

This derivative represents the change in yawing moment due to side velocity. At speeds above 40 knots the principal contribution to this derivative is aerodynamic, being produced by side loads on the vehicle body and vertical tail. The momentum component results from the product of ram force air components at the cruise engine inlets and their moment arms. The farther these inlets are located in front of the aircraft center of gravity, the more destabilizing they are. The interference component increases from zero at hover to a maximum value near a velocity of 20 knots and is constant with further increases in velocity. This component primarily results from the engine-induced side flows in the vicinity of the vertical tail and fuselage.

N_r (Figure 11)

The final derivative considered indicates the change in yawing moment due to yawing rate. The only component having significance is that due to the aerodynamic forces on the fuselage side area and vertical tail and differential drag on the wing panels due to yawing rate. The effect of vertical tail on the magnitude of this derivative is the largest.

SECTION III

LONGITUDINAL DERIVATIVE VARIATION AND THE EFFECT ON THE CHARACTERISTIC ROOTS

Data are presented in this section that indicate the change in both the damping and oscillatory characteristics of the roots of the longitudinal equations of motion of the XV-4B aircraft resulting from changes in aircraft velocity and stability derivatives. During the study, velocity was varied from one foot per second to 150 knots and the stability derivatives were varied as much as ± 100 percent from nominal. The technique used to indicate changes in the aircraft dynamic characteristics makes use of the root locus method of plotting the real and imaginary components of the roots of the characteristic equation. The stability derivatives that were varied for the longitudinal motion study were X_u, M_u, Z_w, M_w, and M_q.

The equations of motion used as a basis of this part of the study were uncoupled from the lateral-directional equations and linearized using small perturbation techniques. The resulting stability axis equations with $\gamma_o = 0$ are:

$$\dot{u} + W_o q + g\,\theta\cos\gamma_o = X_u u + X_q q + X_w w$$

$$\dot{w} + U_o q = Z_u u + Z_q q + Z_w w$$

$$\dot{q} = M_u u + M_q q + M_w w$$

Transforming these equations using the techniques of the Laplace transform; equating pitch rate, q, to angular velocity, $\dot{\theta}$ [(made possible by the assumption of uncoupled equations)]; and converting to matrix notation yields;

$$\begin{vmatrix} s - X_u & -X_w & -(sX_q - g\cos\gamma_o) \\ -Z_u & s - Z_w & -s(U_o + Z_q) \\ -M_u & -M_w & (s^2 - M_q s) \end{vmatrix} \begin{vmatrix} u(s) \\ w(s) \\ \theta(s) \end{vmatrix} = 0$$

Expanding the first matrix yields a characteristic equation of fourth order in the transform variable, s. The constants

in this equation are combinations of the derivatives and other items that make up the terms of the matrix. The resulting characteristic equation is:

$$As^4 + Bs^3 + Cs^2 + Ds + E = 0$$

This equation has four separate roots having the general form:

$$s = \omega_n \pm \omega_n \sqrt{\zeta^2 - 1}$$

For simplicity during presentation, the notation

$$s = \sigma + j\omega$$

is used in the root locus plots. A negative value for σ in these plots indicates that the dynamic motion is decreasing in amplitude toward equilibrium, i.e., the motion is stable. An increase in magnitude of $j\omega$ indicates an increase in frequency of the dynamic motion of the aircraft. Roots having $j\omega = o$ are non-oscillatory. Values for all roots of the derivatives varied are listed in Appendix II, but only the oscillatory roots shown on the root locus plots. Figure 12 and 20 show all roots for the Phase I and Phase II nominal derivatives as related to speed changes.

Root locus plots of the longitudinal roots are shown in Figures 12 through 19 for the Phase I configuration and Figures 20 through 24 for Phase II configuration. Arrowheads on the plots indicate the direction of the movement of the roots as the absolute value of the derivative is increased.

Longitudinal - Phase I

Figure 12 - Velocity Change Study

This figure shows a change in the basic Phase I longitudinal dynamic characteristics as a function of speed. The two phugoid roots vary from unstable oscillatory to two stable aperiodic roots near 100 knots. The two other roots of the quadratic are stable non-oscillatory roots that fluctuate slightly in value and then join together to become the oscillatory short period between 40 and 60 knots.

Figure 13 - 1 foot/second

M_u is the predominate derivative affecting the unstable phugoid roots at this speed and, as shown in Figure 4, it derives most of its value from a change in the momentum of the air entering the engine inlets. The non-oscillatory roots are not plotted but can be found in Appendix II. M_u was varied ±50% about its basic value. A ±50% variation produced no change in the damping ratio, ζ, but a 0.14 radian/second change in the undamped natural frequency, ω_n. M_w, when varied ±50% about the nominal value, caused a change in damping ratio value of 0.05. Decreasing the value of the derivative decreased the negative damping and moved the characteristic root toward a stable condition. The primary influence on the magnitude of M_w at this velocity is the interference factor as shown in Figure 6.

Figure 14 - 10 knots

Very little change was produced in the phugoid roots by changing velocity from 1 ft/second to 10 knots. The ±100% M_q and the ±50% M_w variations produced only a slight change in frequency. M_u was also varied ±50%, again affecting frequency but not damping ratio.

Figure 15 - 20 knots

The same percentage variations in the derivatives as at the lower speeds produced about the same overall effect at 20 knots. The influence of M_q is slightly greater due to the increase in velocity. The dominant influence on M_q is aerodynamic as shown in Figure 2

Figure 16 - 40 knots

The general variations of the phugoid roots by varying the derivatives are about the same as for the lower velocities except for M_q. The percentage variation of M_q was reduced to ±50% but the range of the root variation remained about the same as at 20 knots with ±100% variation because of the influence of the increased velocity. The root became more stable by setting M_q more negative and M_w to a smaller positive value. The natural frequency and negative damping of the basic root decreased slightly from the 20 knots case (see Figure 12).

Figure 17 - 60 knots

At this velocity, highly damped short-period roots have developed from the non-oscillatory roots. Variation of all five of the derivatives produced different effects on the short period. Setting the value of M_w more negative increased the frequency and slightly decreased the positive damping. Increasing M_q increased both the undamped natural frequency and damping of the short period root. Making the value of Z_w more negative increased the frequency and the damping. Increasing M_u positively, decreased natural frequency and damping.

Although speed has moved the basic value of the phugoid root toward a stable position, the effect of derivative variation is about the same as it was for the 40 knot case. M_w, which has reversed its sign from positive to negative, must still be more negative if this root is to become stable. Making M_q more negative at this speed has a greater effect on frequency than at the lower speeds discussed above.

Figure 18 - 70 knots

Increasing the speed from 60 to 70 knots has decreased the damping and increased the natural frequency of the short period roots. The effects of varying Z_w and M_u have been reduced, and the effects of M_q and M_w variations have increased.

The basic value of the phugoid has become lightly damped. Varying the derivatives the same amount as done for the 60 knots case produced very small changes.

Figure 19 - 100 knots

By increasing the velocity from 70 to 100 knots, the phugoid roots reduced to two non-oscillatory roots. The values of these stable roots are listed in Appendix II.

The change in velocity caused the short-period root to increase in frequency from 4.5 to 9.5 radians per second with an increase in total damping, $-\sigma$, but some reduction in damping ratio, ζ. The effect of varying Z_w on these roots changed only slightly with the speed increase. Increasing M_q again increased undamped natural frequency and damping

as before, but to a much larger extent. A decrease in value of M_w also increased the undamped natural frequency but reduced the damping ratio, keeping constant total damping, σ.

Phase II

Figure 20 - Velocity Influence Only

This figure provides an insight into the nature of the Phase II flight condition during which the two cruise engines are deflected from the lifting mode of Phase I into a thrusting mode for forward flight. All derivatives used in this plot are basic values. As shown the short period damping ratio, ζ, is reduced from around 0.7 at 70 knots to about 0.4 at 150 knots; however, the time to decay decreases, as shown by the increased total damping. The undamped natural frequency, ω_n, increased from 0.5 to 1.5 rad/sec with the same increased speed. The phugoid root fluctuated with speed, with both frequency and damping remaining low.

With only four engines lifting, a trim angle of attack of 5 degrees was required throughout the velocity range.

Figure 21 - 70 knots

At this speed, the effect of ±50% M_u variation on the short period and the phugoid is comparatively small. Varying the other derivatives (M_q, M_w, and Z_w) had a small effect on the phugoid but a significantly greater effect on the short period. Increasing the absolute value of M_w (more negative) increased the natural frequency of the short period at constant total damping, thus decreasing the damping ratio. Increasing the absolute values of Z_w and M_q (more negative) increased the damping and the undamped natural frequency of the aircraft motion with little effect on $j\omega$.

Figure 22 - 100 knots

At this velocity setting M_w at a more negative value increased the natural frequency of both the short-period and phugoid motions at constant total damping, $-\sigma$, very much as at 70 knots (Figure 21) and for the short period at the same conditions with the Phase I configuration (Figure 19). Z_w and M_q also influenced frequency and damping similarly to

their effects in Phase II at 70 knots and the Phase I configuration at 100 knots.

The basic phugoid roots, which changed from stable oscillatory roots at 70 knots to stable non-oscillatory roots at 100 knots for the Phase I flight condition, remained oscillatory and stable for the same speed change in the Phase II configuration. At 100 knots, Phase II, the derivatives M_u and M_w produced opposite effects on the phugoid; that is, as M_u became more negative the roots became non-oscillatory, and as M_w became more negative, the roots became more oscillatory. All the varied derivatives affected the phugoid damping ratio. They showed a variation in the low natural frequencies of this root from 0 to 0.1 rad/sec.

Figure 23 - 130 knots

At this velocity the short-period basic roots have moved to a higher frequency while maintaining approximately the same damping ratio (note the change in ordinate from Figure 22 to Figure 23). The effects of varying the derivatives are similar to the effects seen at the 100 knots in the Phase I configuration, except that M_w variations now produce much larger excursions in the root.

The phugoid root variation remains about the same with derivative changes as at 100 knots, with only a slight increase in the frequency of the basic root.

Figure 24 - 150 knots

At this velocity again the basic short-period roots have changed from their values at 130 knots, increasing in frequency while the damping ratio remains at about 0.5. The same three derivatives, M_w, M_q, and Z_w still have about the same effect on the roots at this velocity, only with slightly larger magnitude changes. It should be noted that the Z_w variation would have had about the same effect as the M_q variation on the root if it had been varied ±50% instead of ±20%.

The phugoid roots are again about the same as for the other speeds examined in Phase II, with the one exception that the positive 50% variation of M_u does not produce non-oscillatory roots as it had done at the 100 and 130 knot Phase II cases examined.

SECTION IV

LATERAL/DIRECTIONAL DERIVATIVE VARIATION AND THE EFFECT ON THE CHARACTERISTIC ROOTS

In this section, the same study techniques are used as for the longitudinal derivative variation reported in Section III. This section, however, considers only the lateral/directional equations of motion. The derivatives that were varied were Y_v, N_v, L_v, N_r, and L_p.

Based on $\gamma_o = o$ the equations of motion using the lateral/directional derivatives are:

$$\dot{v} + U_o r - g\phi \cos \gamma_o = Y_r r + Y_v v + Y_p p$$

$$\dot{p} - \dot{r} \frac{I_{xz}}{I_{xx}} = L_r r + L_v v + L_p p$$

$$\dot{r} - \dot{p} \frac{I_{xz}}{I_{zz}} = N_v v + N_r r + N_p p$$

The modified lateral/directional equations as converted to the matrix form in Laplace operator notation, with $\beta = u/U_o$, $p = \dot{\phi}$ and $r = \dot{\psi}$, are:

$$\begin{vmatrix} (s-Y_v) & -(\frac{sY_p}{U_o} + \frac{g}{U_o}\cos\gamma_o) & [s(1 - \frac{Y_r}{U_o}) - \frac{g}{U_o}\sin\gamma_o] \\ -L_\beta & (s^2 - sL_p) & -(\frac{I_{xz}}{I_{xx}} s^2 + SL_r) \\ N_\beta & -(\frac{I_{xz}}{I_{zz}} s^2 + sN_p & (s^2 - sN_r) \end{vmatrix} \begin{vmatrix} \beta(s) \\ \phi(s) \\ \psi(s) \end{vmatrix} = 0$$

Expanding the determinant and setting the result equal to zero yields the characteristic equation of motions of the aircraft:

$$AS^4 + BS^3 + CS^2 + DS + E = 0$$

As before, the roots to this equation are expressed in the form:

$$S = \sigma + j\omega$$

and plotted using root locus techniques. Values for all the roots based on the varied derivatives are included in Appendix II. Most plots indicate only the oscillatory roots since a large amount of overlay would occur if all the root variations for the non-oscillatory conditions were plotted.

Plots of the lateral/direction roots are shown in Figures 25 through 32 for the Phase I configuration and Figures 33 through 37 for the Phase II configuration. Arrowheads on the plots indicate the direction of the movement of the roots as the absolute value of the derivative is increased.

Phase I

Figure 25 -- Velocity Variation Only

This figure indicates the change in the basic lateral/directional characteristic roots as a function of aircraft velocity. The natural frequency of the Dutch roll root varies from 1.0 to 1.2 rad/sec in the speed range from 1 ft/sec to 100 knots and the damping ratio varies from -0.5 at 1 ft/sec to -0.2 at 100 knots. Dutch roll is unstable. The spiral root remains near zero and the roll subsidence has a value of 1.2. Both are stable.

Figure 26 -- 1 ft/sec -- L_v is the primary derivative that affects the lateral/directional dutch roll at this velocity. The damping ratio remained relatively constant at -0.5 with frequency changing from .2 to 1.2 the value of the derivative decreases. Y_v produced the very small change in the roots. The L_v derivative when varied (not plotted) also produced a large change in the non-oscillatory roll subsidence root, varying from -.257 to -1.295 for a ± 100% change.

Figure 27 -- 10 knots

The L_v effect on the dutch roll and roll subsidence roots remained essentially the same as at the 1 ft/sec velocity with some reduction in dutch roll damping ratio although the effect of Y_v is still small; its effect has increased from the 1 ft/sec case. L_p has an effect now, but this effect is still very small. Making either Y_v or L_p more negative reduces the negative damping of the aircraft motion at roughly constant frequency.

Figure 28 -- 20 knots

At 20 knots, L_v is still the dominate dutch roll derivative with the total curve shifted to a less unstable condition. At low frequencies, as L_v approaches zero, a dynamically stable motion develops. Although variation of the other derivatives still has a small effect on dutch roll, this effect is increasing. N_v, which previously had almost no effect, now reduces the negative damping as its value is made more positive.

Figure 29 -- 40 knots

At this velocity, the basic root is less unstable, having a negative damping ratio of -.35 at a natural frequency of about 1.2 radians/sec. Setting Y_v, L_p, or N_v more negative tends to move the root toward a more stable condition; this change in N_v increases the frequency, also. The effect of the N_v variation has grown considerably at this speed, now being equal to the effect of Y_v and L_p. L_v is still the dominant derivative at this speed requiring a comparatively smaller change in the positive direction to produce Dutch roll stability.

Phase II

Figure 33 -- Velocity Variation Only

Neutral stability for the Dutch roll roots occurred around 115 knots. The value of the spiral non-oscillatory root varied -0.01 to -0.07 while velocity varied from 70 to 150 knots. The roll subsidence root varied from -1.1 to -1.5 for the same velocity range.

Figure 34 -- 70 knots

The effects of the derivative variations on the Dutch roll are very similar to those obtained for the Phase I 70 knot case, except that the basic root is more stable with the two cruise engines diverted for cruise thrust. In general, increasing the absolute value of N_v, L_p, Y_v, and N_r tends to decrease the negative damping; this N_r variation also increases the frequency even more, its principal effect.

Figure 35 -- 100 knots

Comparing Figure 32 with Figure 35, it becomes evident that the contrast between the two phases is even greater than it was at 70 knots. In the Phase II plot the basic root is stable whereas the Phase I root is unstable, having a damping ratio near -0.1. Varying L_p did not produce as much change in the roots as it did in Phase I. In general, most of the root differences between the two phases come from the change in α from 0 for the Phase I configuration to 5 degrees for the Phase II configuration.

Figure 36 -- 130 knots

At 130 knots, the trends of the Phase II root location with derivative variation are similar to the 100 knot case. L_v variation has less influence than N_v. Varying L_p has caused a slightly greater movement of the root; a movement that is primarily due to the velocity increase.

Figure 37 -- 150 knots

The basic root at this velocity has moved to a slightly more stable position, with an increase in frequency. N_v has become the dominant derivative, exerting the greatest change in the root when varied; the effects of all the other derivatives diminish. N_v affects frequency more than the other derivatives do, while all other derivatives have a greater effect on damping of the motion.

CONCLUSIONS

1. Of the 10 derivatives evaluated, M_u in the longitudinal (Phugoid) mode and L_v in the lateral/directional (Dutch roll) mode cause the biggest change in the dynamic characteristics at hover and low airspeeds when varied. With a lift jet near hover, the predominant item affecting M_u is the momentum of the air entering the engine inlets. In the lateral case there is still a momentum effect, but it is only half the strength of the interference effect produced by the lift jet exhaust on the body, wing, and vertical tail. In the longitudinal case, M_u diminishes in value at higher speeds, and at 60 knots has no more effect than M_q, X_u, Z_w, M_w, when varied the same amount. L_v on the other hand remained greatly effective up to 100 knots.

2. As speed is increased on a jet lift V/STOL, M_q and M_w become more predominant in their effect on the short period with M_u becoming completely ineffective. This is true throughout Phase I and Phase II.

3. The effect of L_v variation, which is the predominant influence near hover, reduces only slightly up to 100 knots but drops rather sharply with the initiation of Phase II (2 engines diverted to cruise). Two other derivatives which make their influence felt when varied at the higher speeds are N_v and L_p, N_v having stronger influence in Phase II.

4. Based on the above conclusions it can be seen that by properly locating the wing relative to the jet exhaust and the engine inlets relative to the center of gravity, it would be possible to control the values of M_u and L_v to make most jet lift V/STOL aircraft nearly stable at near-hover or low speeds.

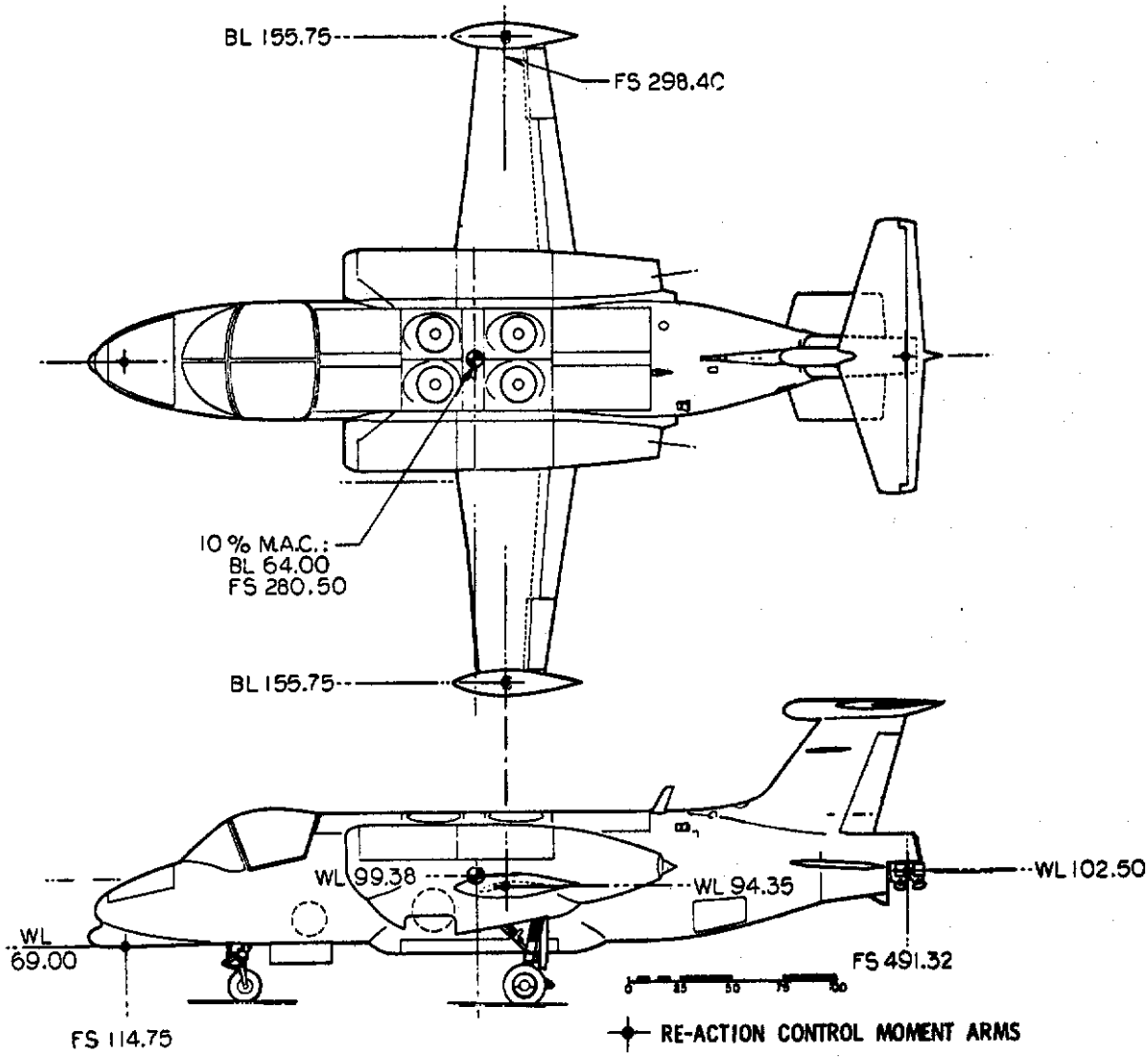

Figure 1. XV-4B General Arrangement

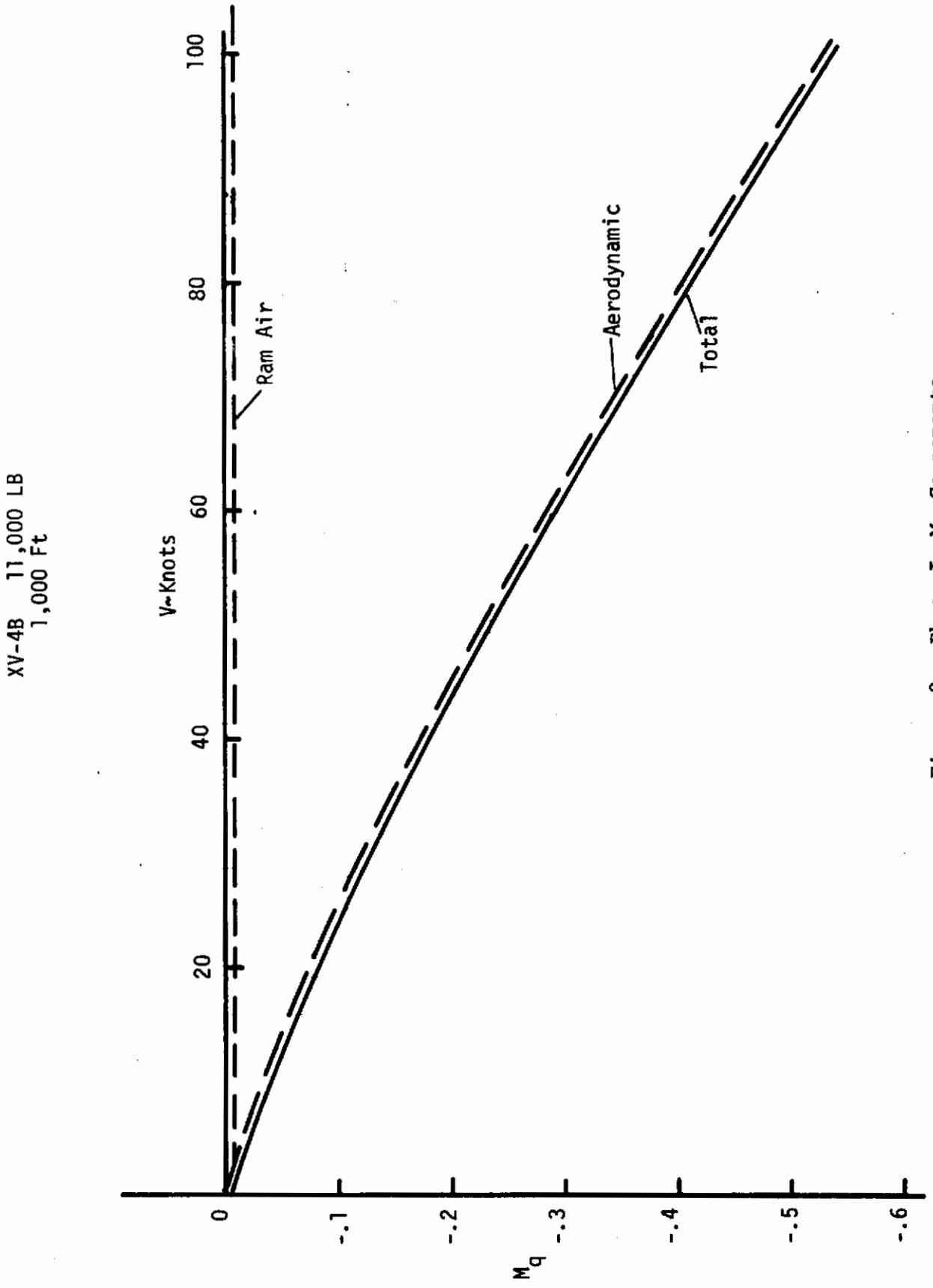

Figure 2. Phase I, M_q Components

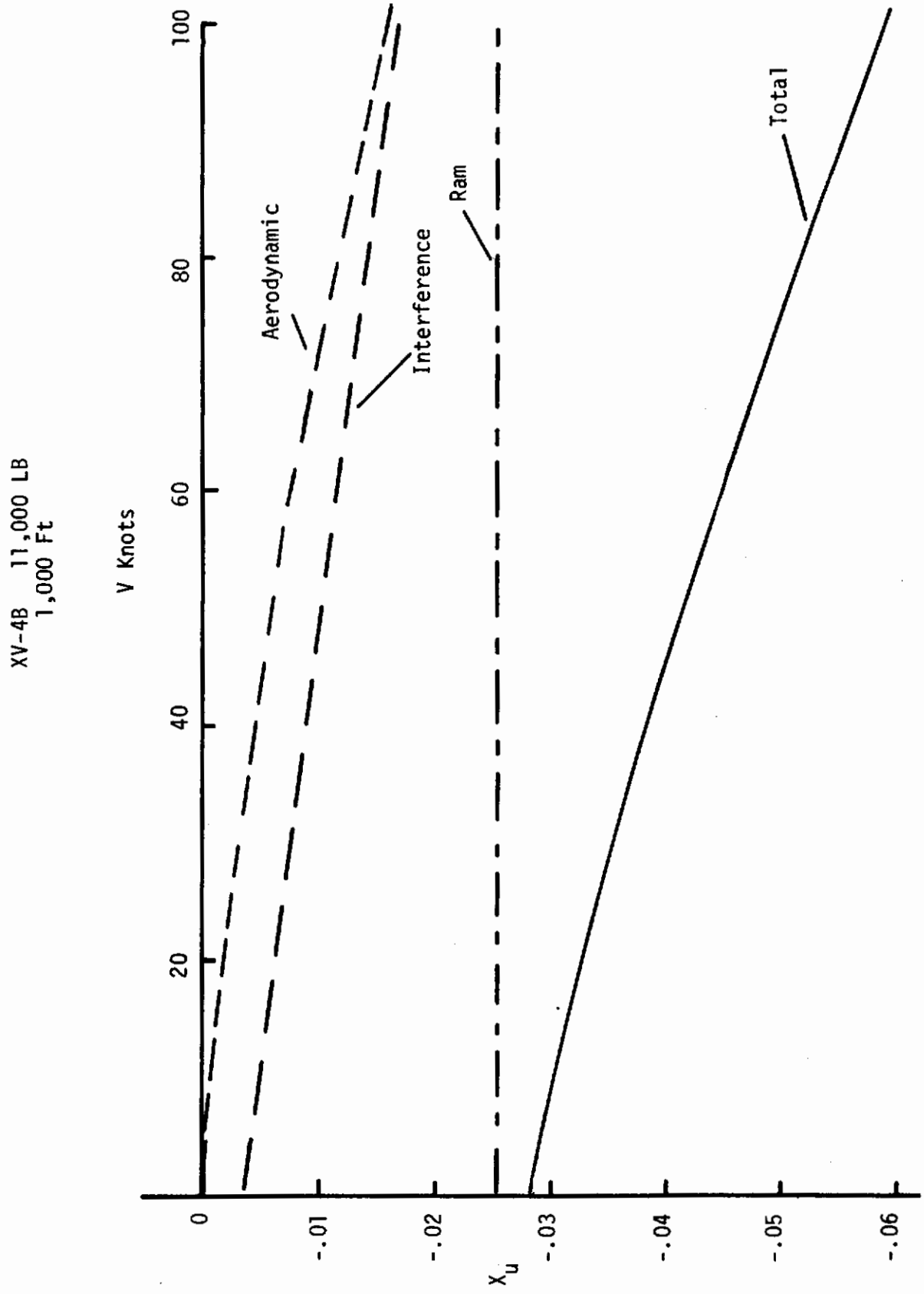

Figure 3. Phase I, X_u Components

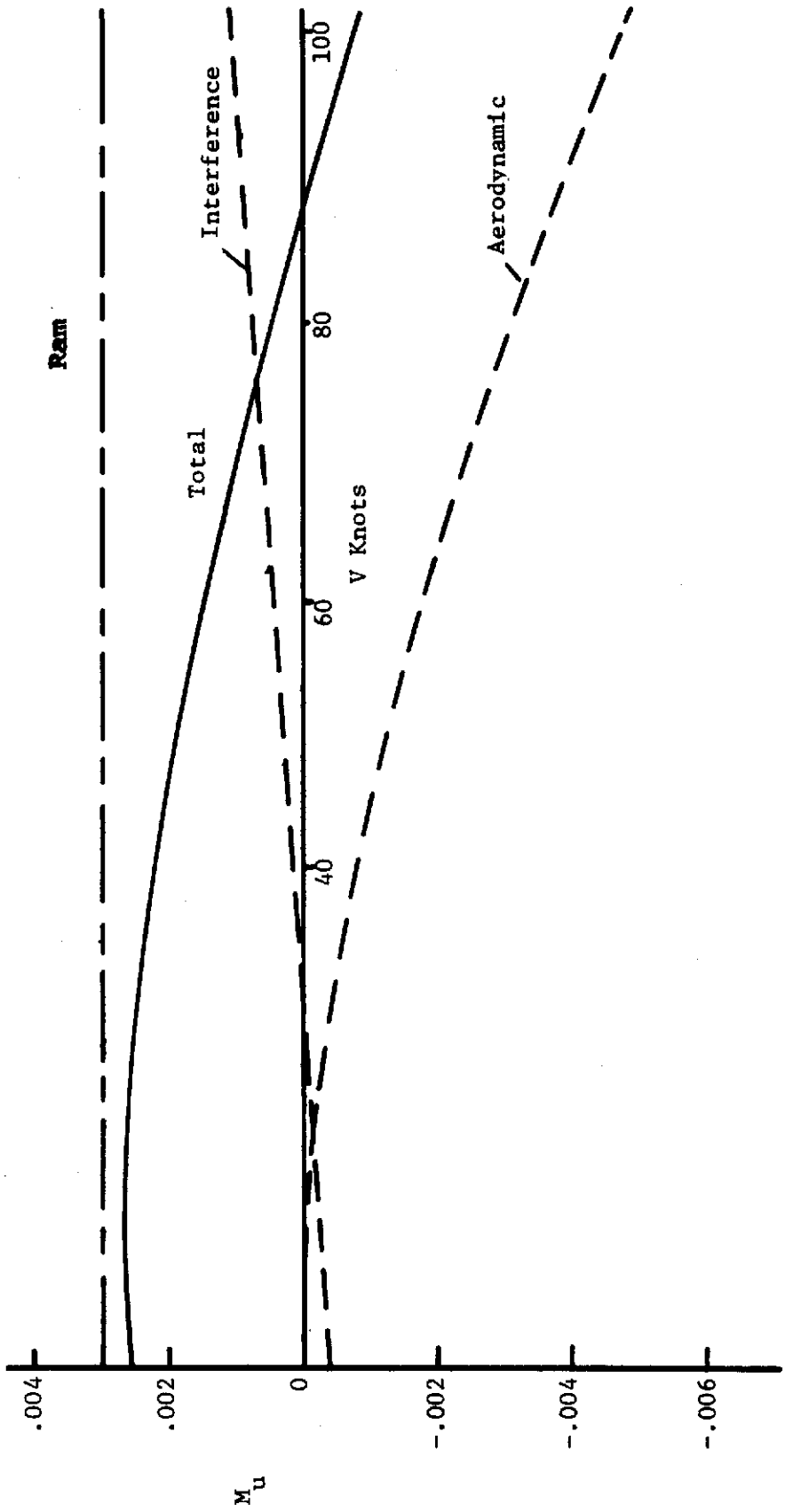

Figure 4. Phase I, M_u Components

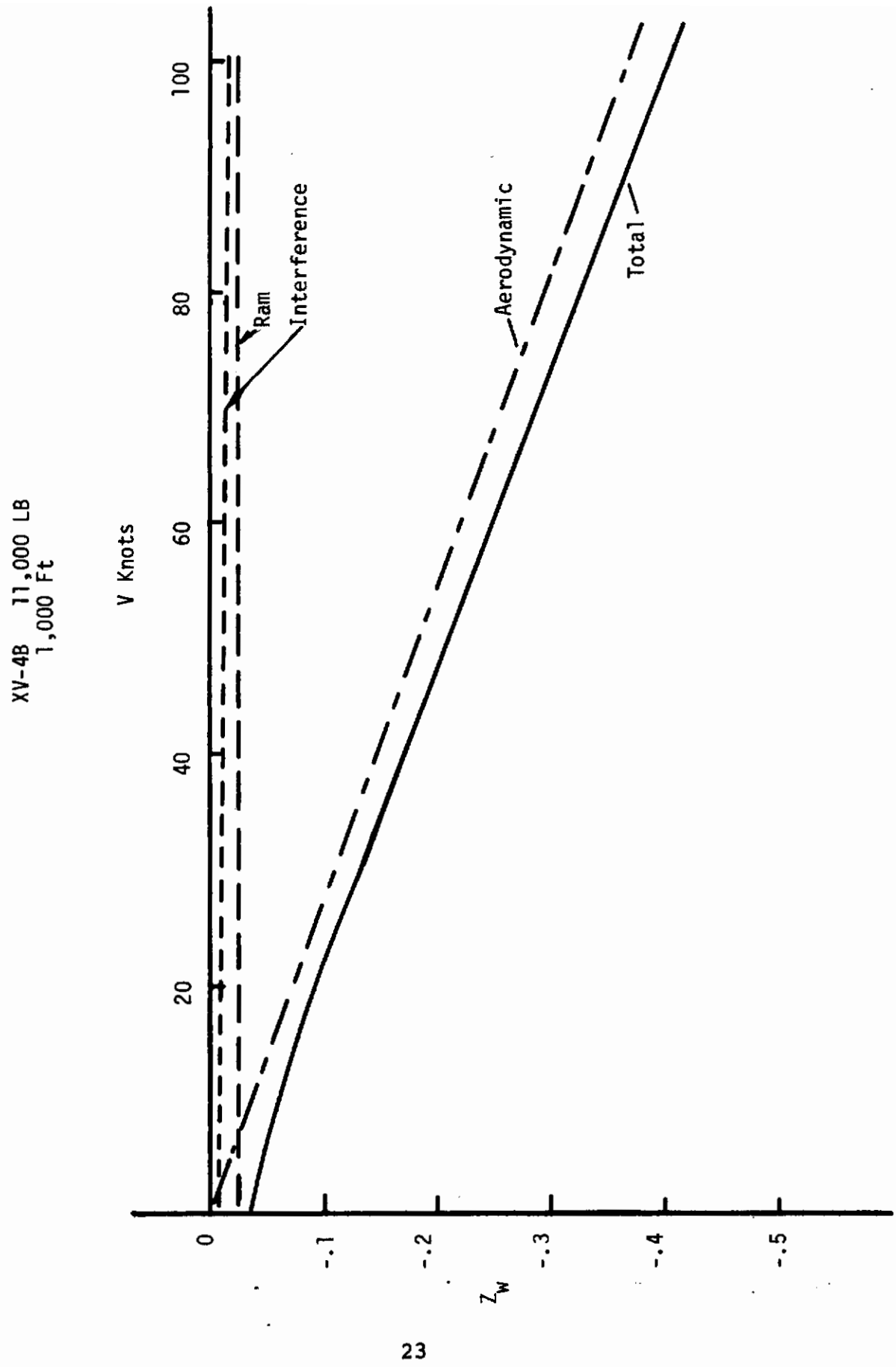

Figure 5. Phase I. Z_w Components

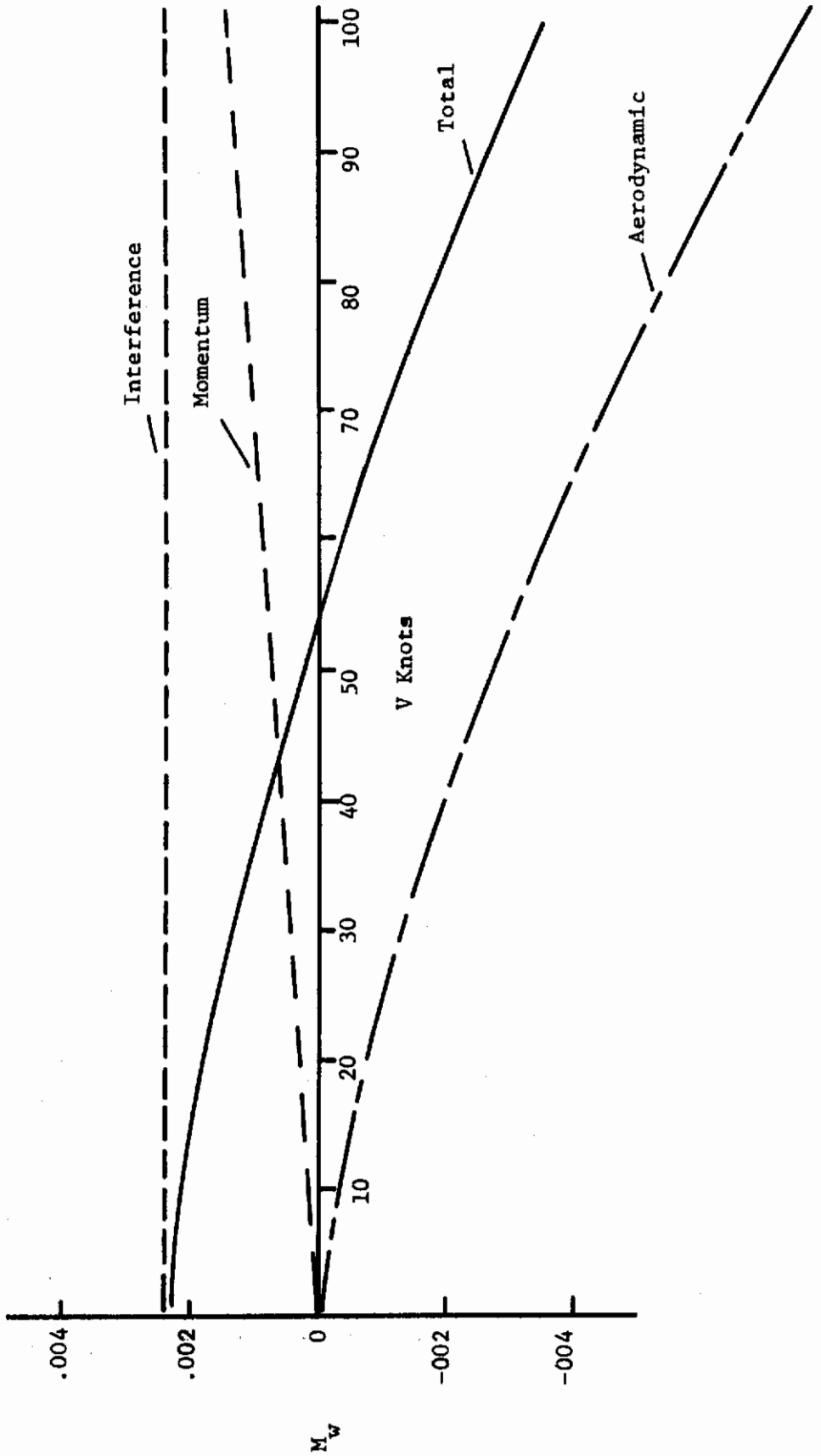

Figure 6. Phase I, M_w Components

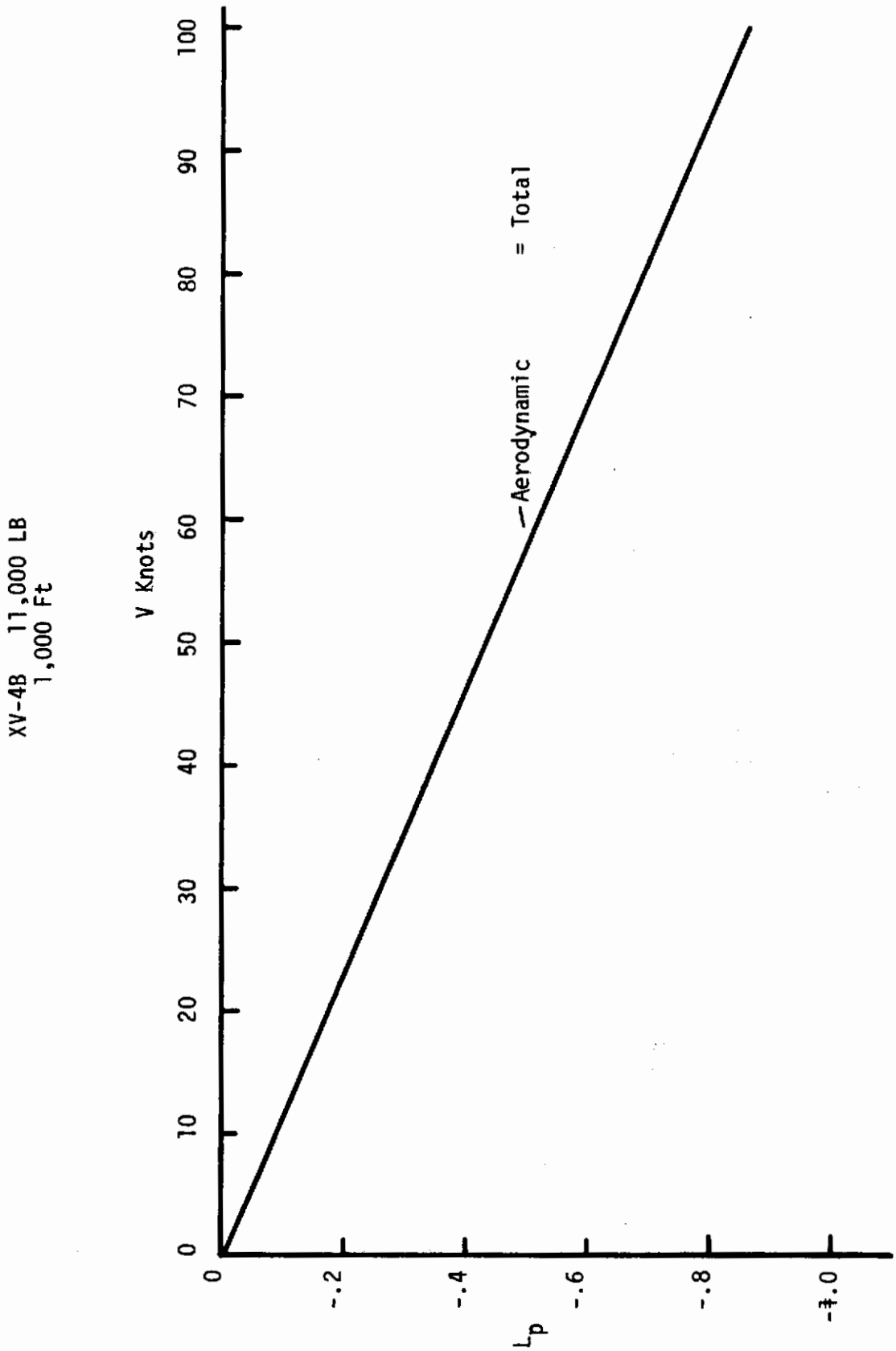

Figure 7. Phase I, L_p Components

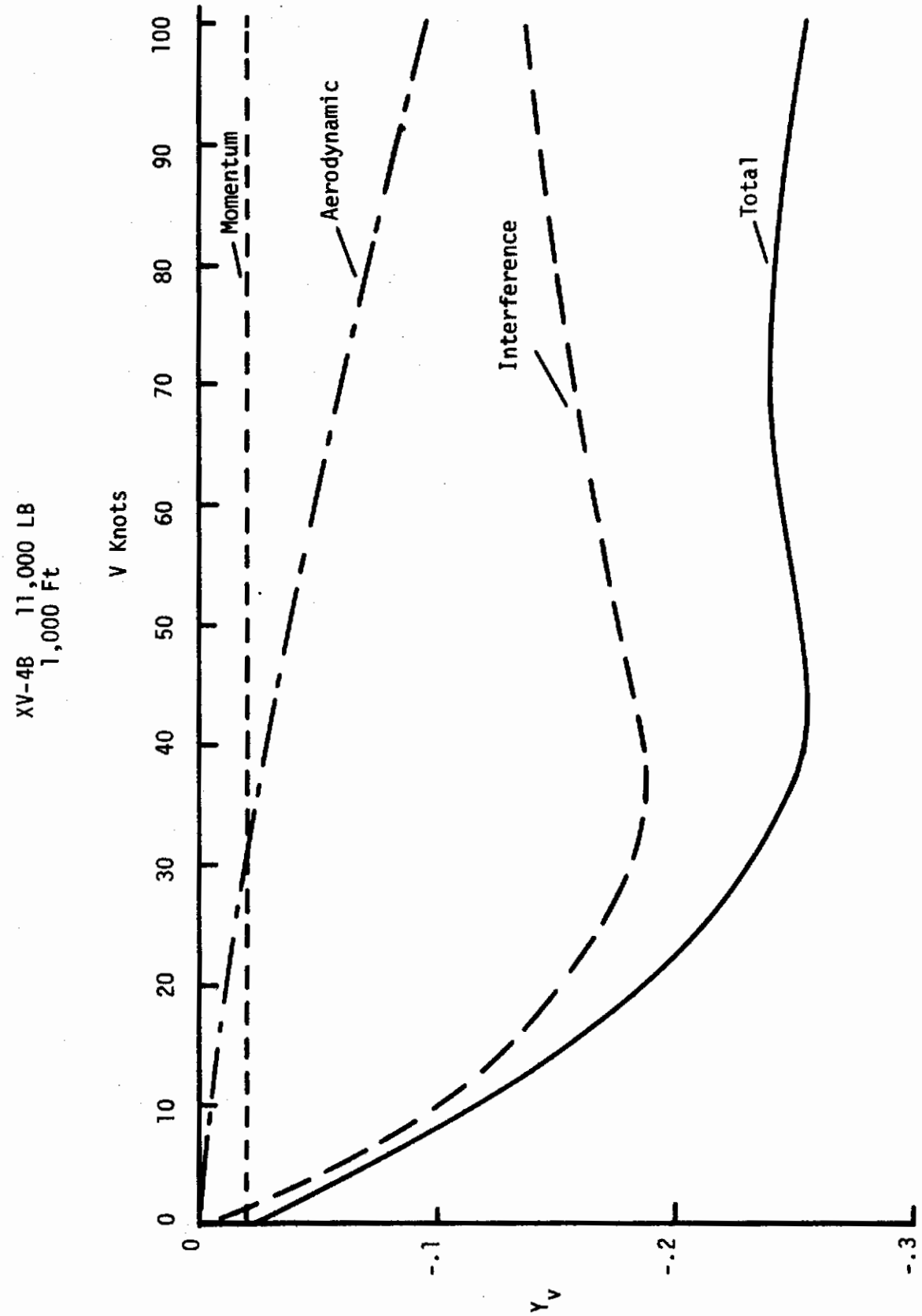

Figure 8. Phase I, Y_v Components

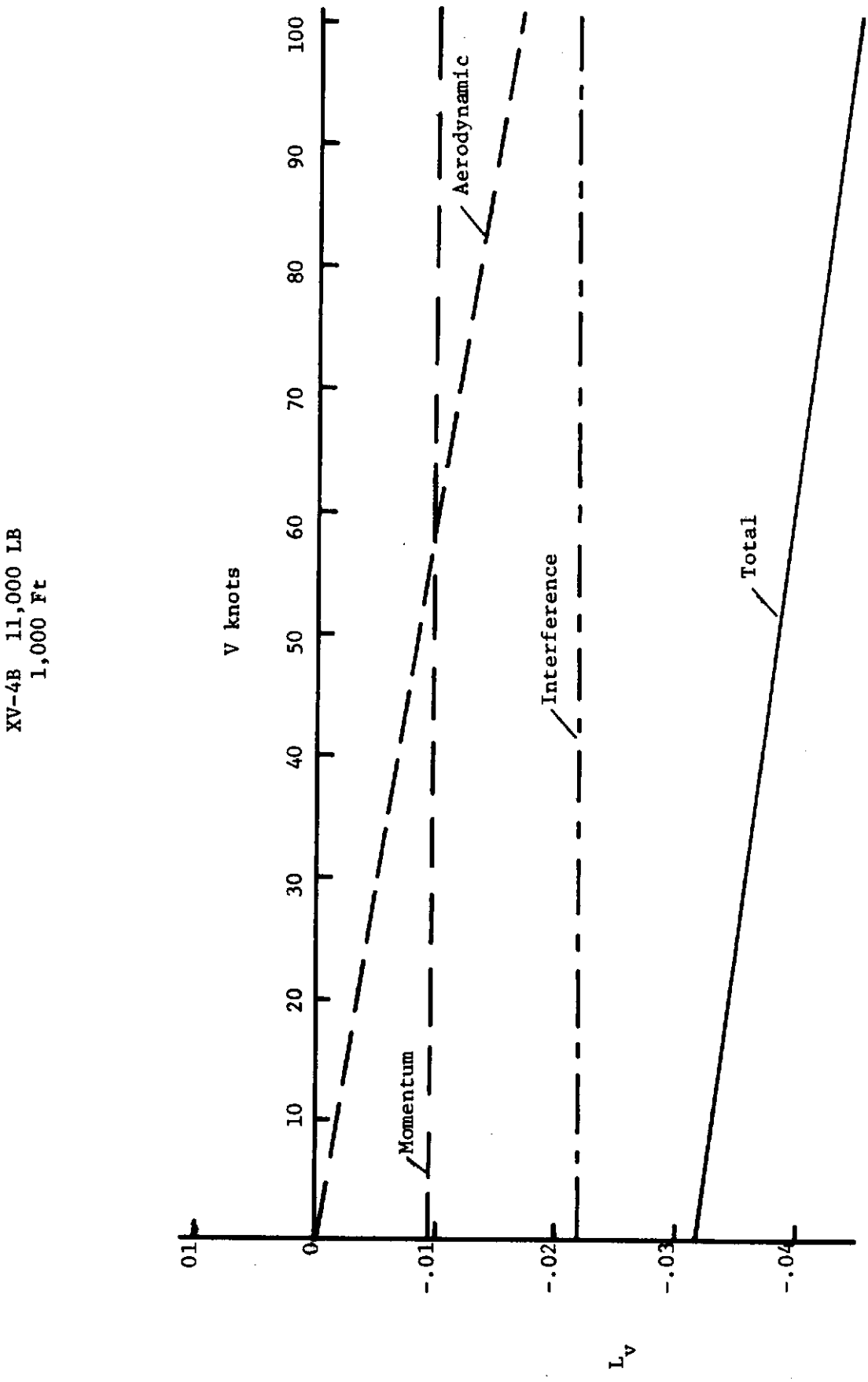

Figure 9. Phase I, L_v Components

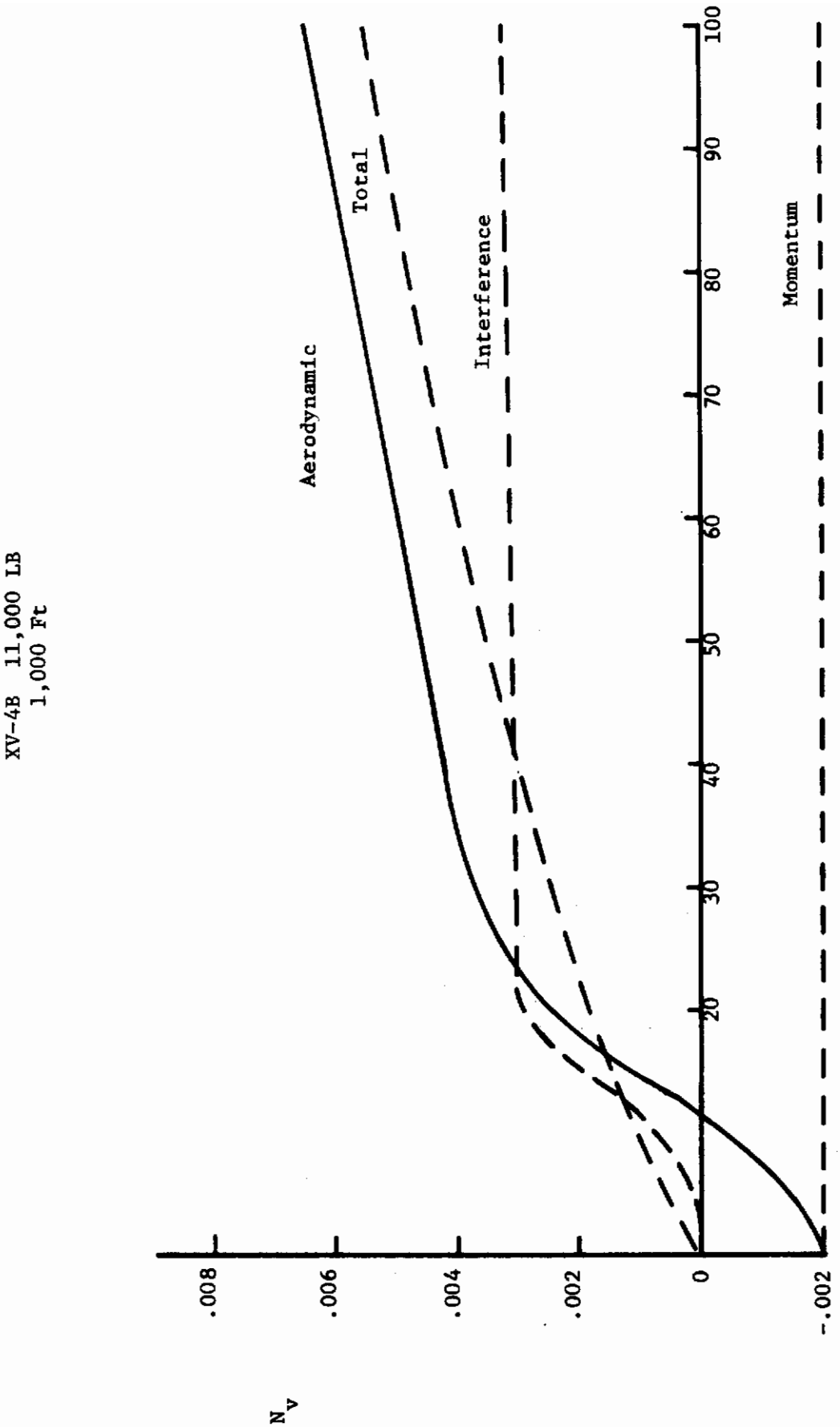

Figure 10. Phase I, N_v Components

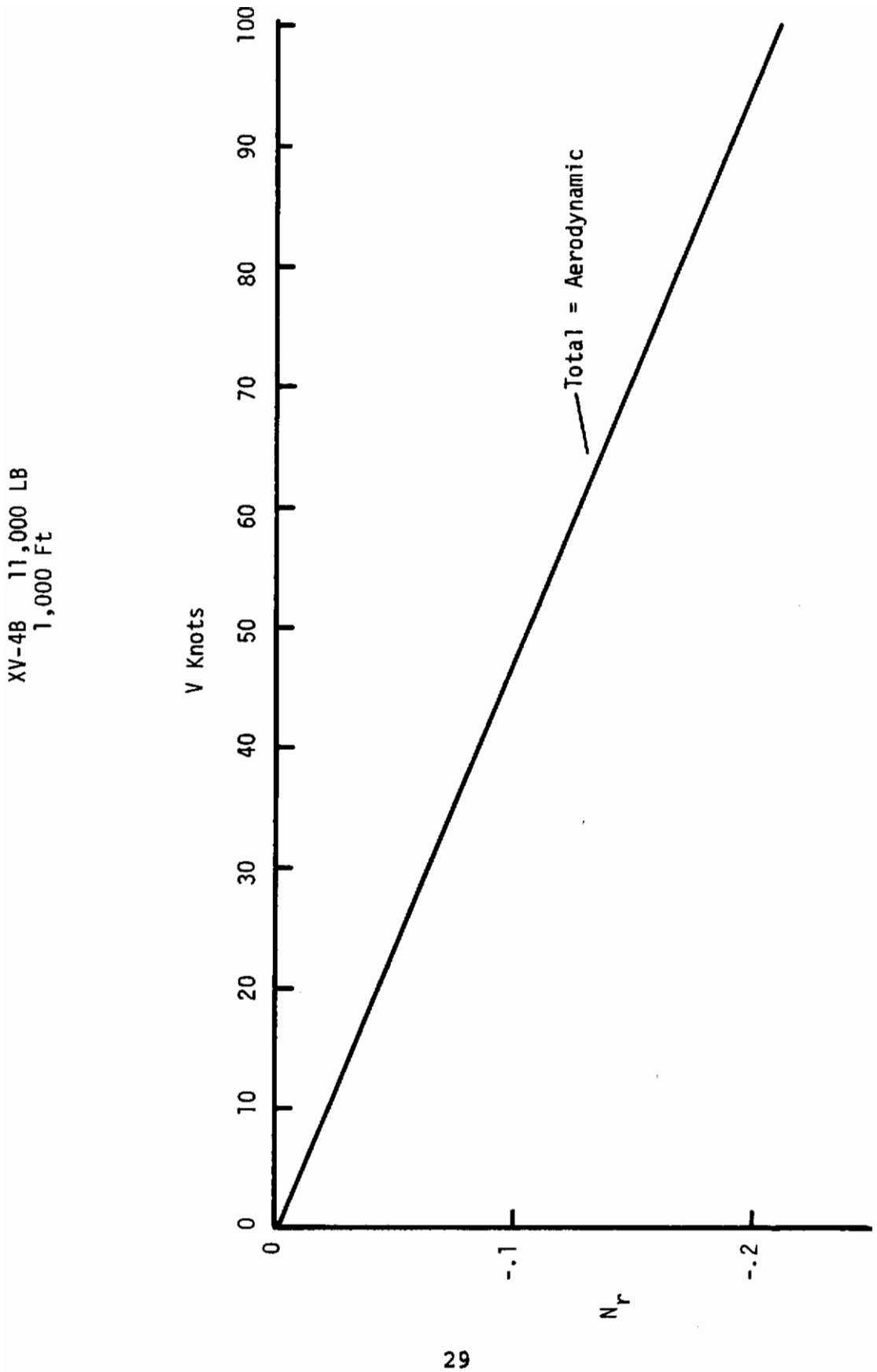

Figure 11. Phase I, N_r Components

XV-4B Phase I

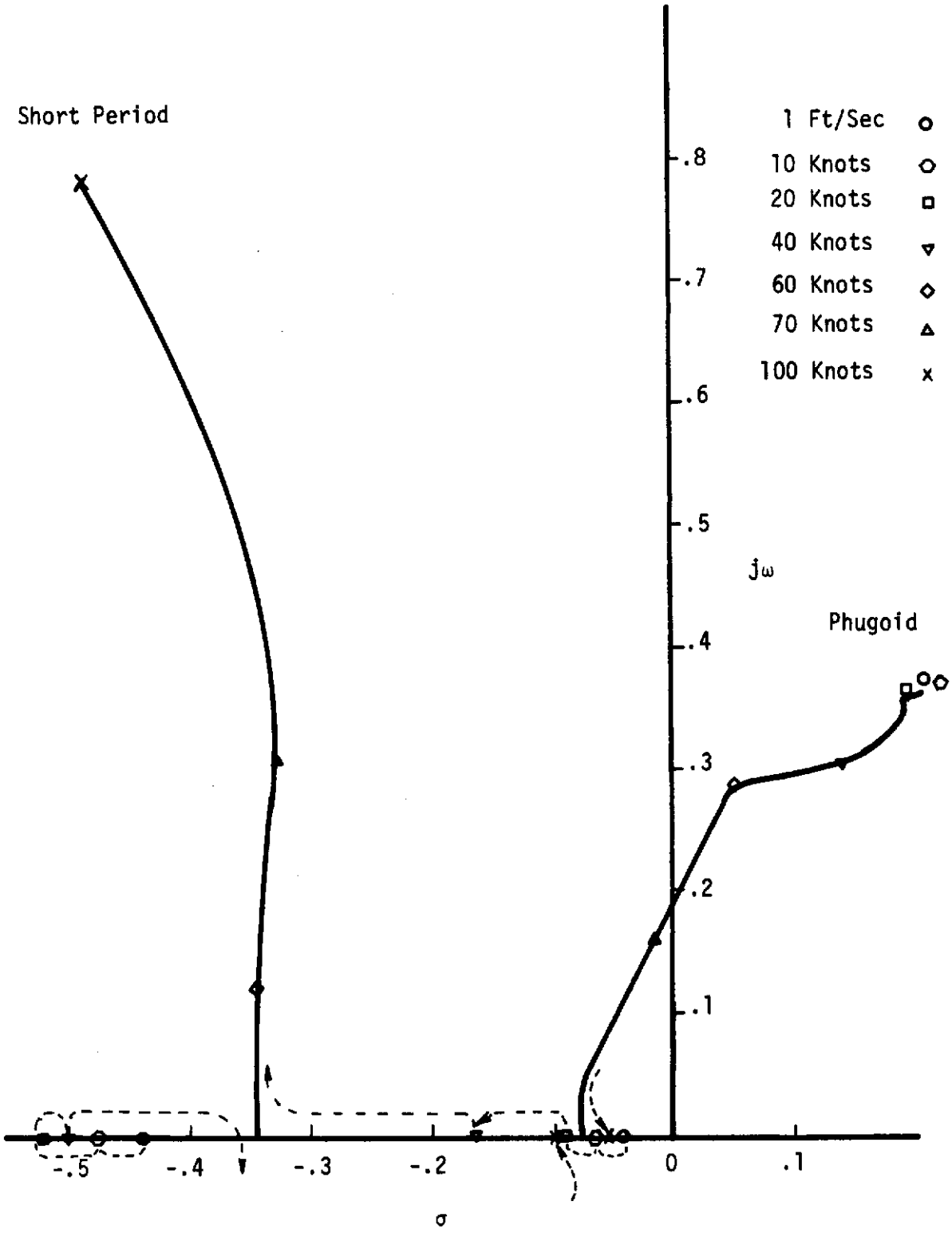

Figure 12. Phase I, Longitudinal Root Variation with Velocity

The effects of M_q, X_u, Z_w are negligible

M_u and M_w are positive.

Arrows indicate direction of absolute value increase.

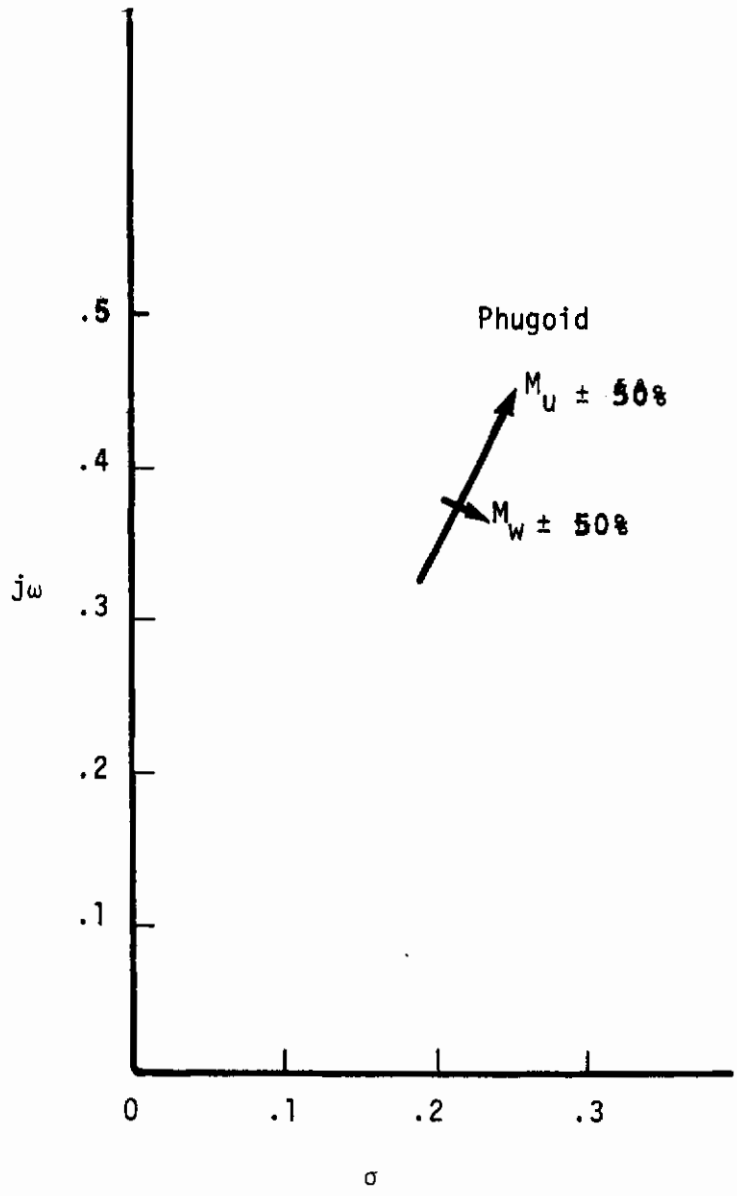

Figure 13. Phase I, Longitudinal Derivative Variation 1 Ft/Sec

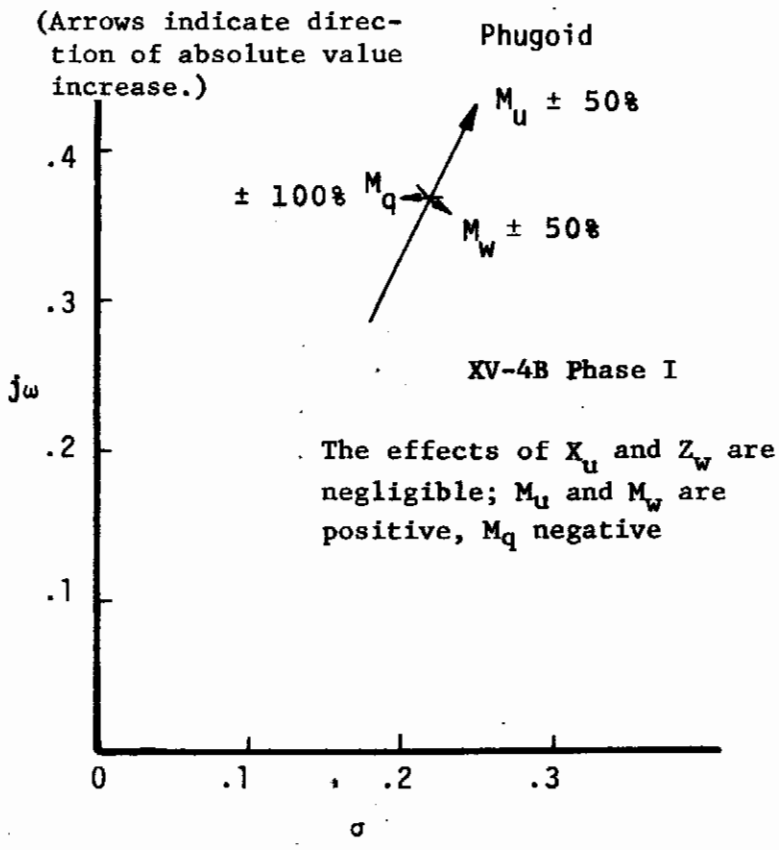

Figure 14. Phase I, Longitudinal Derivative Variation, 10 Knots

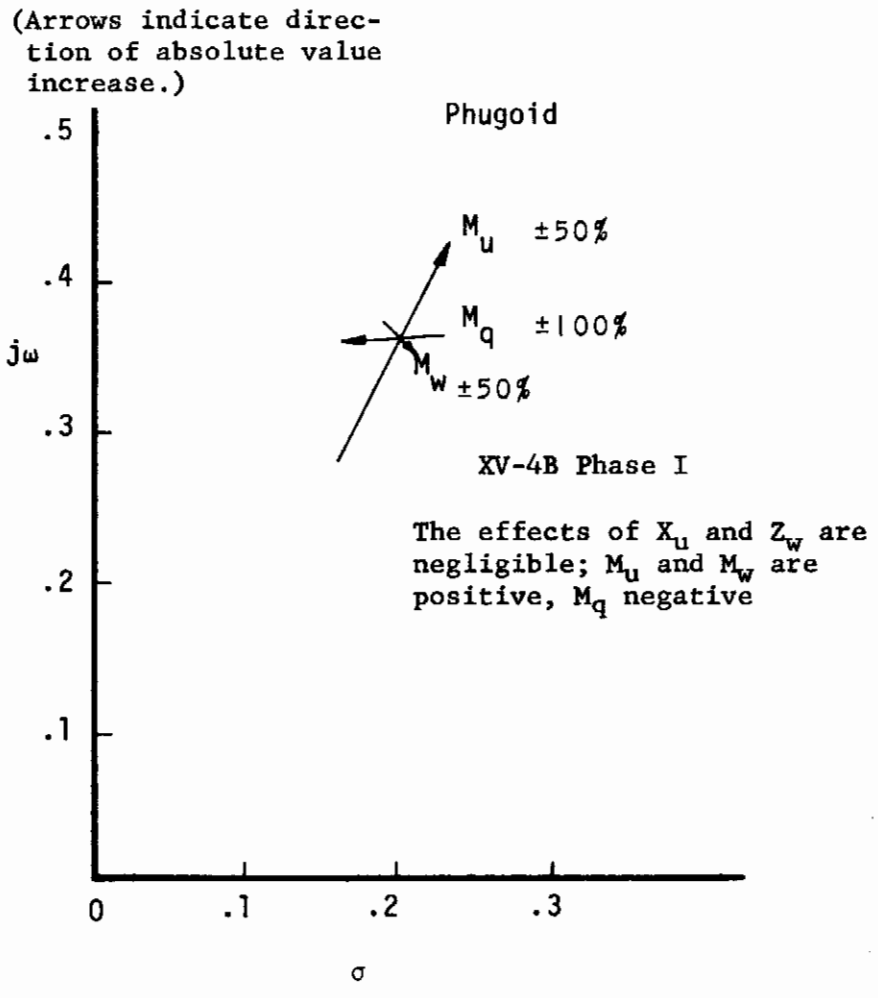

Figure 15. Phase I, Longitudinal Derivative Variation, 20 Knots

The effect of X_u and Z_w are negligible

M_u and M_w are positive, M_q negative

Arrows indicate direction of absolute value increase.

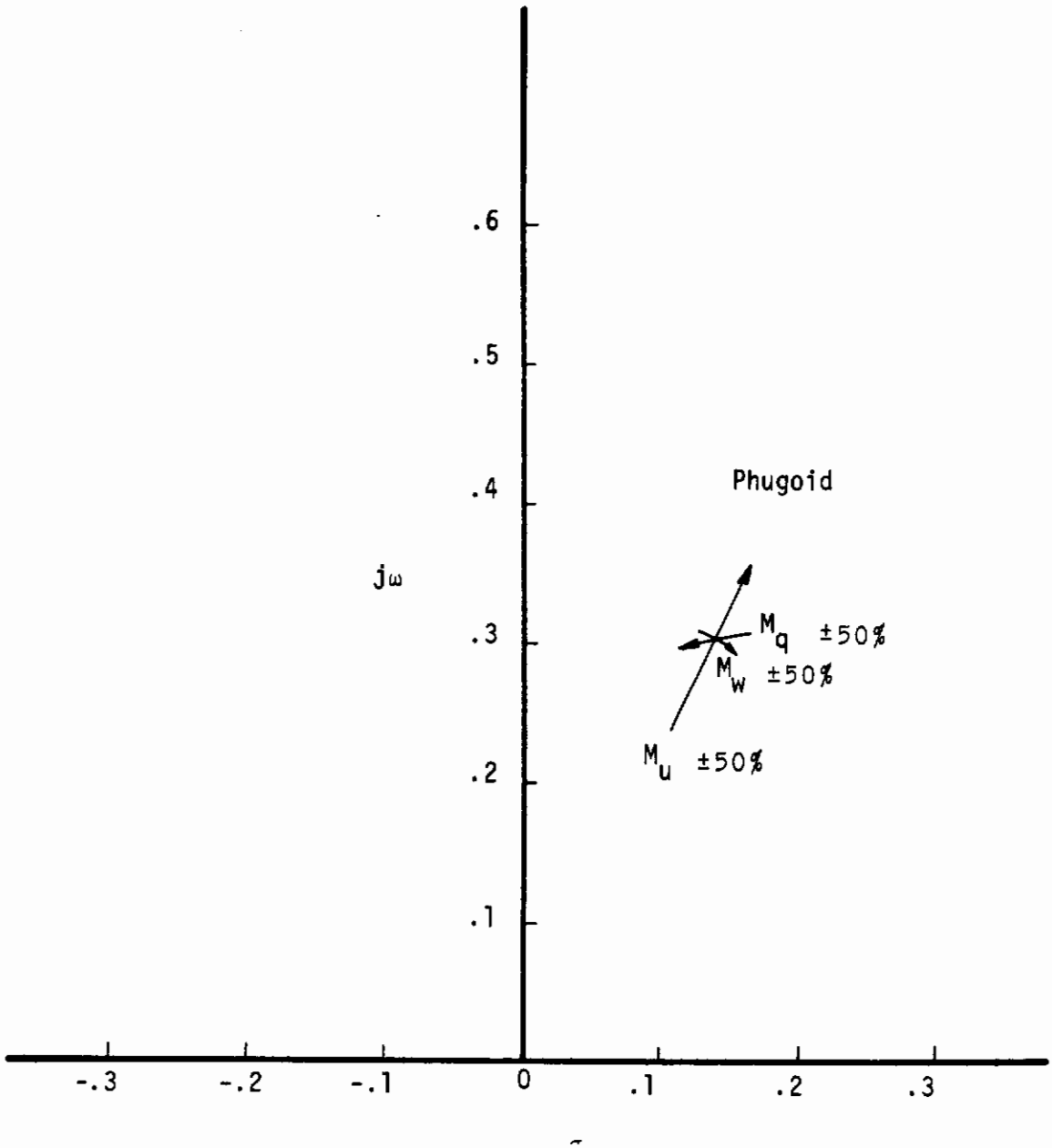

Figure 16. Phase I, Longitudinal Derivative Variation, 40 Knots

XV-4B Phase I

The effect of Z_w is negligible on the phugoid
The effect of X_w is negligible on all roots
Z_w, M_q and M_w are negative, M_u is positive

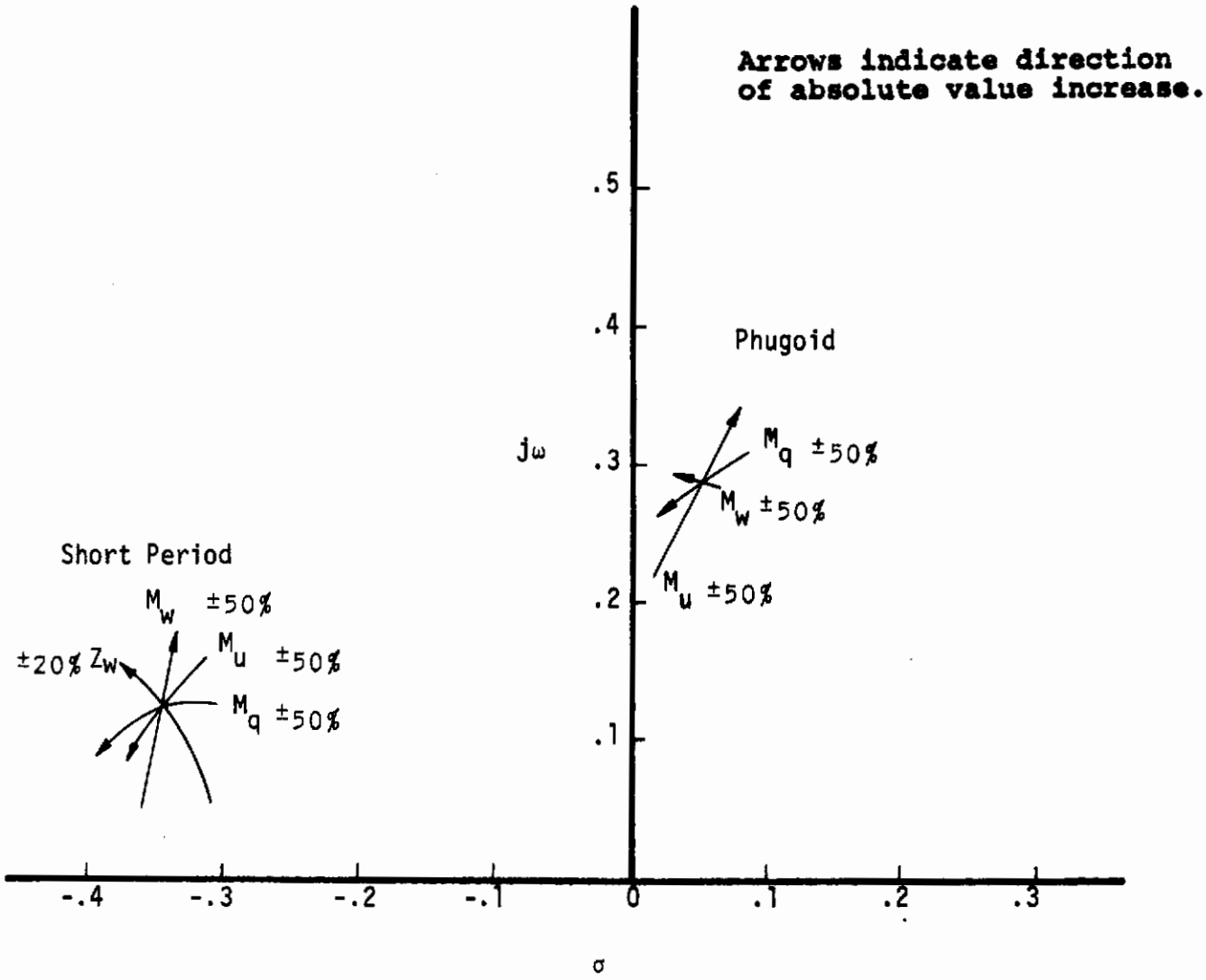

Figure 17. Phase I, Longitudinal Derivative Variation, 60 Knots

XV-4B Phase I

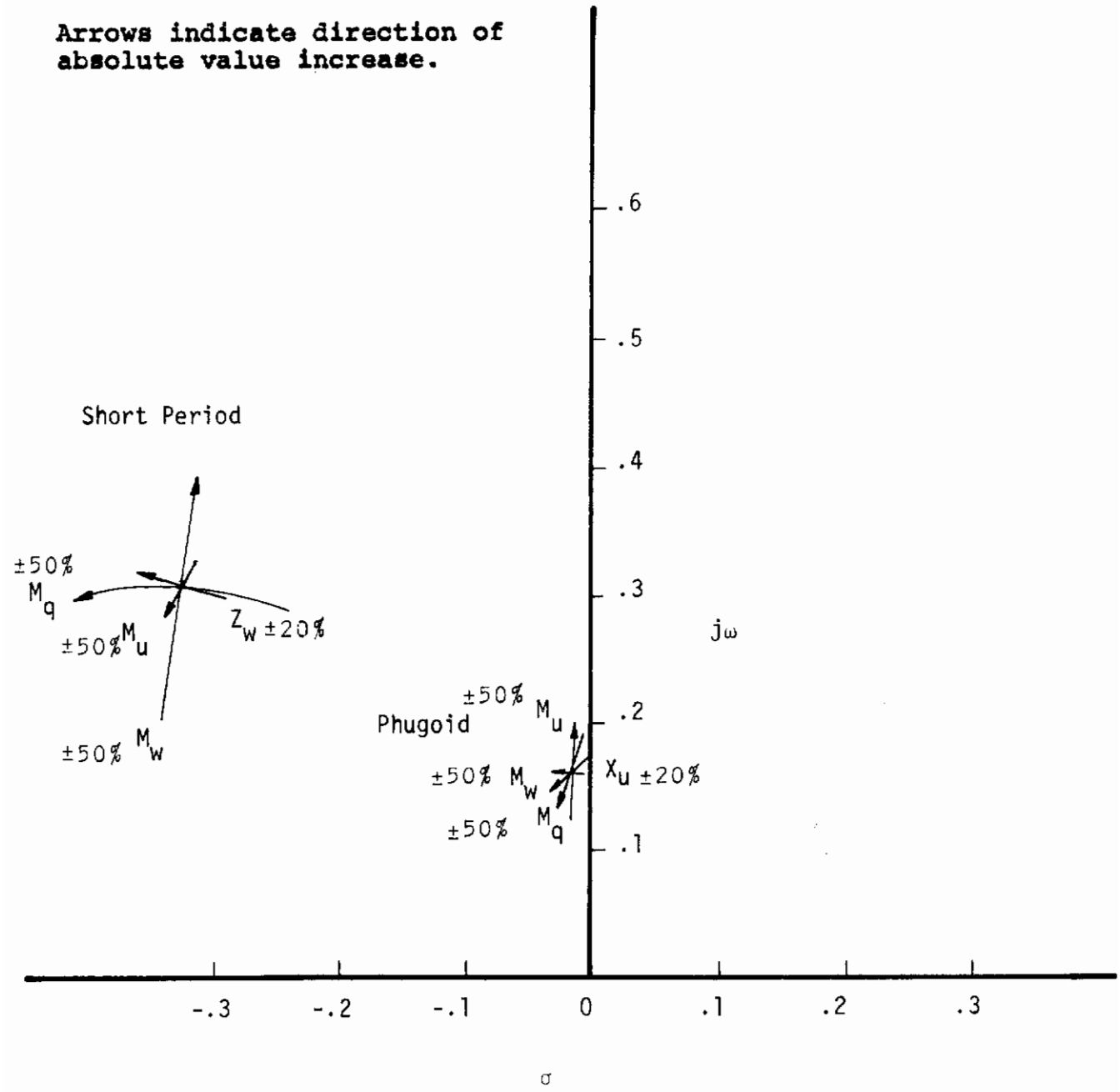

The effect of Z_w on the phugoid root is negligible
The effect of X_u on the short period root is negligible
M_u is positive, W_w, M_q, X_u, and Z_w are negative

Figure 18. Phase I, Longitudinal Derivative Variation, 70 Knots

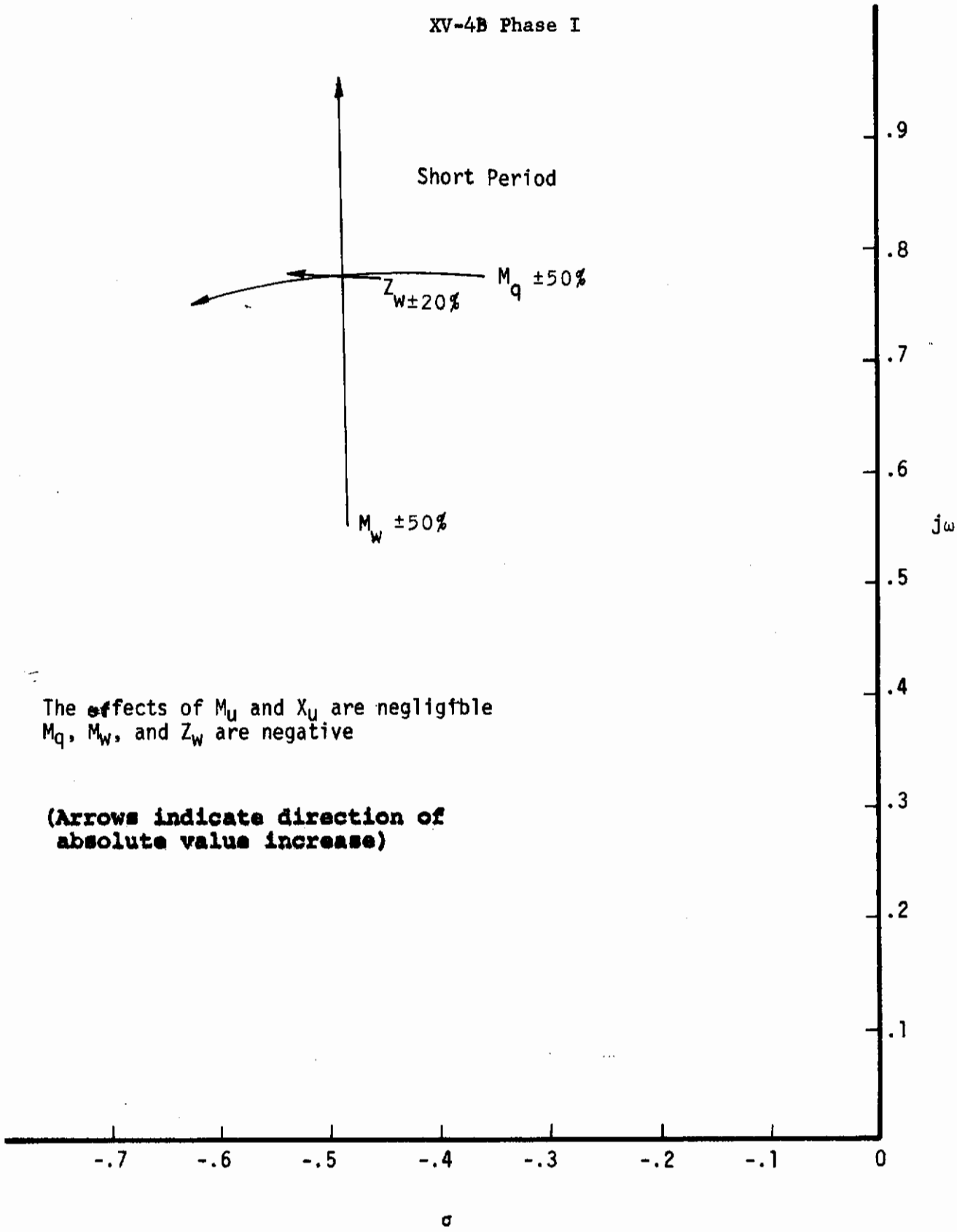

Figure 19. Phase I, Longitudinal Derivative Variation, 100 Knots

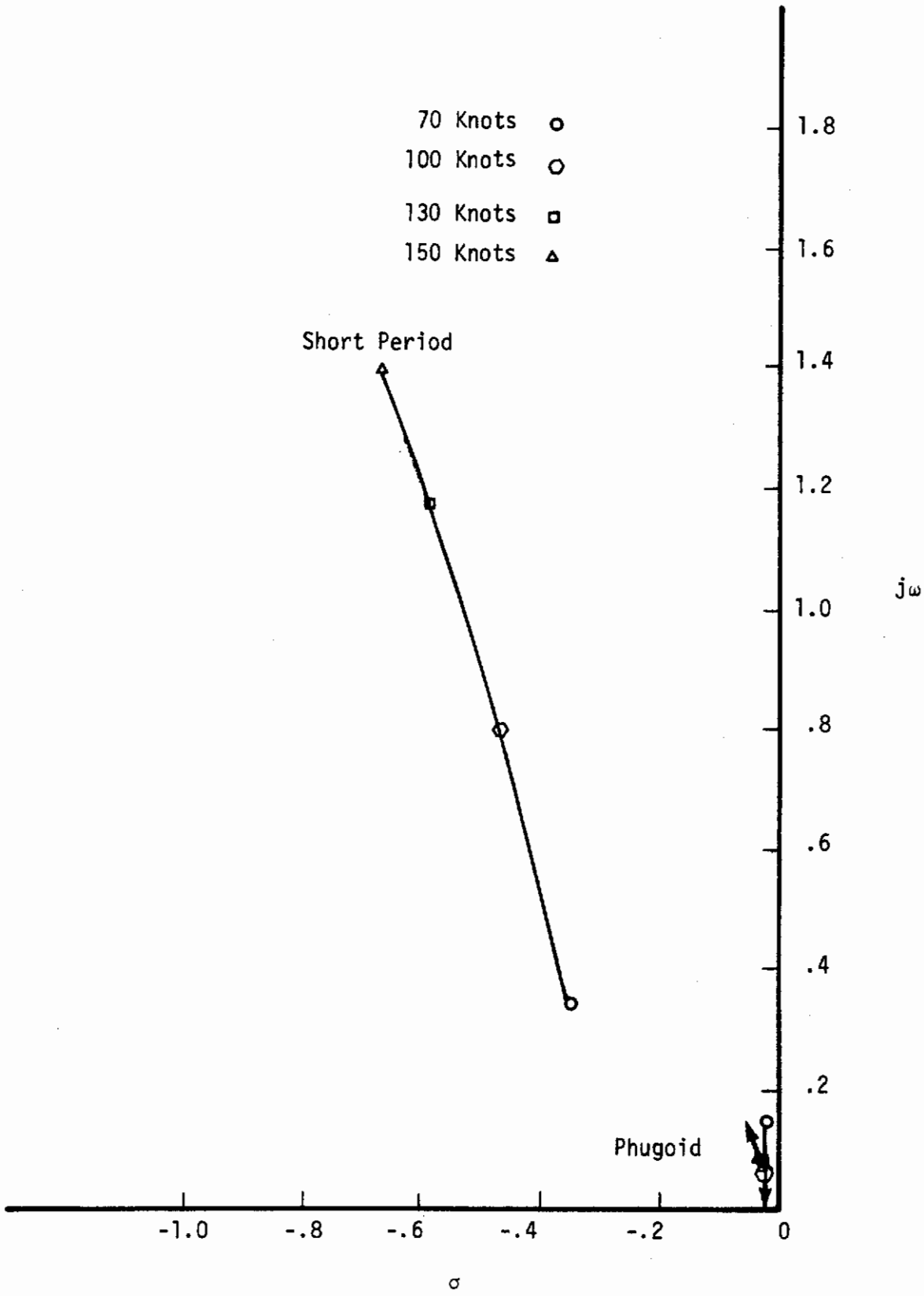

Figure 20. Phase II, Longitudinal Root Variation with Velocity

The effects of X_w are negligible
The effect of Z_w on the phugoid is negligible
M_u is positive
Z_w, M_q and M_w are negative

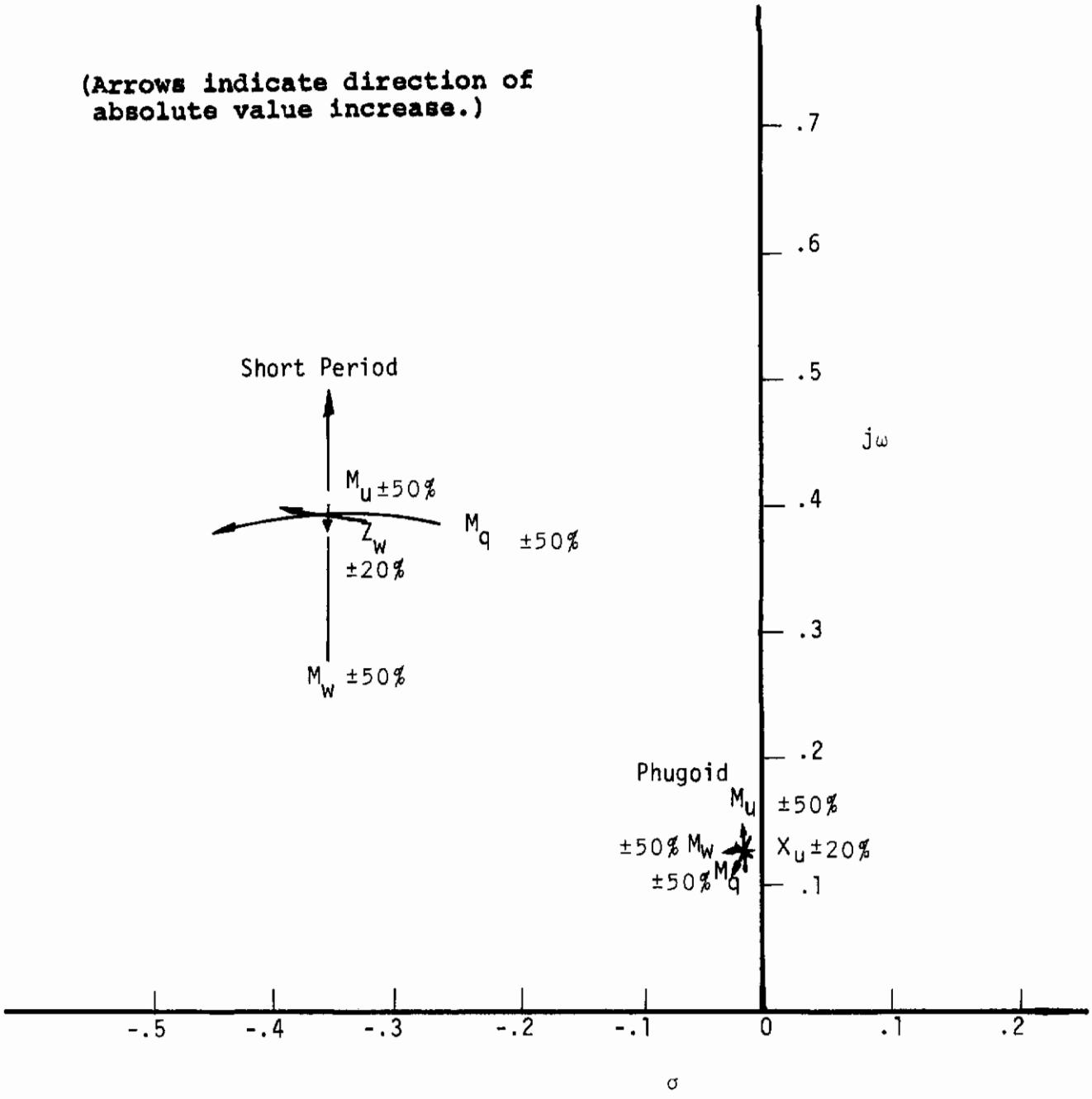

Figure 21. Phase II, Longitudinal Derivative Variation, 70 Knots

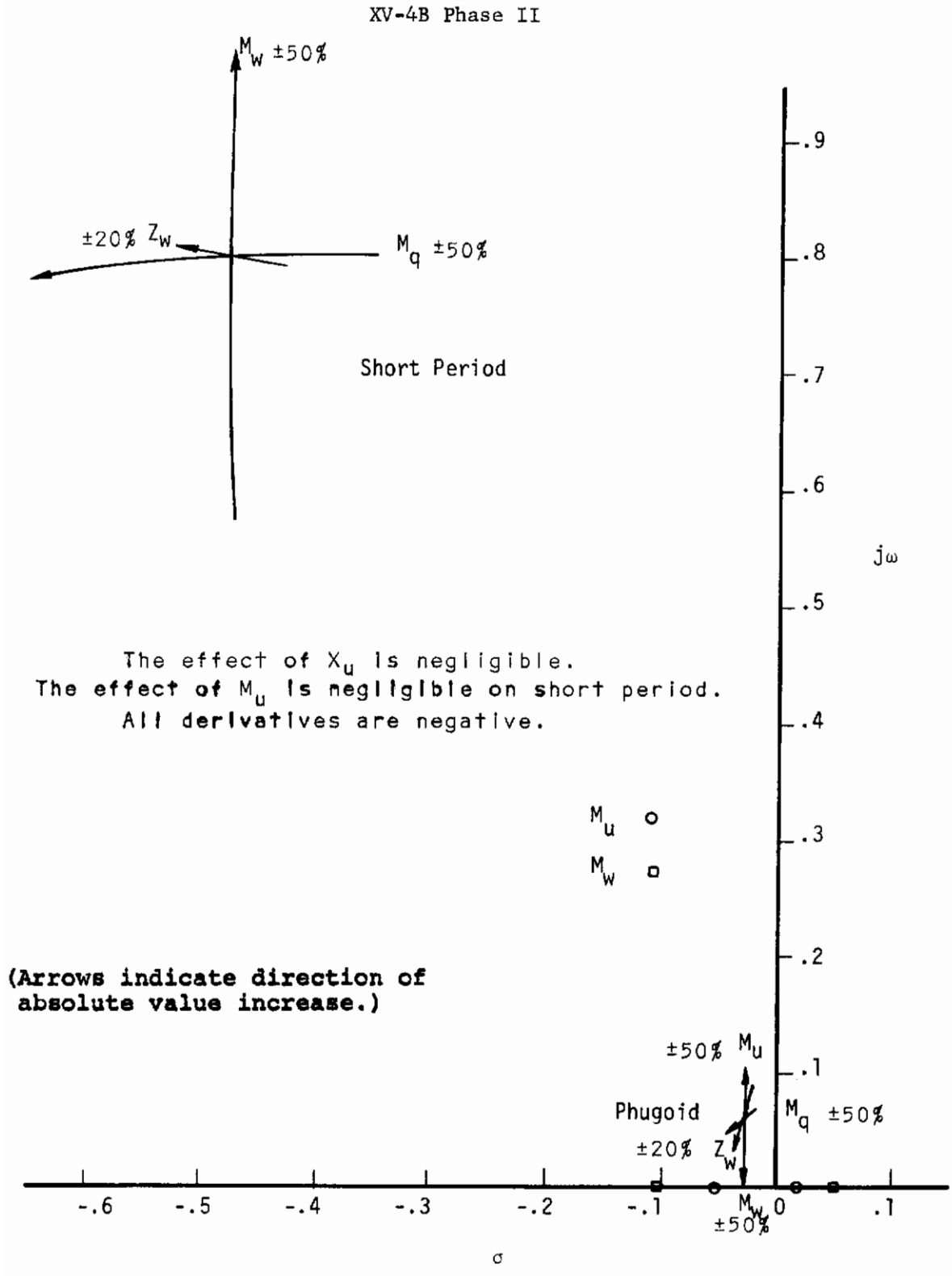

Figure 22. Phase II, Longitudinal Derivative Variation, 100 Knots

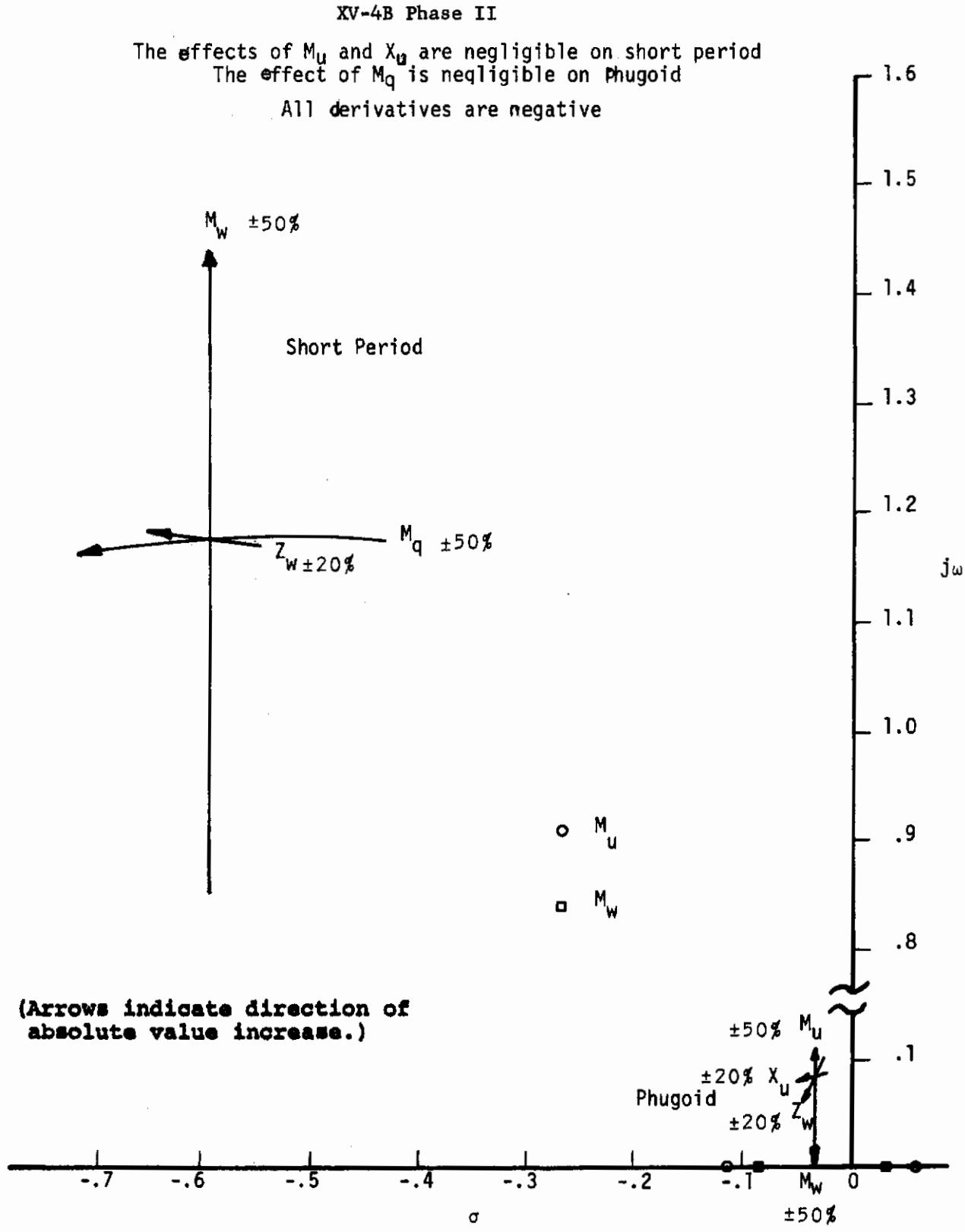

Figure 23. Phase II, Longitudinal Derivative Variation, 130 Knots

XV-4B Phase II

Effect of M_u and X_u negligible on short period

Effect of M_q negligible on phugoid

All derivatives are negative

(Arrows indicate direction of absolute value increase.)

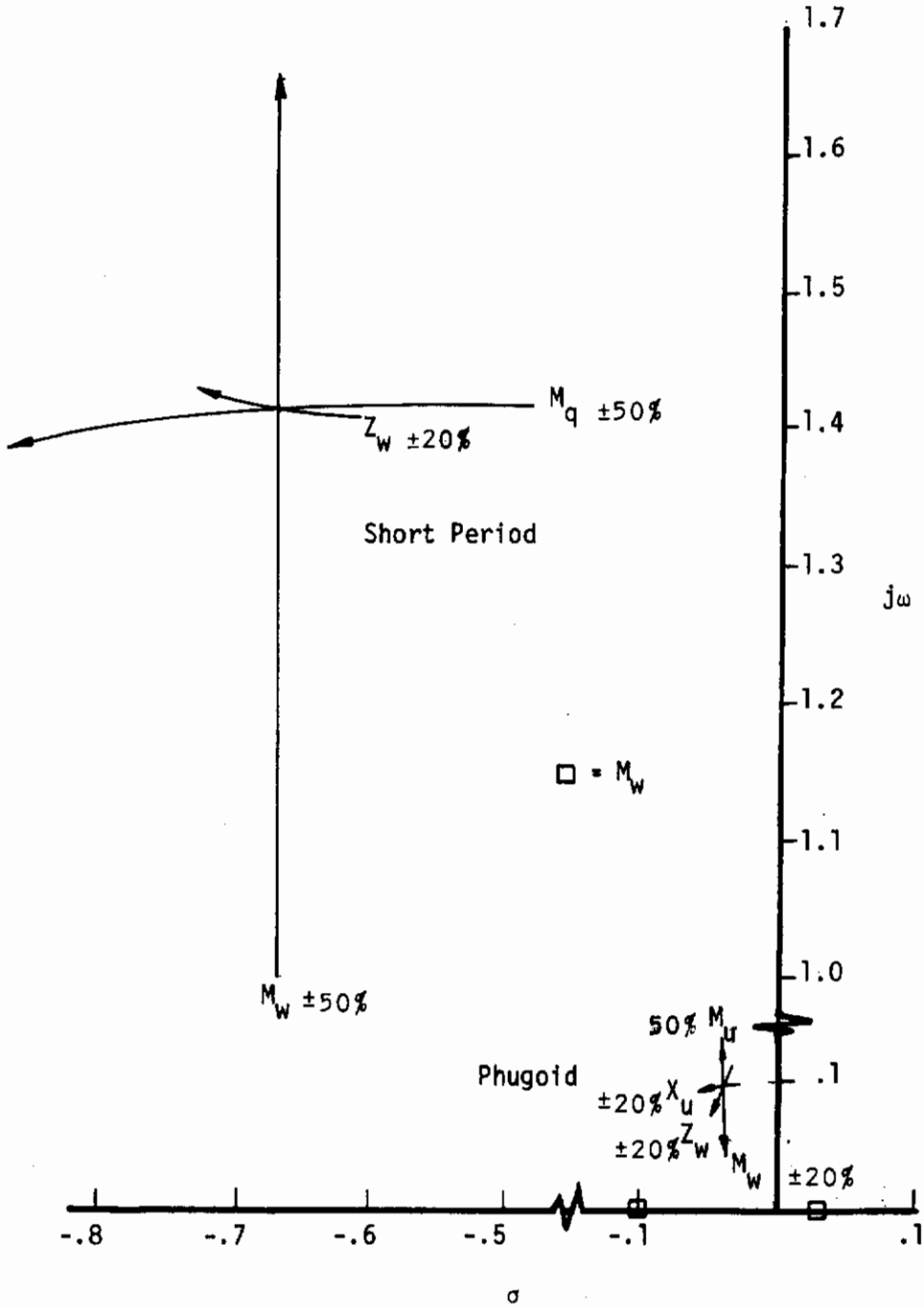

Figure 24. Phase II, Longitudinal Derivative Variation, 150 Knots

XV-4B Phase I

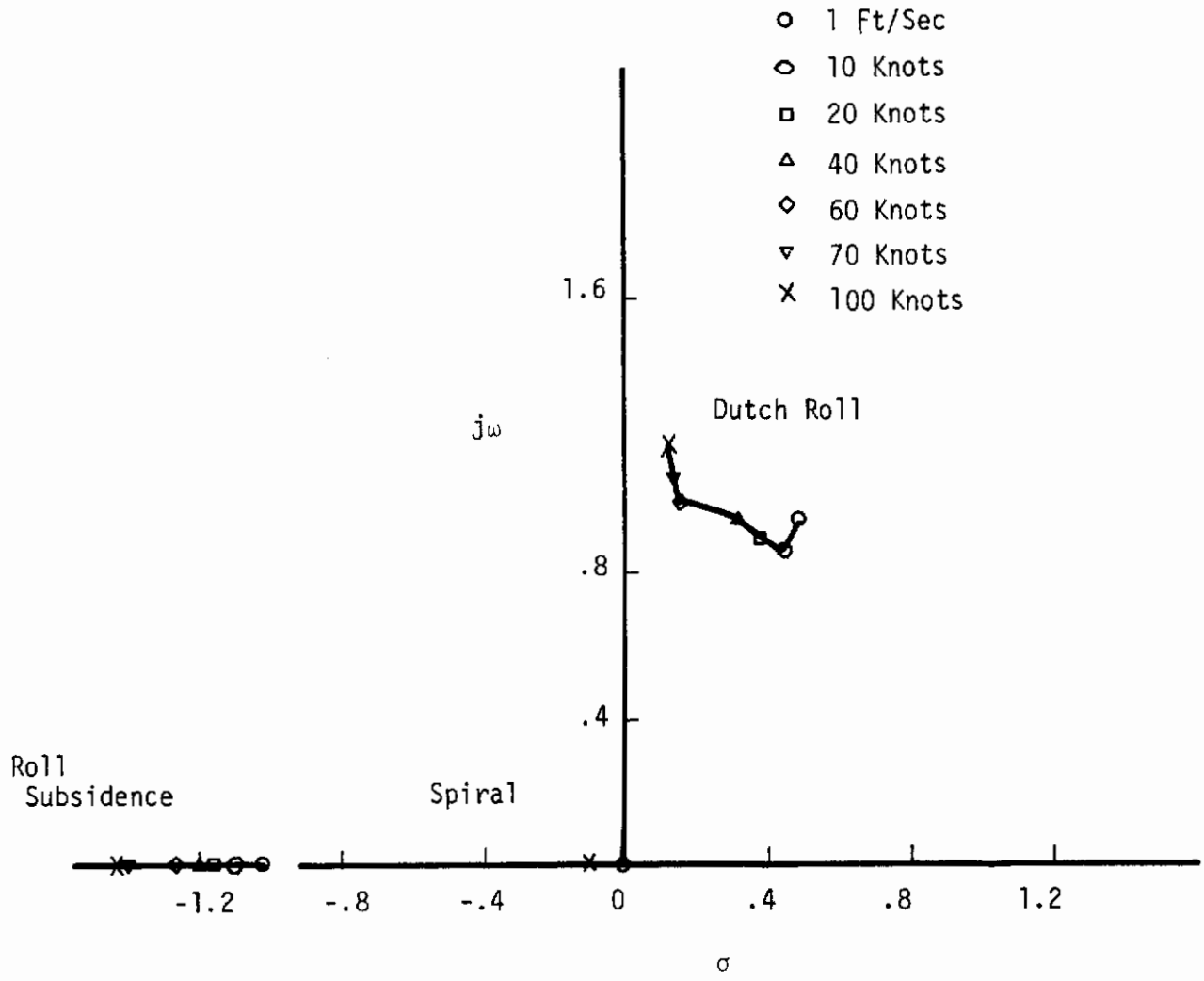

Figure 25. Phase I, Lateral Root Variation with Velocity

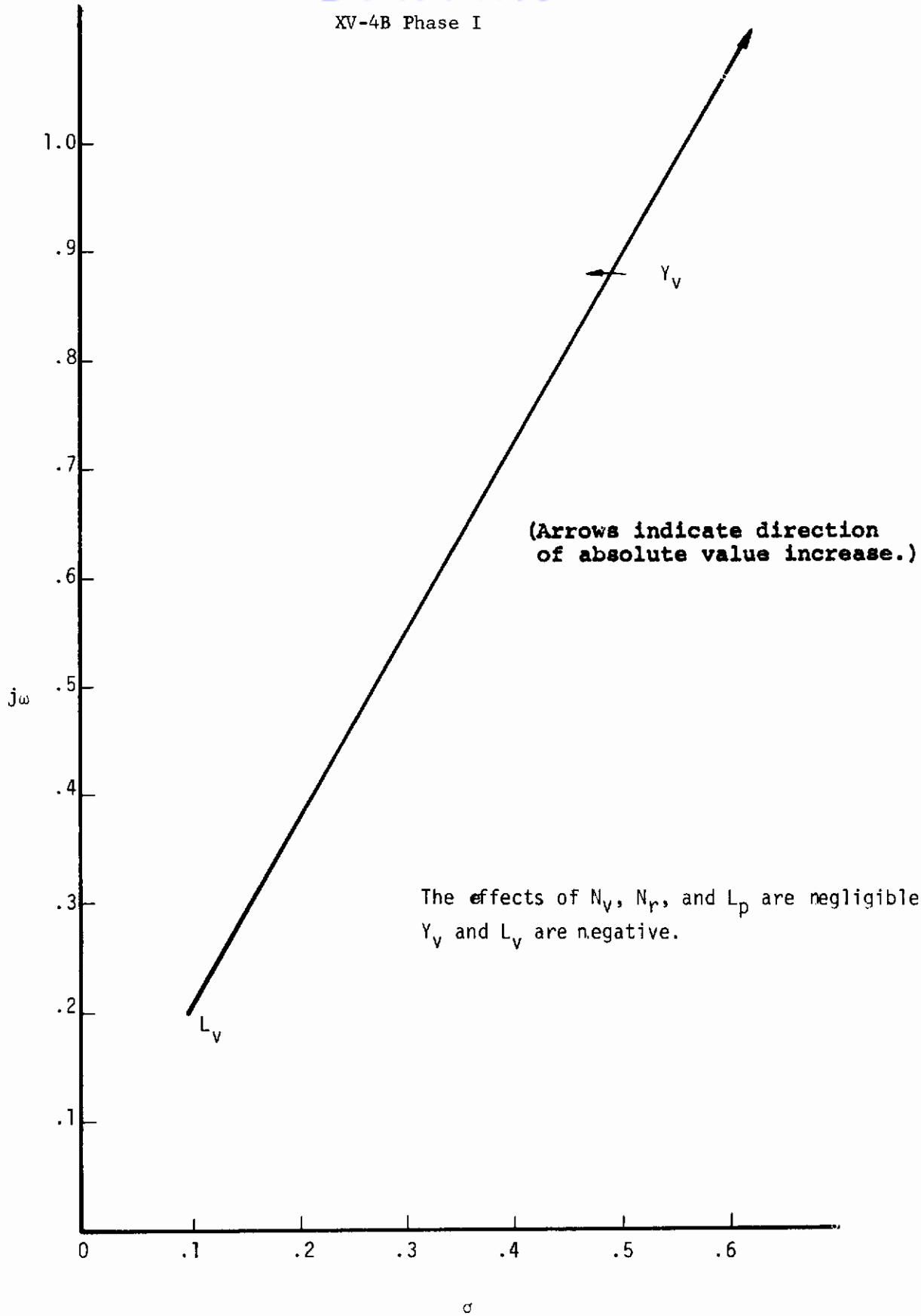

Figure 26. Phase I, Lateral Derivative Variation 1 Ft/Sec

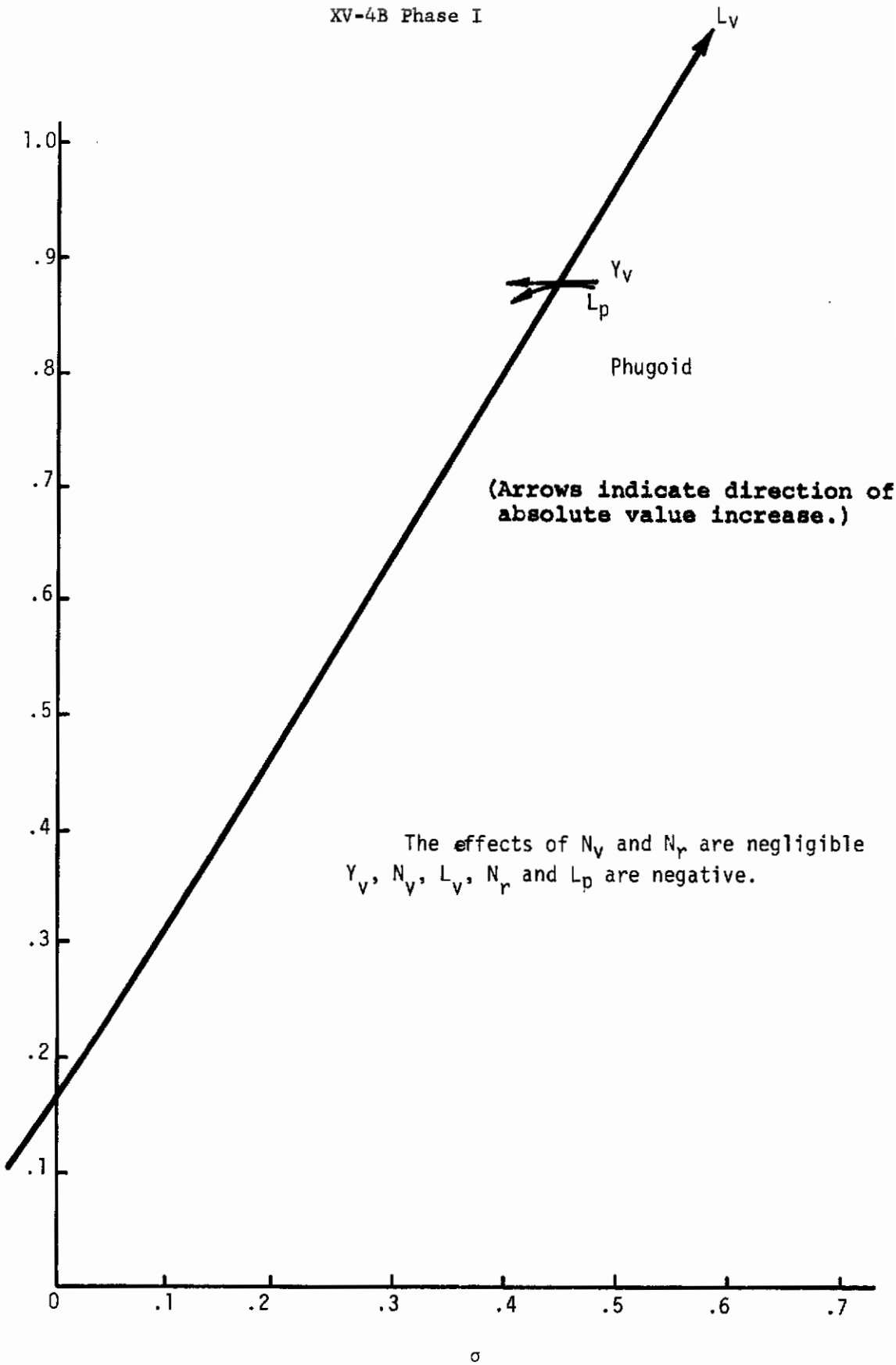

Figure 27. Phase I, Lateral Derivative Variation, 10 Knots

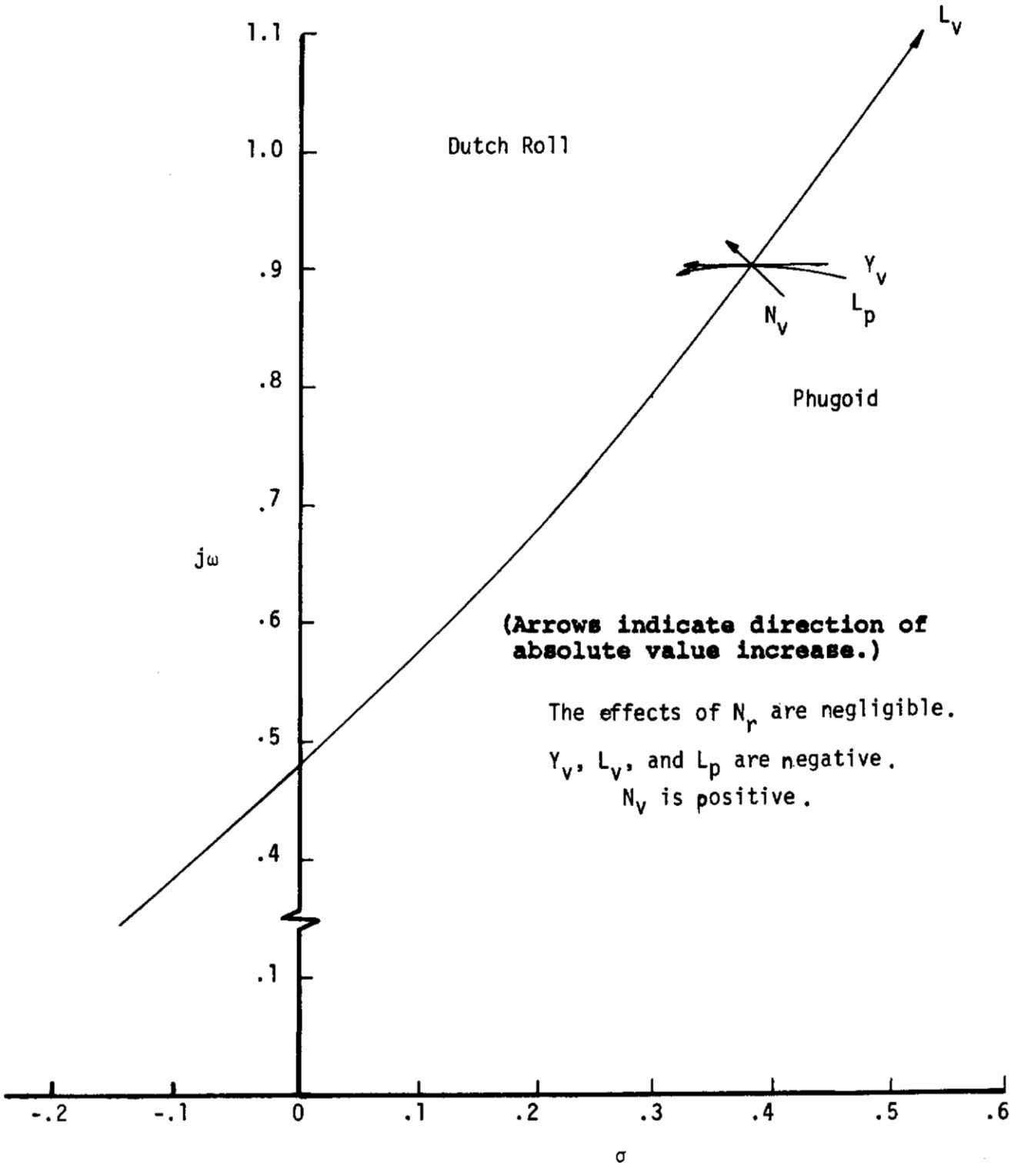

Figure 28. Phase I, Lateral Derivative Variation, 20 Knots

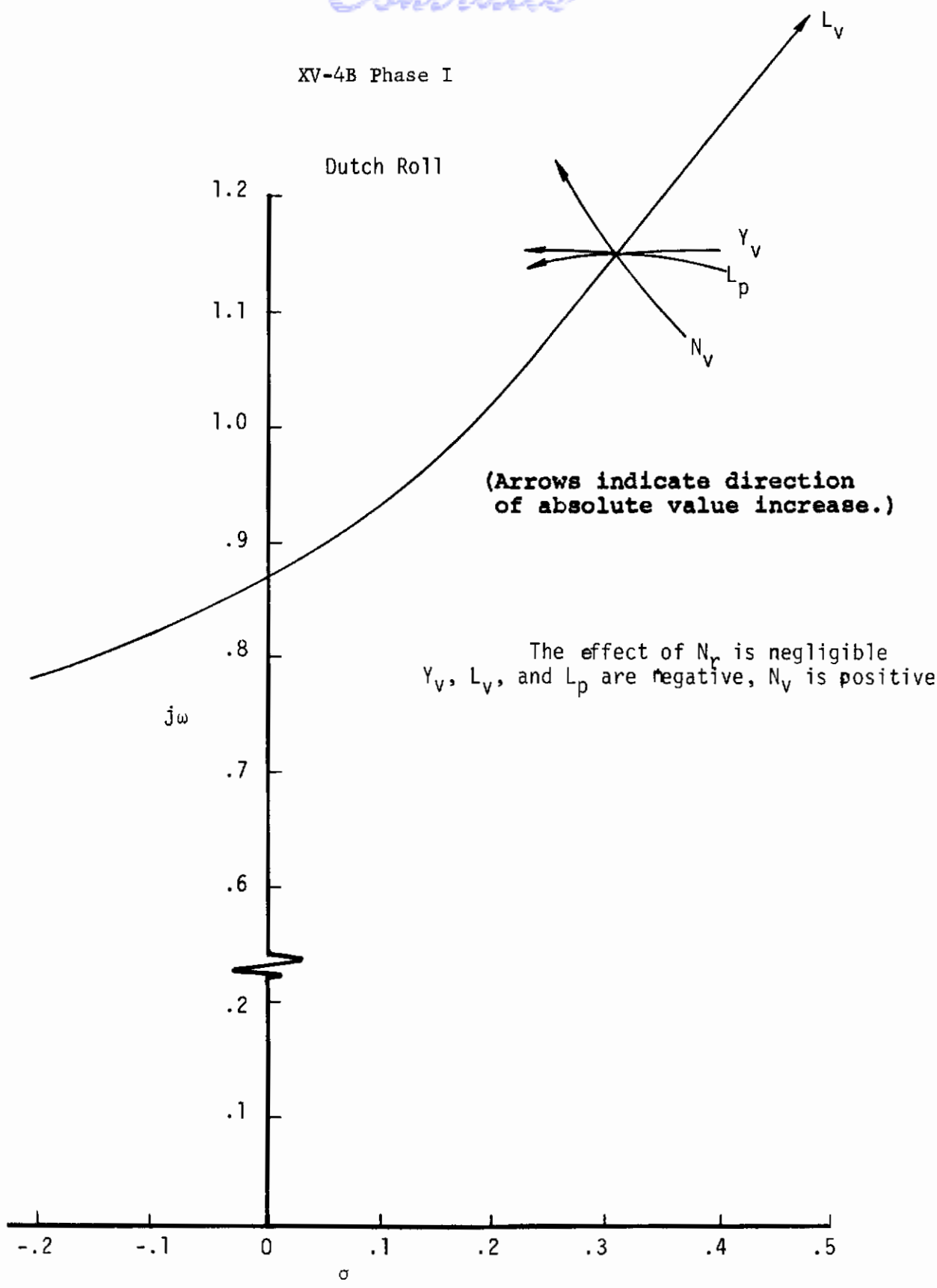

Figure 29. Phase I, Lateral Derivative Variation, 40 Knots

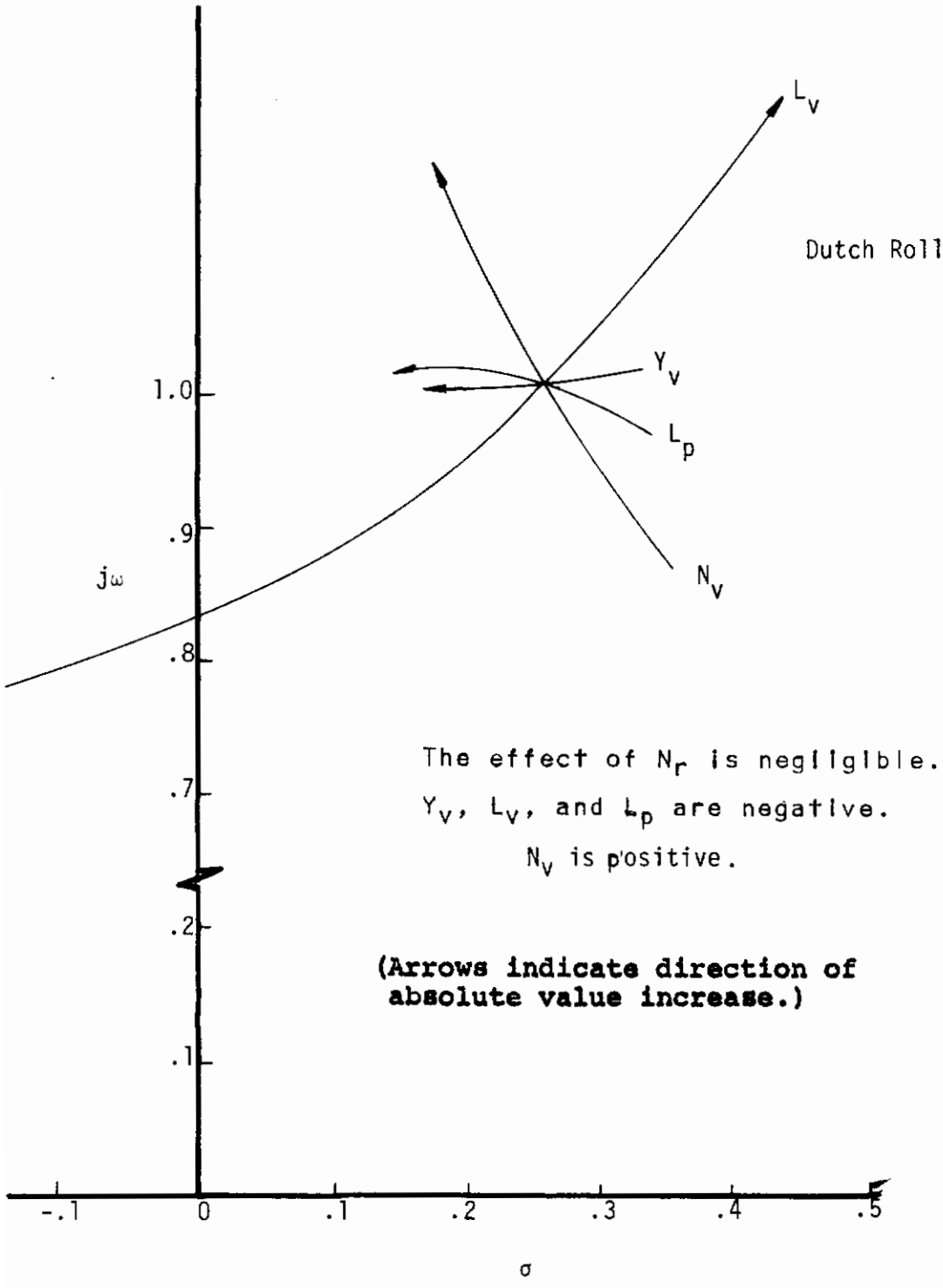

Figure 30. Phase I, Lateral Derivative Variation, 60 Knots

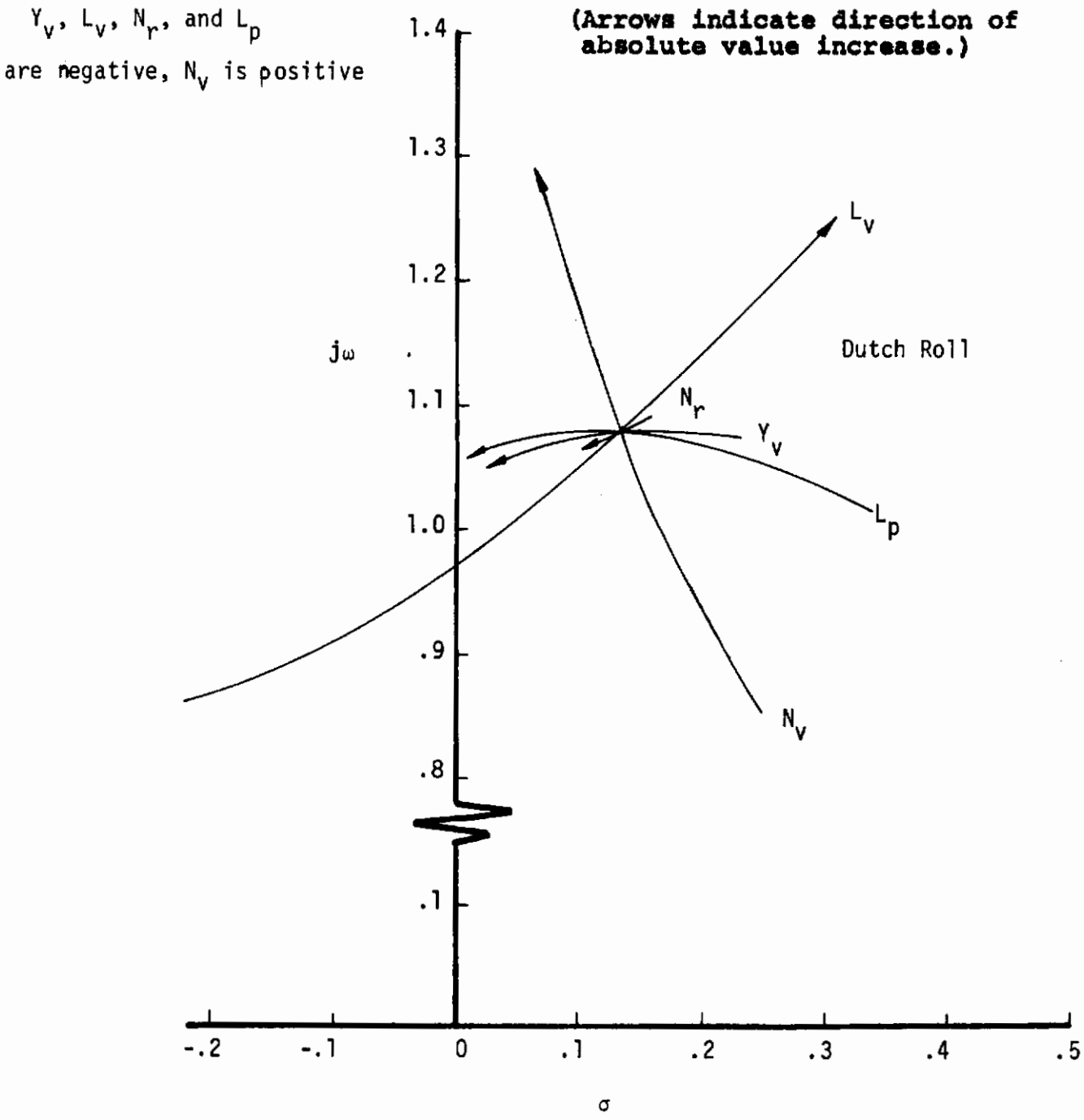

Figure 31. Phase I, Lateral Derivative Variation, 70 Knots

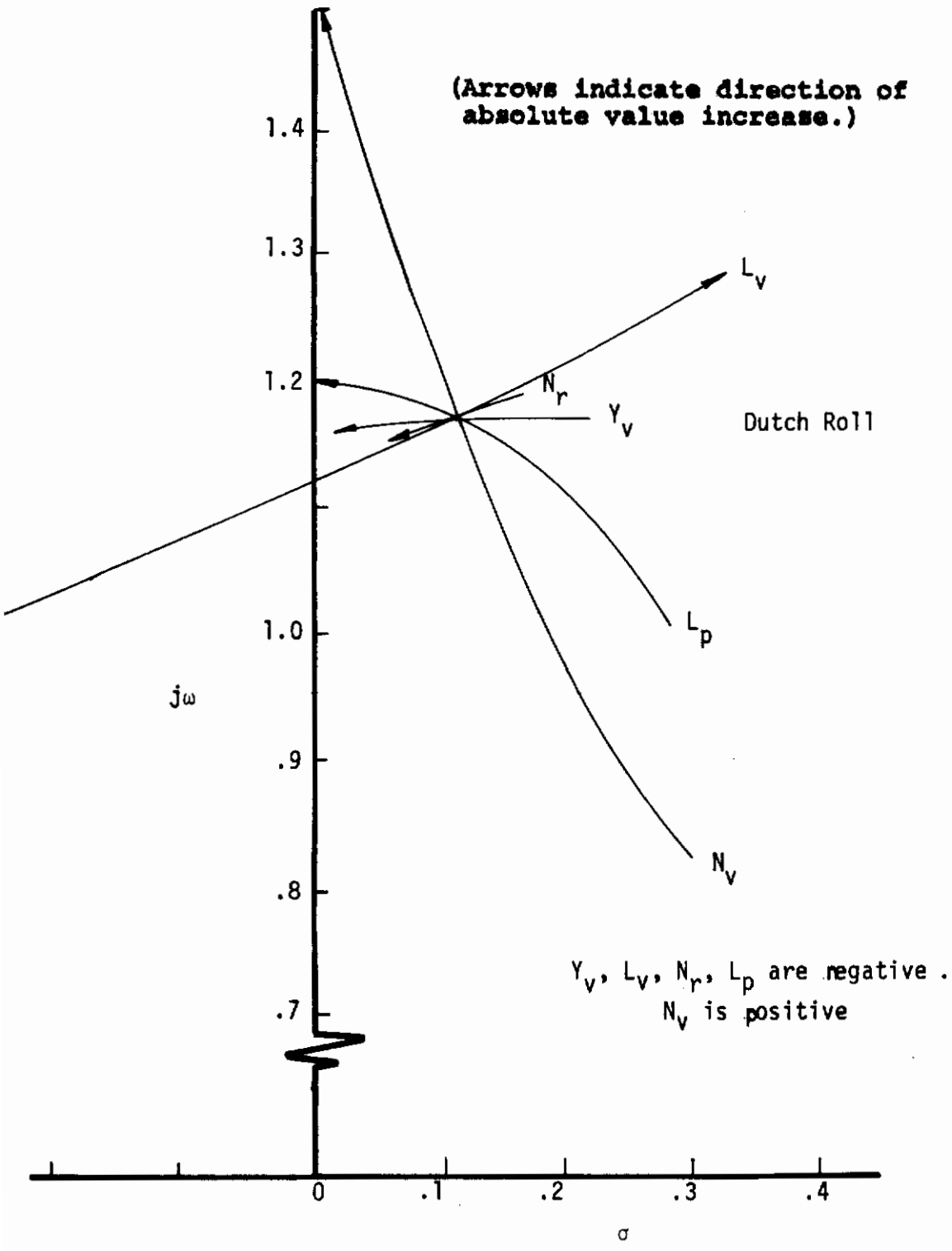

Figure 32. Phase I, Lateral Derivative Variation, 100 Knots

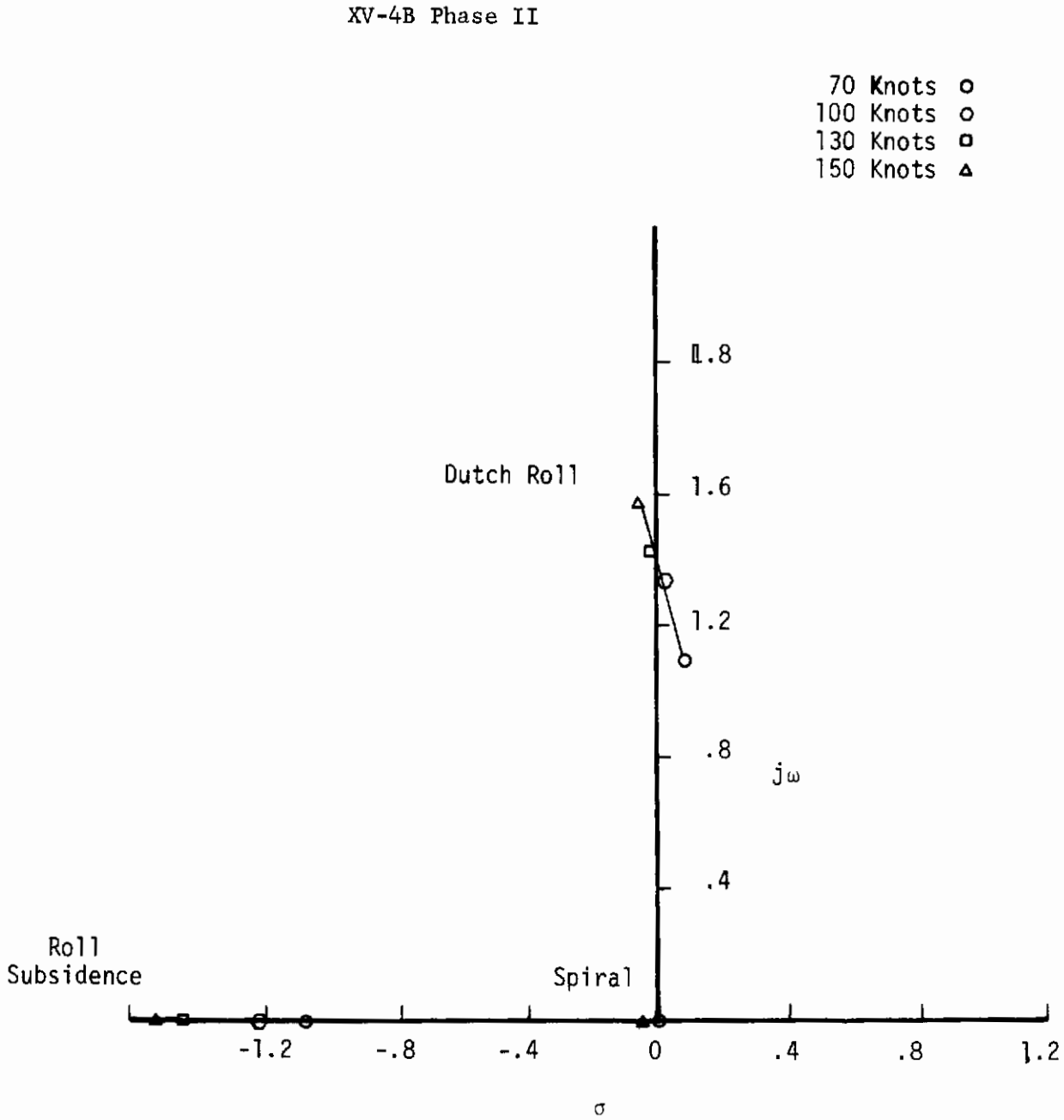

Figure 33. Phase II, Lateral Root Variation with Velocity

N_v is positive.
Y_v, L_v, N_r, and L_p are negative.

Dutch Roll

(Arrows indicate direction of absolute value increase.)

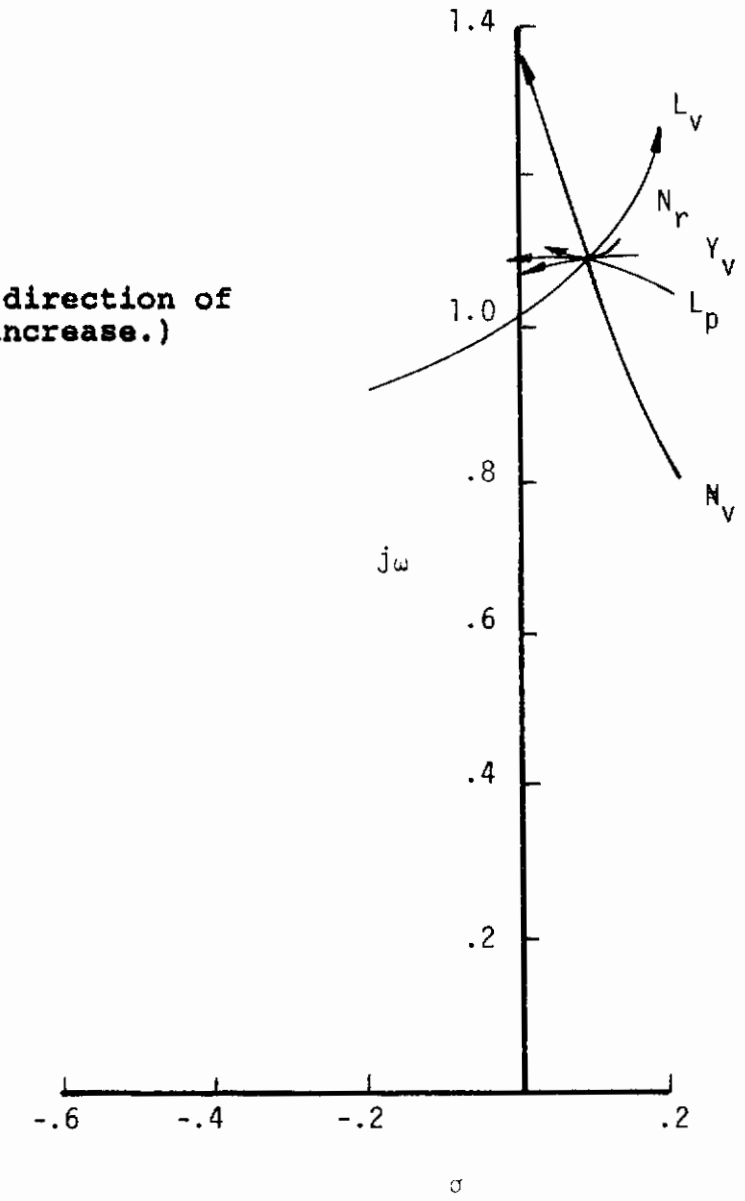

Figure 34. Phase II, Lateral Derivative Variation, 70 Knots

XV-4B Phase II

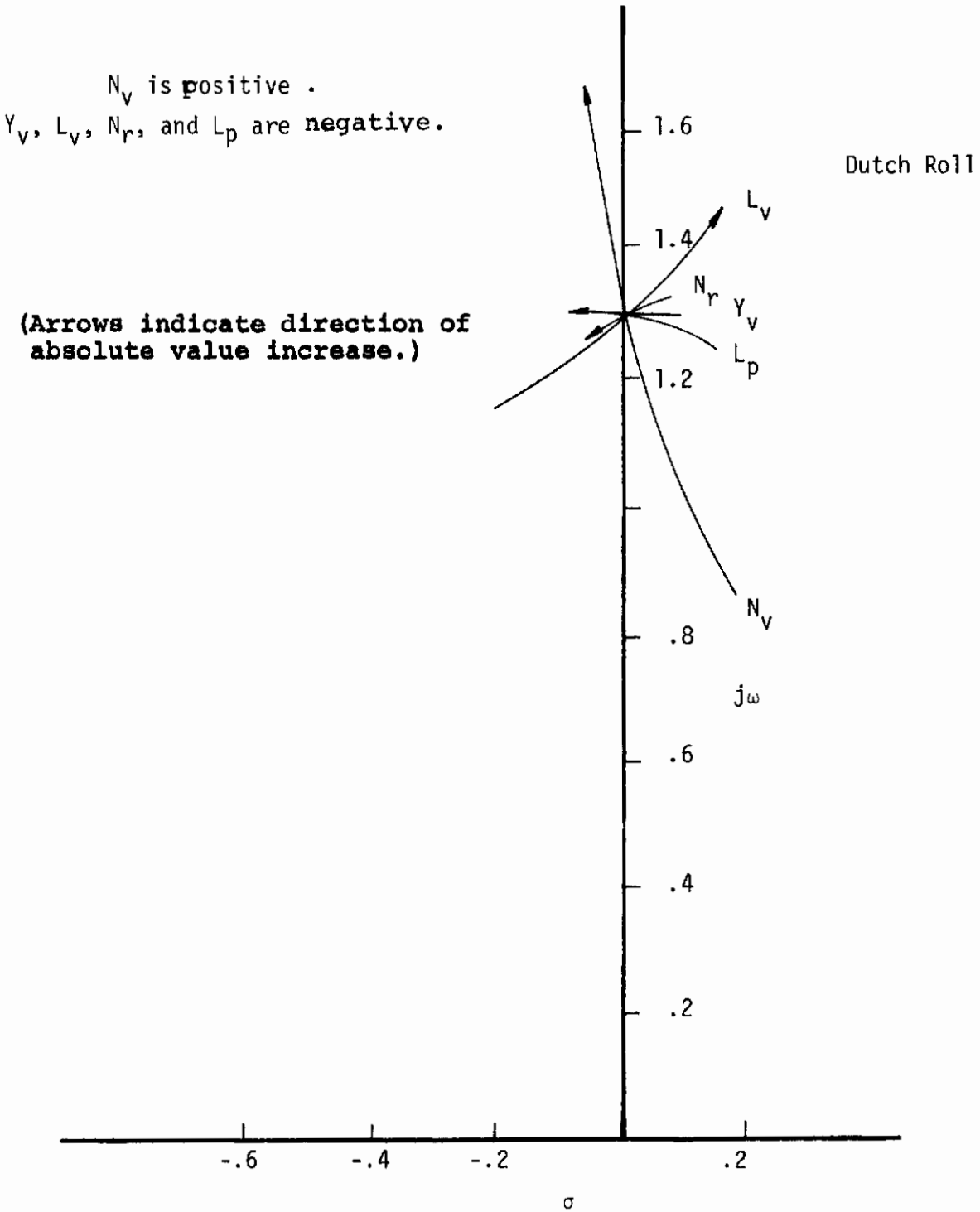

Figure 35. Phase II, Lateral Derivative Variation, 100 Knots

N_v is positive.

Y_v, L_v, N_r, and L_p are negative.

(Arrows indicate direction of absolute value increase.)

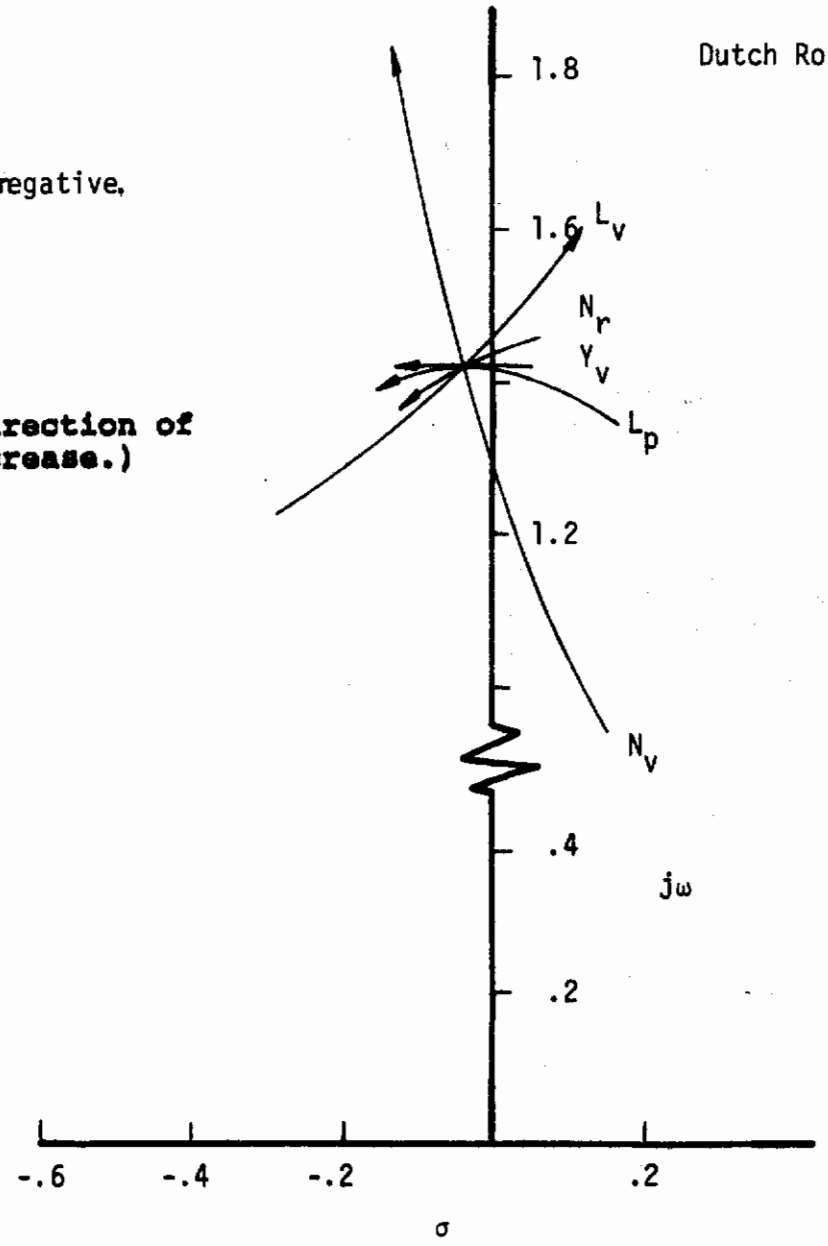

Figure 36. Phase II, Lateral Derivative Variation, 130 Knots

N_v is positive.

Y_v, L_v, N_r, and L_p are negative.

(Arrows indicate direction of absolute value increase.)

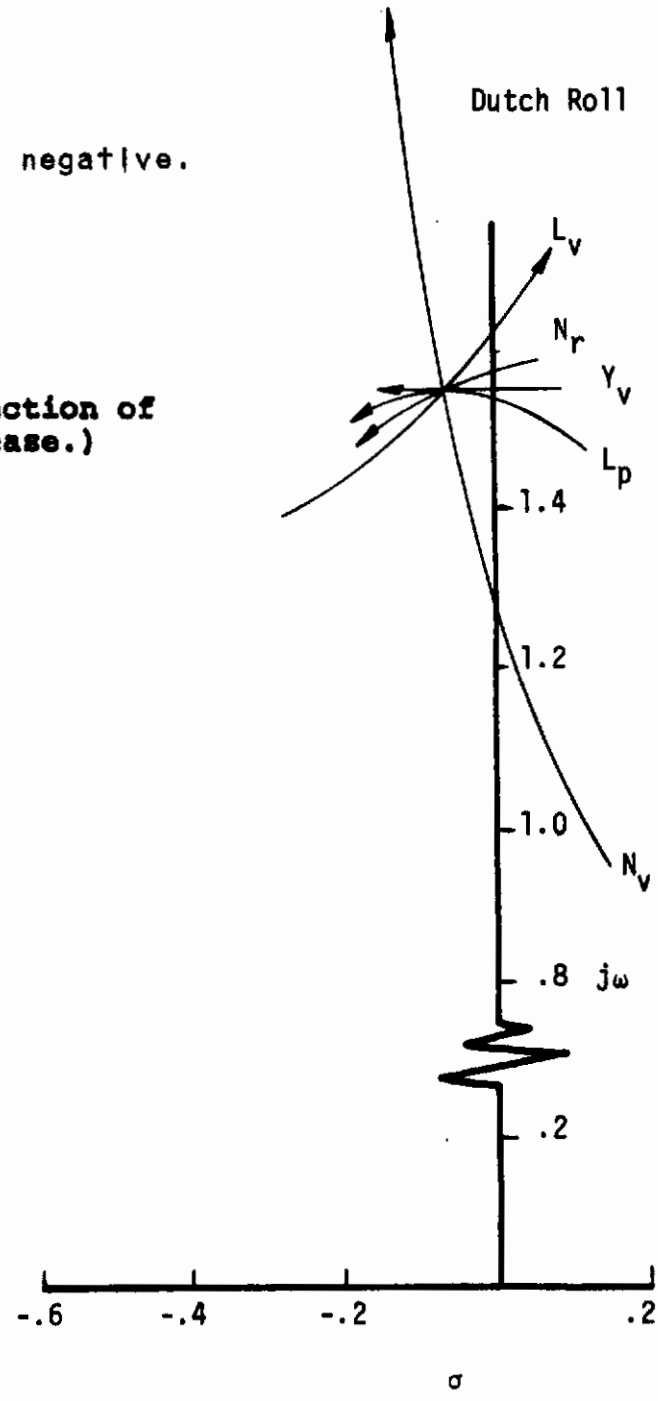

Figure 37. Phase II, Lateral Derivative Variation, 150 Knots

APPENDIX I

XV-4B Phase I (Hover and Near Hover) and Phase II (Transition) Basic Derivatives and Trim Conditions

Table I -- Stability Derivatives

XV-4B PHASE I DERIVATIVES

11,000 lb. - 1000 Ft.

VEL(Kts)	1 Ft/Sec	10.0	20.0	40.0	60.0	70.0	100.0
γ_v(DEG)	-9.45	-7.85	-6.7	-4.67	-2.06	-1.0	+6.1
Se(DEG)	-6.5	-4.84	-2.8	-0.26	+2.85	+4.3	+8.9
C-RPM(%)	93.3	93.6	93.3	93.5	93.8	93.5	91.25
L-RPM(%)	92.8	93.2	93.3	93.5	92.56	92.0	91.25
θ(DEG)	0.0	0.0	0.0	0.0	0.0	0.0	0.0
α(DEG)	0.0	0.0	0.0	0.0	0.0	0.0	0.0
δ_F(DEG)	40.0	40.0	40.0	40.0	40.0	40.0	40.0
Mw	+.00225	+.002	+.00175	+.0005	-.0005	-.001	-.0035
Zw	-.016	-.052	-.085	-.165	-.245	-.282	-.416
Xw	+.016	+.02	+.024	+.032	+.04	+.044	+.055
Mu	+.00253	+.00271	+.00279	+.00171	+.0014	+.00049	-.000873
Zu	+.0325	+.024	+.016	0.0	-.02	-.029	-.060
Xu	-.0285	-.032	-.0335	-.039	-.044	-.0475	-.056
Mq	-.005	-.019	-.100	-.175	-.295	-.350	-.540
Zq	0.0	0.0	0.0	0.0	0.0	0.0	0.0
Xq	0.0	0.0	0.0	0.0	0.0	0.0	0.0
N_{z_α}	+.000623	+.015	+.0715	+.30	+.645	+.873	+1.78
Mδe	-4.0	-4.41	-4.78	-5.26	-5.43	-5.4	-5.0
Zδe	0.0	-.183	-.46	-2.2	-5.50	-6.42	-12.8
Xδe	0.0	-.0005	-.003	-.0125	-.0275	-.0375	-.0705
Mγ_v	+1.925	+2.10	+2.25	+2.50	+2.6	+2.60	+2.7
Xγ_v	+29.6	+32.2	+34.3	+36.7	+29.9	+29,8	+25.2
Zγ_v	-3.0	-2.29	-1.7	0.0	+2.29	+4.58	+9.16
Mδ_{TA}	-.000012	-.0000107	-.0000103	-.00000756	+.0000026	+.000003	+.000013
Xδ_{TA}	0.0	+.0000319	+.0000816	+.00159	+.000149	+.000014	+.000057
Zδ_{TA}	-.0028	-.00277	-.00275	-.00265	-.00266	-.0026	-.0257
Nv	-.002	-.000436	+.00262	+.00415	+.00495	+.00535	+.00655
Lv	-.032	-.0334	-.0345	-.0375	-.04	-.041	-.045
Yv	-.021	-.125	-.175	-.255	-.240	-.240	-.255
Nr	-.01	-.026	-.034	-.090	-.124	-.15	-.230
Lr	0.0	+.021	+.060	+.230	+.344	+.425	+.640
Yr	0.0	+.055	+.11	+.22	+.33	+.385	+.55
Yp	0.0	-.025	-.05	-.095	-.14	-.165	-.235
Lp	-.02	-.100	-.220	-.320	-.50	-.80	-.86
Np	0.0	+.004	+.008	+.017	+.0255	+.0298	+.042
Nδr	-10.05	-10.25	-10.5	-11.10	-11.10	-11.10	-11.35
Lδr	-2.175	-2.10	-2.10	-1.65	-1.70	-1.655	-1.00
Yδr	+19.5	+21.4	+23.0	+24.7	+25.8	+24.1	+27.7
Nδa	+.545	-.54	-.542	-.537	-0.37	-.4775	-.480
Lδa	-10.6	-10.8	-11.2	-11.35	-11.9	-12.1	-13.35
Yδa	0.0	0.0	0.0	0.0	0.0	0.0	0.0

Table II -- Stability Derivatives

XV-4B PHASE II DERIVATIVES

11,000 lb, - 1000 Ft.

VEL(Kts)	70	100	130	150
γ_v(DEG)	+2.57	+3.6	+4.0	+4.2
Se(DEG)	-3.80	-2.25	-.45	+1.2
C-RPM(%)	76.5	86.2	90,6	91.7
L-RPM(%)	99.76	93.95	87.1	73.0
θ(DEG)	5.0	5.0	5.0	5.0
α(DEG)	5.0	5.0	5.0	5.0
δ_F(DEG)	40.0	40.0	40.0	40.0
Mw	-.0014	-.00375	-.00625	-.00785
Zw	-.312	-.420	-.496	-.56
Xw	+.064	+.071	+.077	+.082
Mu	+.0001745	-.00074	-.00129	-.0017
Zu	-.062	-.118	-.174	-.214
Xu	-.060	-.068	-.076	-.082
Mq	-.370	-.516	-.680	-.77
Zq	0	0	0	0
Xq	0	0	0	0
N_{z_α}	+.867	+1.78	+3.02	+4.00
Mδe	-5.43	-6.62	-7.70	-7.61
Zδe	-6.43	-10.5	-14.65	-13.75
Xδe	-.03	-.07	-.125	-.177
Mγv	+2.3	+2.2	+1.8	+1.2
Xγv	+23.0	+16.0	+7.5	+2.29
Zγv	6.88	11.45	9.16	+2.29
$M_{\delta_{TL}}$	-.0000245	+.00001215	+.0000328	+.000101
$X_{\delta_{TL}}$	0	-.0000575	-.0001455	-.000384
$Z_{\delta_{TL}}$	-.0025	-.0025	-.00244	-.00193
$M_{\delta_{TC}}$	-.0000145	-.0000356	-.0000256	-.0000094
$X_{\delta_{TC}}$	+.00281	+.00256	+.00286	+.00297
$Z_{\delta_{TC}}$	0	0	0	0
Nv	+.0063	+.00733	+.0065	+.0075
Lv	-.0268	-.0325	+.0446	-.0478
Yv	-.192	-.188	-.208	-.16
Nr	-.152	-.22	-.31	-.36
Lr	+.56	+0.8	+.96	+1.1
Yr	+.13	+.3	+.459	+.58
Nδr	-11.25	-11.4	-11.8	-12.0
Lδr	-0.5	+.82	+3.0	+5.00
Yδr	+20.8	+22.8	+24.2	+25.6
Nδa	-0.4	-.304	-.156	-.052
Lδa	-12.28	-13.1	-14.55	-15.15
Yδa	0	0	0	0
Yp	-.165	-.267	-.348	-.40
Lp	-0.6	-.84	-1.1	-1.24
Np	0	-.008	-.011	-.014

APPENDIX II

Tables of Derivative and Total Root Variation for the XV-4B in the Phase I and Phase II Configurations

XV-4B PHASE I

1 FT/SEC

DERIVATIVE	VALUE	% CHANGE	ROOTS 1 & 2		ROOTS 3 & 4	
			Real	Imag.	Real	Imag.
M_u	+ .001625	-50	+ .1898	+ .3228	- .0560	+ 0
			+ .1898	- .3228	- .3732	+ 0
	+ .001897	-25	+ .1979	+ .3397	- .0503	+ 0
			+ .1979	- .3397	- .3951	+ 0
	+ .00253	0	+ .2150	+ .3740	- .0417	+ 0
			+ .2150	- .3740	- .4378	+ 0
	+ .003163	+25	+ .2300	+ .4030	- .0366	+ 0
			+ .2300	- .4030	- .4730	+ 0
	+ .003795	+50	+ .2435	+ .4283	- .0331	+ 0
			+ .2435	- .4283	- .5033	+ 0
M_q	- .0000	-100	+ .2167	+ .3740	- .0417	+ 0
			+ .2167	- .3740	- .4361	+ 0
	- .0025	-50	+ .2158	+ .3740	- .0417	+ 0
			+ .2158	- .2740	- .4369	+ 0
	- .0050	0	+ .2150	+ .3740	- .0417	+ 0
			+ .2150	- .3740	- .4378	+ 0
	- .0075	+50	+ .2142	+ .3740	- .0417	+ 0
			+ .2142	- .3740	- .4386	+ 0
	- .0100	+100	+ .2133	+ .3740	- .0417	+ 0
			+ .2133	- .3740	- .4395	+ 0

XV-4B PHASE I

1 FT/SEC

DERIVATIVE	VALUE	% CHANGE	ROOTS 1 & 2	ROOTS 3 & 4
			Real Imag.	Real Imag.
M_w	+ .0010	-50	+ .2105 + .3743	- .0289 + 0
			+ .2105 - .3743	- .4416 + 0
	+ .0015	-25	+ .2127 + .3741	- .0353 + 0
			+ .2127 - .3741	- .4397 + 0
	+ .0020	0	+ .2150 + .3740	- .0417 + 0
			+ .2150 - .3740	- .4378 + 0
	+ .0025	+25	+ .2172 + .3738	- .0481 + 0
			+ .2172 - .3738	- .4358 + 0
	+ .0030	+50	+ .2194 + .3737	- .0545 + 0
			+ .2194 - .3737	- .4338 + 0
X_u	- .0228	-20	+ .2168 + .3741	- .0417 + 0
			+ .2168 - .3741	- .4358 + 0
	- .0257	-10	+ .2159 + .3740	- .0417 + 0
			+ .2159 - .3740	- .4368 + 0
	- .0285	0	+ .2150 + .3740	- .0417 + 0
			+ .2150 - .3740	- .4378 + 0
	- .0314	+10	+ .2141 + .3739	- .0417 + 0
			+ .2141 - .3739	- .4388 + 0
	- .0342	+20	+ .2132 + .3739	- .0417 + 0
			+ .2132 - .3739	- .4398 + 0

XV-4B PHASE I

1 FT/SEC

DERIVATIVE	VALUE	% CHANGE	ROOTS 1 & 2		ROOTS 3 & 4	
			Real	Imag.	Real	Imag.
Z_w	- .0154	-20	+ .2150	+ .3740	- .0411	+ 0
			+ .2150	- .3740	- .4378	+ 0
	- .0158	-10	+ .2150	+ .3740	- .0415	+ 0
			+ .2150	- .3740	- .4375	+ 0
	- .0160	0	+ .2150	+ .3740	- .0417	+ 0
			+ .2150	- .3740	- .4378	+ 0
	- .0176	-10	+ .2150	+ .3740	- .0433	+ 0
			+ .2150	- .3740	- .4378	+ 0
	- .0192	-20	+ .2150	+ .3740	- .0449	+ 0
			+ .2150	- .3740	- .4377	+ 0
Y_v	- 0.	-100	+ .5027	+ .8803	- .0099	+ 0
			+ .5027	- .8803	- 1.026	+ 0
	- .0105	-50	+ .4992	+ .8803	- .0099	+ 0
			+ .4992	- .8803	- 1.029	+ 0
	- .0210	0	+ .4957	+ .8803	- .0097	+ 0
			+ .4957	- .8803	- 1.033	+ 0
	- .0315	+50	+ .4922	+ .8803	- .0099	+ 0
			+ .4922	- .8803	- 1.036	+ 0
	- .0420	+100	+ .4887	- .8802	- .0099	+ 0
			+ .4887	+ .8802	- 1.040	+ 0

XV-4B PHASE I

1 FT/SEC

DERIVATIVE	VALUE	% CHANGE	ROOTS 1 & 2		ROOTS 3 & 4	
			Real	Imag.	Real	Imag.
N_β	0.0	-100	+ .4932	+ .8772	- .0100	+ 0
	(0.0)		+ .4932	- .8772	- 1.028	+ 0
(N_v)						
	- .001	-50	+ .4944	+ .8787	- .0099	+ 0
	(-.001)		+ .4944	- .8787	- 1.030	+ 0
	- .002	0	+ .4957	+ .8803	- .0099	+ 0
	(-.002)		+ .4957	- .8803	- 1.033	+ 0
	- .003	+50	+ .4969	+ .8819	- .0098	+ 0
	(-.003)		+ .4969	- .8819	- 1.035	+ 0
	- .004	+100	+ .4981	+ .8835	- .0098	+ 0
	(-.004)		+ .4981	- .8835	- 1.038	+ 0
I_β	0.0	-100	+ .1029	+ .2028	0	+ 0
	(0.0)		+ .1029	- .2028	- .2571	+ 0
(L_v)						
	- .016	-50	+ .3923	+ 7014	- .0098	+ 0
	(-.016)		+ .3923	- .7014	- .8262	+ 0
	- .032	0	+ .4957	+ .8803	- .0099	+ 0
	(-.032)		+ .4957	- .8803	- 1.033	+ 0
	- .048	+50	+ .5685	+ 1.006	- .0099	+ 0
	(-.048)		+ .5685	- 1.006	- 1.178	+ 0
	- .064	+100	+ .6267	+ 1.107	- .0099	+ 0
	(-.064)		+ .6267	- 1.107	- 1.295	+ 0

XV-4B PHASE I

1 FT/SEC

DERIVATIVE	VALUE	% CHANGE	ROOTS 1 & 2	ROOTS 3 & 4
			Real Imag.	Real Imag.
N_r	0.0	-100	+ .4957 + .8803	+ 0.000 + 0
			+ .4957 - .8803	- 1.033 + 0
	- .005	-50	+ .4957 + .8803	- .0049 + 0
			+ .4957 - .8803	- 1.033 + 0
	- .010	0	+ .4957 + .8803	- .0099 + 0
			+ .4957 - .8803	- 1.033 + 0
	- .015	+50	+ .4956 + .8803	- .0148 + 0
			+ .4956 - .8803	- 1.033 + 0
	- .020	+100 .	+ .4956 + .8803	- .0198 + 0
			+ .4956 - .8803	- 1.033 + 0
L_p	0.0	-100	+ .5024 + .8803	- .0099 + 0
			+ .5024 - .8803	- 1.026 + 0
	- .01	-50	+ .4990 + .8803	- .0099 + 0
			+ .4990 - .8803	- 1.029 + 0
	- .02	0	+ .4957 + .8803	- .0099 + 0
			+ .4957 - .8803	- 1.033 + 0
	- .03	+50	+ .4923 - .8803	- .0099 + 0
			+ .4923 + .8803	- 1.036 + 0
	- .04	+100	+ .4890 - .8802	- .0099 + 0
			+ .4890 + .8802	- 1.040 + 0

XV-4B PHASE I

10K

DERIVATIVE	VALUE	% CHANGE	ROOTS 1 & 2		ROOTS 3 & 4	
			Real	Imag.	Real	Imag.
M_u	+ .00136	-50	+ .1804	+ .2871	- .0773	+ 0
			+ .1804	- .2871	- .3866	+ 0
	+ .002030	-25	+ .2010	+ .3317	- .0695	+ 0
			+ .2010	- .3317	- .4359	+ 0
	+ .00271	0	+ .2190	+ .3679	- .0653	+ 0
			+ .2190	- .3679	- .4757	+ 0
	+ .00339	+25	+ .2345	+ .3984	- .0628	+ 0
			+ .2345	- .3984	- .5091	+ 0
	+ .00406	++50	+ .2481	+ .4246	- .0612	+ 0
			+ .2481	- .4246	- .5380	+ 0
M_q	+ .0000	-100	+ .2252	+ .3677	- .0653	+ 0
			+ .2252	- .3677	- .4691	+ 0
	- .0095	-50	+ .2221	+ .3678	- .0653	+ 0
			+ .2221	- .3678	- .4723	+ 0
	- .0190	0	+ .2190	+ .3679	- .0653	+ 0
			+ .2190	- .3679	- .4757	+ 0
	- .0285	+50	+ .2159	+ .3680	- .0653	+ 0
			+ .2159	- .3680	- .4790	+ 0
	- .0380	+100	+ .2129	+ .3680	- .0653	+ 0
			+ .2129	- .3680	- .4824	+ 0

XV-4B PHASE I

10K

DERIVATIVE	VALUE	% CHANGE	ROOTS 1 & 2		ROOTS 3 & 4	
			Real	Imag.	Real	Imag.
M_w	+ .00075	-50	+ .2117	+ .3750	- .0590	+ 0
			+ .2117	- .3750	- .4675	+ 0
	+ .00113	-25	+ .2154	+ .3714	- .0622	+ 0
			+ .2154	- .3714	- .4715	+ 0
	+ .0015	0	+ .2190	+ .3679	- .0653	+ 0
			+ .2190	- .3679	- .4757	+ 0
	+ .00188	+25	+ .2226	+ .3644	- .0684	+ 0
			+ .2226	- .3644	- .4798	+ 0
	+ .00225	+50	+ .2262	+ .3610	- .0715	+ 0
			+ .2262	- .3610	- .4840	+ 0
X_u	- .0256	-20	+ .2211	+ .3681	- .0652	+ 0
			+ .2211	- .3681	- .4736	+ 0
	- .0288	-10	+ .2201	+ .3680	- .0653	+ 0
			+ .2201	- .3680	- .4746	+ 0
	- .0320	0	+ .2190	+ .3679	- .0653	+ 0
			+ .2190	- .3679	- .4757	+ 0
	- .0352	+10	+ .2179	+ .3678	- .0654	+ 0
			+ .2179	- .3678	- .4767	+ 0
	- .0384	+20	+ .2169	+ .3677	- .0654	+ 0
			+ .2169	- .3677	- .4777	+ 0

XV-4B PHASE I

10K

DERIVATIVE	VALUE	% CHANGE	ROOTS 1 & 2		ROOTS 3 & 4	
			Real	Imag.	Real	Imag.
Z_w	- .0416	-20	+ .2189	+ .3674	- .0551	+ 0
			+ .2189	- .3674	- .4753	+ 0
	- .0468	-10	+ .2189	+ .3677	- .0601	+ 0
			+ .2189	- .3677	- .4755	+ 0
	- .0520	0	+ .2190	+ .3679	- .0653	+ 0
			+ .2190	- .3679	- .4757	+ 0
	- .0572	+10	+ .2190	+ .3681	- .0704	+ 0
			+ .2190	- .3681	- .4758	+ 0
	- .0724	+20	+ .2191	+ .3681	- .0853	+ 0
			+ .2191	- .3681	- .4764	+ 0
Y_v	- 0.	+100	+ .4871	+ .8792	- .0261	+ 0
			+ .4871	- .8792	- 1.074	+ 0
	- .06250	+50	+ .4662	+ .8796	- .0261	+ 0
			+ .4662	- .8796	- 1.095	+ 0
	- .1250	0	+ .4458	+ .8793	- .0261	+ 0
			+ .4458	- .8793	- 1.116	+ 0
	- .1875	+50	+ .4258	+ .8783	- .0261	+ 0
			+ .4258	- .8783	- 1.139	+ 0
	- .2500	+100	+ .4063	+ .8783	- .0261	+ 0
			+ .4063	- .8783	- 1.162	+ 0

XV-4B PHASE I

10 K

DERIVATIVE	VALUE	% CHANGE	ROOTS 1 & 2		ROOTS 3 & 4	
			Real	Imag.	Real	Imag.
N_β	0.0	-100	+ .4441	+ .8806	- .0260	+ 0
	(0.0)		+ .4441	- .8806	- 1.113	+ 0
(N_v)						
	- .00368	-50	+ .4449	+ .8799	- .0261	+ 0
	(-.000218)		+ .4449	- .8799	- 1.115	+ 0
	- .00738	0	+ .4458	+ .8793	- .0261	+ 0
	(-.000436)		+ .4458	- .8793	- 1.120	+ 0
	- .01105	+50	+ .4466	+ .8787	- .0262	+ 0
	(-.000654)		+ .4466	- .8787	- 1.120	+ 0
	- .01472	+100	+ .4475	+ .8780	- .0262	+ 0
	(-.000872)		+ .4475	- .8780	- 1.124	+ 0
L_β	0.0	-100	+ .2588	+ .1012	- .0661	+ 0
	(0.0)		+ .2588	- .1012	- .2365	+ 0
(L_v) .						
	- .283	-50	+ .3396	+ .6995	- .0262	+ 0
	(.0167)		+ .3396	- .6995	- .9030	+ 0
	- .563	0	+ .4458	+ .8793	- .0261	+ 0
	(-.0334)		+ .4458	- .8793	- 1.116	+ 0
	- .846	+50	+ .5216	+ 1.006	- .0261	+ 0
	(-.0501)		+ .5216	- 1.006	- 1.268	+ 0
	- 1.145	+100	+ .5851	+ 1.112	- .0261	+ 0
	(-.0668)		+ .5851	- 1.112	- 1.395	+ 0

XV-4B PHASE I

10K

DERIVATIVE	VALUE	% CHANGE	ROOTS 1 & 2	ROOTS 3 & 4
			Real Imag.	Real Imag.
N_r	0.0	-100	+ .4458 + .8790	- .0002 + 0
			+ .4458 - .8790	- 1.116 + 0
	- .0130	-50	+ .4458 + .8792	- .0132 + 0
			+ .4458 - .8792	- 1.116 + 0
	- .0260	0	+ .4458 + .8793	- .0261 + 0
			+ .4458 - .8793	- 1.116 + 0
	- .0390	+50	+ .4458 + .8794	- .0391 + 0
			+ .4458 - .8794	- 1.116 + 0
	- .0520	+100	+ .4458 + .8796	- .0521 + 0
			+ .4458 - .8796	- 1.117 + 0
L_p	0	-100	+ .4796 + .8790	- .0261 + 0
			+ .4796 - .8790	- 1.083 + 0
	- .0500	-50	+ .4796 + .8794	- .0261 + 0
			+ .4796 - .8794	- 1.099 + 0
	- .1000	0	+ .4458 + .8793	- .0261 + 0
			+ .4458 - .8793	- 1.116 + 0
	- .1500	+50	+ .4293 + .8787	- .0262 +)
			+ .4293 - .8787	- 1.134 + 0
	- .2000	+100	+ .4132 + .8777	- .0262 + 0
			+ .4132 - .8777	- 1.152 + 0

XV-4B PHASE I

20K

DERIVATIVE	VALUE	% CHANGE	ROOTS 1 & 2		ROOTS 3 & 4	
			Real	Imag.	Real	Imag.
M_u	+ .0014	-50	+ .1563	+ .2844	- .0945	+ 0
			+ .1563	- .2844	- .4367	+ 0
	+ .002092	-25	+ .1779	+ .3297	- .0923	+ 0
			+ .1779	- .3297	- .4820	+ 0
	+ .00279	0	+ .1959	+ .3661	- .0911	+ 0
			+ .1959	- .3661	- .5193	+ 0
	+ .003489	+25	+ .2115	+ .3967	- .0903	+ 0
			+ .2115	- .3967	- .5512	+ 0
	+ .004180	+50	+ .2252	+ .4232	- .0898	+ 0
			+ .2252	- .4232	- .5791	+ 0
M_q	- .0000	-100	+ .2275	+ .3659	- .0911	+ 0
			+ .2275	- .3659	- .4824	+ 0
	- .0500	-50	+ .2114	+ .3665	- .0911	+ 0
			+ .2114	- .3665	- .5002	+ 0
	- .1000	0	+ .1959	+ .3661	- .0911	+ 0
			+ .1959	- .3661	- .5193	+ 0
	- .1500	+50	+ .1812	+ .3647	- .0911	+ 0
			+ .1812	- .3647	- .5398	+ 0
	- .2000	+100	+ .1671	+ .3626	- .0911	+ 0
			+ .1671	- .3626	- .5617	+ 0

XV-4B PHASE I

20K

DERIVATIVE	VALUE	% CHANGE	ROOTS 1 & 2 Real	ROOTS 1 & 2 Imag.	ROOTS 3 & 4 Real	ROOTS 3 & 4 Imag.
M_w	+ .0005	-50	+ .1877	+ .3743	- .0892	+ 0
			+ .1877	- .3743	- .5047	+ 0
	+ .00075	-25	+ .1918	+ .3702	- .0901	+ 0
			+ .1918	- .3702	- .5120	+ 0
	+ .0010	0	+ .1959	+ .3661	- .0911	+ 0
			+ .1959	- .3661	- .5193	+ 0
	+ .00125	+25	+ .2000	+ .3620	- .0920	+ 0
			+ .2000	- .3620	- .5265	+ 0
	+ .00150	+50	+ .2040	+ .3579	- .0928	+ 0
			+ .2040	- .3579	- .5337	+ 0
X_u	- .0268	-20	+ .1982	+ .3662	- .0908	+ 0
			+ .1982	- .3662	- .5174	+ 0
	- .0303	-10	+ .1970	+ .3662	- .0910	+ 0
			+ .1970	- .3662	- .5184	+ 0
	- .0335	0	+ .1959	+ .3661	- .0911	+ 0
			+ .1959	- .3661	- .5193	+ 0
	- .0369	+10	+ .1948	+ .3660	- .0912	+ 0
			+ .1948	- .3660	- .5202	+ 0
	- .0402	+20	+ .1936	+ .3659	- .0913	+ 0
			+ .1936	- .3659	- .5212	+ 0

XV-4B PHASE I

20K

DERIVATIVE	VALUE	% CHANGE	ROOTS 1 & 2		ROOTS 3 & 4	
			Real	Imag.	Real	Imag.
Z_w	- .0680	-20	+ .1957	+ .3652	- .0745	+ 0
			+ .1957	- .3652	- .5183	+ 0
	- .0768	-10	+ .1958	+ .3656	- .0831	+ 0
			+ .1958	- .3656	- .5188	+ 0
	- .0850	0	+ .1959	+ .3661	- .0911	+ 0
			+ .1959	- .3661	- .5193	+ 0
	- .0935	+10	+ .1960	+ .3665	- .0993	+ 0
			+ .1960	- .3665	- .5198	+ 0
	- .1020	+20	+ .1961	+ .3669	- .1075	+ 0
			+ .1961	- .3669	- .5203	+ 0
Y_v	- 0.	-100	+ .4415	+ .9011	- .0297	+ 0
			+ .4415	- .9011	- 1.105	+ 0
	- .0875	-50	+ .4114	+ .9018	- .0297	+ 0
			+ .4114	- .9018	- 1.133	+ 0
	- .1750	0	+ .3822	+ .9010	- .0297	+ 0
			+ .3822	- .9010	- 1.162	+ 0
	- .2625	+50	+ .3539	+ .8989	- .0297	+ 0
			+ .3539	- .8989	- 1.193	+ 0
	- .350	+100	+ .3264	+ .8955	- .0297	+ 0
			+ .3264	- .8955	- 1.225	+ 0

XV-4B PHASE I

20K

DERIVATIVE	VALUE	% CHANGE	ROOTS 1 & 2		ROOTS 3 & 4	
			Real	Imag.	Real	Imag.
N_β	0.0	-100	+ .4001	+ .8794	- .0342	+ 0
	(0.0)		+ .4001	- .8794	- 1.193	+ 0
(N_v)						
	.04425	-50	+ .3912	+ .8902	- .0320	+ 0
	(.00131)		+ .3912	- .8902	- 1.177	+ 0
	.0886	0	+ .3822	+ .9010	- .0297	+ 0
	(.00262)		+ .3822	- .9010	- 1.162	+ 0
	.1330	+50	+ .3733	+ .9120	- .0274	+ 0
	(.00393)		+ .3733	- .9120	- 1.146	+ 0
	.1770	+100	+ .3644	+ .9229	- .0251	+ 0
	(.00524)		+ .3644	- .9229	- 1.131	+ 0
L_β	0.0	-100	- .1610	+ .3414	+ .1441	+ 0
	(0.0)		- .1610	- .3414	- .2491	+ 0
(L_v)						
	-.5825	-50	+ .2656	+ .7253	- .0250	+ 0
	(-.01725)		+ .2656	- .7253	- .9331	+ 0
	-1.165	0	+ .3822	+ .9010	- .0297	+ 0
	(-.0345)		+ .3822	- .9010	- 1.162	+ 0
	-1.745	+50	+ .4626	+ 1.024	- .0312	+ 0
	(-.0517)		+ .4626	- 1.024	- 1.321	+ 0
	-2.330	+100	+ .5268	+ 1.122	- .0319	+ 0
	(-.0690		+ .5268	- 1.122	- 1.449	+ 0

XV-4B PHASE I

20K

DERIVATIVE	VALUE	% CHANGE	ROOTS 1 & 2		ROOTS 3 & 4	
			Real	Imag.	Real	Imag.
N_r	0.0	-100	+ .3824	+ .9014	+ .0046	+ 0
			+ .3824	- .9014	- 1.162	+ 0
	- .017	-50	+ .3823	+ .9012	- .0125	+ 0
			+ .3823	- .9012	- 1.162	+ 0
	- .034	0	+ .3822	+ .9010	- .0297	+ 0
			+ .3822	- .9010	- 1.162	+ 0
	- .051	+50	+ .3821	+ .9009	- .0468	+ 0
			+ .3821	- .9009	- 1.162	+ 0
	- .068	+100	+ .3821	+ .9007	- .0640	+ 0
			+ .3821	- .9007	- 1.161	+ 0
L_p	0	-100	+ .4535	+ .8973	- .0302	+ 0
			+ .4535	- .8973	- 1.081	+ 0
	- .11	-50	+ .4172	+ .9003	- .0299	+ 0
			+ .4172	- .9003	- 1.120	+ 0
	- .22	0	+ .3822	+ .9010	- .0247	+ 0
			+ .3822	- .9010	- 1.162	+ 0
	- .33	+50	+ .3487	+ .8997	- .0294	+ 0
			+ .3487	- .8977	- 1.206	+ 0
	- .44	+100	+ .3167	+ .8964	- .0291	+ 0
			+ .3167	- .8964	- 1.253	+ 0

XV-4B PHASE I

40 K

DERIVATIVE	VALUE	% CHANGE	ROOTS 1 & 2		ROOTS 3 & 4	
			Real	Imag.	Real	Imag.
M_u	+ .000855	-50	+ .1067	+ .2365	- .1538	+ 0
			+ .1067	- .2365	- .4386	+ 0
	+ .001282	-25	+ .1251	+ .2741	- .1600	+ 0
			+ .1251	- .2741	- .4693	+ 0
	+ .00171	0	+ .1401	+ .3041	- .1635	+ 0
			+ .1401	- .3041	- .4958	+ 0
	+ .002137	+25	+ .1530	+ .3294	- .1658	+ 0
			+ .1530	- .3294	- .5192	+ 0
	+ .002565	+50	+ .1644	+ .3516	- .1674	+ 0
			+ .1644	- .3516	- .5404	+ 0
M_q	- .0875	-50	+ .1653	+ .3064	- .1635	+ 0
			+ .1653	- .3064	- .4586	+ 0
	- .1312	-25	+ .1524	+ .3056	- .1635	+ 0
			+ .1524	- .3056	- .4766	+ 0
	- .1750	0	+ .1401	+ .3041	- .1635	+ 0
			+ .1401	- .3041	- .4958	+ 0
	- .2188	+25	+ .1285	+ .3018	- .1635	+ 0
			+ .1285	- .3018	- .5163	+ 0
	- .2625	+50	+ .1176	+ .2990	- .1635	+ 0
			+ .1176	- .2990	- .5381	+ 0

XV-4B PHASE I

40K

DERIVATIVE	VALUE	% CHANGE	ROOTS 1 & 2	ROOTS 3 & 4
			Real Imag.	Real Imag.
M_w	+ .00025	-50	+ .1312 + .3104	- .1696 + 0
			+ .1312 - .3104	- .4718 + 0
	+ .000375	-25	+ .1357 + .3072	- .1664 + 0
			+ .1357 - .3072	- .4840 + 0
	+ .00050	0	+ .1401 + .3041	- .1635 + 0
			+ .1401 - .3041	- .4958 + 0
	+ .000625	+25	+ .1495 + .3009	- .1608 + 0
			+ .1495 - .3009	- .5072 + 0
	+ .00075	+50	+ .1488 + .2977	- .1583 + 0
			+ .1488 - .2977	- .5182 + 0
X_u	- .0312	-20	+ .1428 + .3042	- .1628 + 0
			+ .1428 - .3042	- .4941 + 0
	- .0351	-10	+ .1415 + .3041	- .1631 + 0
			+ .1415 - .3041	- .4949 + 0
	- .0390	0	+ .1401 + .3041	- .1635 + 0
			+ .1401 - .3041	- .4958 + 0
	- .0429	+10	+ .1388 + .3040	- .1638 + 0
			+ .1388 - .3040	- .4466 + 0
	- .0468	+20	+ .1374 + .3039	- .1642 + 0
			+ .1374 - .3039	- .4975 + 0

XV-4B PHASE I

40K

DERIVATIVE	VALUE	% CHANGE	ROOTS 1 & 2		ROOTS 3 & 4	
			Real	Imag.	Real	Imag.
Z_w	- .1320	-20	+ .1399	+ .3020	- .1332	+ 0
			+ .1399	- .3020	- .4925	+ 0
	- .1485	-10	+ .1400	+ .3031	- .1485	+ 0
			+ .1400	- .3031	- .4941	+ 0
	- .1650	0	+ .1401	+ .3041	- .1635	+ 0
			+ .1401	- .3041	- .4958	+ 0
	- .1815	+10	+ .1402	+ .3050	- .1782	+ 0
			+ .1402	- .3050	- .4976	+ 0
	- .1980	+20	+ .1402	+ .3059	- .1927	+ 0
			+ .1402	- .3059	- .4996	+ 0
Y_v	0	-100	+ .4026	+ .9563	- .0641	+ 0
			+ .4026	- .9563	-1.141	+ 0
	- .1275	-50	+ .3575	+ .9567	- .0641	+ 0
			+ .3575	- .9567	-1.178	+ 0
	- .2550	0	+ .3140	+ .9540	- .0640	+ 0
			+ .3140	- .9540	-1.218	+ 0
	- .3825	+50	+ .2723	+ .9486	- .0640	+ 0
			+ .2723	- .9486	-1.262	+ 0
	- .510	+100	+ .2325	- .9405	-1.310	+ 0

XV-4B PHASE I

40K

DERIVATIVE	VALUE	% CHANGE	ROOTS 1 & 2		ROOTS 3 & 4	
			Real	Imag.	Real	Imag.
N_β	0.0	-100	+ .3701	+ .8800	- .0925	+ 0
	(0.0)		+ .3701	- .8800	- 1.302	+ 0
(N_v)						
	+ .1405	-50	+ .3418	+ .9167	- .0781	+ 0
	(+.002075)		+ .3418	- .9167	- 1.260	+ 0
	+ .280	0	+ .3140	+ .9540	- .0640	+ 0
	(+.00415)		+ .3140	- .9540	- 1.218	+ 0
	+ .4210	+50	+ .2864	+ .9927	- .0502	+ 0
	(+.006225)		+ .2864	- .9927	- 1.177	+ 0
	+ .560	+100	+ .2599	+ 1.032	- .0370	+ 0
	(+.0083)		+ .2599	- 1.032	- 1.137	+ 0
L_β	0.0	-100	- .1970	+ .5898	+ .1816	+ 0
	(0.0)		- .1970	- .5898	- .4420	+ 0
(L_v)						
	- 1.265	-50	+ .1764	+ .7960	- .0370	+ 0
	(-.01875)		+ .1764	- .7960	- .9702	+ 0
	- 2.530	0	+ .3140	+ .9540	- .0640	+ 0
	(-.0375)		+ .3140	- .9540	- 1.218	+ 0
	- 3.800	+50	+ .4063	+ 1.069	- .0734	+ 0
	(-.05625)		+ .4063	- 1.069	- 1.393	+ 0
	- 5.06	+100	+ .4780	+ 1.160	- .0781	+ 0
	(-.075)		+ .4780	- 1.160	- 1.532	+ 0

XV-4B PHASE I

40K

DERIVATIVE	VALUE	% CHANGE	ROOTS 1 & 2		ROOTS 3 & 4	
			Real	Imag.	Real	Imag.
N_r	0.0	-100	+ .3167	+ .9579	.0250	+ 0
			+ .3167	- .9579	- 1.222	+ 0
	- .045	-50	+ .3152	+ .9560	- .0193	+ 0
			+ .3152	- .9560	- 1.220	+ 0
	- .090	0	+ .3140	+ .9540	- .0640	+ 0
			+ .3140	- .9540	- 1.218	+ 0
	- .135	+50	+ .3129	+ .9520	- .1093	+ 0
			+ .3129	- .9520	- 1.216	+ 0
	- .180	+100	+ .3120	+ .9500	- .1552	+ 0
			+ .3120	- .9500	- 1.214	+ 0
L_p	0	-100	+ .4120	+ .9364	- .0692	+ 0
			+ .4120	- .9364	- 1.086	+ 0
	- .16	-50	+ .3616	+ .9476	- .0665	+ 0
			+ .3616	- .9476	- 1.149	+ 0
	- .32	0	+ .3140	+ .9540	- .0640	+ 0
			+ .3140	- .9540	- 1.218	+ 0
	- .48	+50	+ .2692	+ .9561	- .0617	+ 0
			+ .2692	- .9561	- 1.293	+ 0
	- .64	+100	+ .2274	+ .9546	- .0595	+ 0
			+ .2274	- .9546	- 1.373	+ 0

XV-4B PHASE I

60K

DERIVATIVE	VALUE	% CHANGE	ROOTS 1 & 2		ROOTS 3 & 4	
			Real	Imag.	Real	Imag.
M_u	+ .0007	-50	+ .0180	+ .2182	- .3099	+ .1607
			+ .0180	- .2182	- .3099	- .1607
	+ .001053	-25	+ .0362	+ .2579	- .3282	+ .1400
			+ .0362	- .2579	- .3282	- .1400
	+ .00140	0	+ .0516	+ .2878	- .3436	+ .1221
			+ .0516	- .2878	- .3436	- .1221
	+ .00175	+25	+ .0650	+ .3128	- .3570	+ .1045
			+ .0650	- .3128	- .3570	- .1045
	+ .00210	+50	+ .0770	+ .3343	- .3690	+ .0859
			+ .0770	- .3343	- .3690	- .0859
M_q	- .1476	-50	+ .0884	+ .3079	- .3067	+ .1294
			+ .0884	- .3079	- .3067	- .1294
	- .2213	-25	+ .0685	+ .2987	- .3236	+ .1277
			+ .0685	- .2987	- .3236	- .1277
	- .2950	0	+ .0516	+ .2878	- .3436	+ .1221
			+ .0516	- .2878	- .3436	- .1221
	- .3687	+25	+ .0376	+ .2761	- .3665	+ .1099
			+ .0376	- .2761	- .3665	- .1099
	- .4424	+50	+ .0265	+ .2642	- .3922	+ .0862
			+ .0265	- .2642	- .3922	- .0862

XV-4B PHASE I

60K

DERIVATIVE	VALUE	% CHANGE	ROOTS 1 & 2		ROOTS 3 & 4	
			Real	Imag.	Real	Imag.
M_w	- .00025	-50	+ .0659	+ .2849	- .3579	+ .0544
			+ .0659	- .2849	- .3579	- .0544
	- .000375	-25	+ .0589	+ .2865	- .3508	+ .0941
			+ .0589	- .2865	- .3508	- .0941
	- .00050	0	+ .0516	+ .2878	- .3436	+ .1221
			+ .0576	- .2878	- .3436	- .1221
	- .000625	+25	+ .0440	+ .2889	- .3360	+ .1453
			+ .0440	- .2889	- .3360	- .1453
	- .00075	+50	+ .0362	+ .2897	- .3282	+ .1659
			+ .0362	- .2897	- .3282	- .1659
X_u	- .0352	-20	+ .0551	+ .2872	- .3427	+ .1243
			+ .0551	- .2872	- .3427	- .1243
	- .0396	-10	+ .0534	+ .2879	- .3431	+ .1232
			+ .0534	- .2879	- .3431	- .1232
	- .0440	0	+ .0516	+ .2878	- .3436	+ .1221
			+ .0516	- .2878	- .3436	- .1221
	- .0484	+10	+ .0498	+ .2881	- .3440	+ .1209
			+ .0498	- .2881	- .3440	- .1209
	- .0528	+20	+ .0480	+ .2884	- .3444	+ .1198
			+ .0480	- .2884	- .3444	- .1198

XV-4B PHASE I

60K

DERIVATIVE	VALUE	% CHANGE	ROOTS 1 & 2		ROOTS 3 & 4	
			Real	Imag.	Real	Imag.
Z_w	- .1860	-20	+ .0479	+ .2907	- .3104	+ .0627
			+ .0479	- .2907	- .3104	- .0627
	- .2205	-10	+ .0501	+ .2888	- .3298	+ .2888
			+ .0501	- .2888	- .3298	- .2888
	- .2450	0	+ .0516	+ .2878	- .3436	+ .1221
			+ .0516	- .2878	- .3436	- .1221
	- .2695	+10	+ .0530	+ .2870	- .3572	+ .1370
			+ .0530	- .2870	- .3572	- .1370
	- .3040	+20	- .0548	+ .2862	- .3763	+ .1535
			- .0548	- .2862	- .3763	- .1535
Y_v	0	-100	+ .2961	+1.109	- .0476	+ 0
			+ .2961	-1.109	-1.153	+ 0
	- .120	-50	+ .2970	+1.015	- .0761	+ 0
			+ .2970	-1.015	-1.246	+ 0
	- .240	0	+ .2535	+1.013	- .0760	+ 0
			+ .2535	-1.013	-1.279	+ 0
	- .360	+50	+ .2114	+1.009	- .0759	+ 0
			+ .2114	-1.009	-1.315	+ 0
	- .480	+100	+ .1709	-1.002	- .0758	+ 0
			+ .1709	+1.002	-1.354	+ 0

XV-4B PHASE I

60K

DERIVATIVE	VALUE	% CHANGE	ROOTS 1 & 2		ROOTS 3 & 4	
			Real	Imag.	Real	Imag.
N_β	0.0	-100	+ .3446	+ .8665	- .1320	+ 0
(N_v)	(0.0)		+ .3446	- .8665	-1.405	+ 0
	+ .3030	-50	+ .2884	+ .9542	- .0969	+ 0
	(+ .002975)		+ .2884	- .9542	-1.328	+ 0
	+ .5020	0	+ .2535	+1.013	- .0769	+ 0
	(+ .00495)		+ .2535	-1.013	-1,279	+ 0
	+ .8070	+50	+ .2039	+1.105	- .0474	+ 0
	(+ .007925)		+ .2039	-1.105	-1.208	+ 0
	+1.005	+100	+ .1744	+1.165	- .0312	+ 0
	(+ .0099)		+ .1744	-1.165	-1.166	+ 0
L_β	0.0	-100	- .2049	+ .7573	.1522	+ 0
(L_v)	(0.0)		- .2049	- .7573	.5905	+ 0
	-2.035	-50	+ .1050	+ .8843	- .0313	+ 0
	(- .02)		+ .1050	- .8843	-1.027	+ 0
	-4.060	0	+ .2535	+1.013	- .0760	+ 0
	(- .04)		+ .2535	-1.013	-1.279	+ 0
	-6.10	+50	+ .3546	+1.114	- .0936	+ 0
	(- .06)		+ .3546	-1.114	-1.464	+ 0
	-8.14	+100	+ .4336	+1.196	- .1028	+ 0
	(- .08)		+ .4336	-1,196	-1.613	+ 0

XV-4B PHASE I

60K

DERIVATIVE	VALUE	% CHANGE	ROOTS 1 & 2	ROOTS 3 & 4
			Real Imag.	Real Imag.
N_r	0.0	-100	+ .2624 +1.022	+ .0387 + 0
			+ .2624 -1.022	-1.286 + 0
	- .062	-50	+ .2577 +1.018	- .0179 + 0
			+ .7577 -1.018	-1.283 + 0
	- .124	0	+ .2039 +1.105	- .0474 + 0
			+ .2039 -1.105	-1.208 + 0
	- .186	+50	+ .2499 +1.008	- .1356 + 0
			+ .2499 -1.008	-1.275 + 0
	- .248	+100	+ .2469 +1.003	- .1971 + 0
			+ .2469 -1.003	-1.270 + 0
L_p	0	-100	+ .3870 + .9694	- .0928 + 0
			+ .3870 - .9694	-1.024 + 0
	- .25	-50	+ .3190 + .9989	- .0838 + 0
			+ .3190 - .9989	-1.150 + 0
	- .50	0	+ .2535 +1.013	- .0769 + 0
			+ .2535 -1.013	-1.279 + 0
	- .75	+50	+ .1947 +1.018	- .0694 + 0
			+ .1947 -1.018	-1.421 + 0
	-1.00	+100	+ .1430 +1.016	- .0639 + 0
			+ .1430 -1.016	-1.575 + 0

XV-4B PHASE I

70K

DERIVATIVE	VALUE	% CHANGE	ROOTS 1 & 2		ROOTS 3 & 4	
			Real	Imag.	Real	Imag.
M_u	+ .0002470	-50	- .0183	+ .1218	- .3215	+ .3255
			- .0183	- .1218	- .3215	- .3255
	+ .0003677	-25	- .0176	+ .1435	- .3221	+ .3172
			- .0176	- .1435	- .3221	- .3172
	+ .00049	0	- .0164	+ .1633	- .3234	+ .3087
			- .0164	- .1633	- .3234	- .3087
	+ .00061	+25	- .0161	+ .1750	- .3236	+ .3010
			- .0161	- .1750	- .3236	- .3010
	+ .000733	+50	- .0123	+ .1982	- .3275	+ .2920
			- .0123	- .1982	- .3275	- .2920
M_q	- .1750	-50	- .2414	+ .2892	- .0109	+ .1945
			- .2414	- .2892	- .0109	- .1945
	- .2625	-25	- .2814	+ .3035	- .0146	+ .1767
			- .2814	- .3035	- .0146	- .1767
	- .3500	0	- .3234	+ .3087	- .0164	+ .1633
			- .3234	- .3087	- .0164	- .1633
	- .4375	+25	- .3661	+ .3060	- .0175	+ .1528
			- .3661	- .3060	- .0175	- .1528
	- .5250	+50	- .4091	+ .2957	- .0182	+ .1442
			- .4091	- .2957	- .0182	- .1442

XV-4B PHASE I

70K

DERIVATIVE	VALUE	% CHANGE	ROOTS 1 & 2		ROOTE 3 & 4	
			Real	Imag.	Real	Imag.
M_w	- .0005	-50	- .3397	+ .2059	- .0000	+ .1765
			- .3397	- .2059	- .0000	- .1765
	- .00075	-25	- .3303	+ .2604	- .0094	+ .1704
			- .3303	- .2604	- .0094	- .1704
	- .0010	0	.3234	+ .3087	.0164	+ .1633
			.3234	- .3087	.0164	- .1633
	- .00125	+25	.3187	+ .3524	- .0213	+ .1563
			.3187	- .3524	- .0213	- .1563
	- .0015	+50	- .3157	+ .3923	- .0241	+ .1500
			- .3157	- .3923	- .0241	- .1500
X_u	- .0380	-20	- .3237	+ .3094	- .0113	+ .1635
			- .3237	- .3094	- .0113	- .1635
	- .0428	-10	- .3235	+ .3091	- .0139	+ .1634
			- .3235	- .3091	- .0139	- .1634
	- .0475	0	- .3234	+ .3087	- .0164	+ .1633
			- .3234	- .3087	- .0164	- .1633
	- .0533	+10	- .3231	+ .3083	- .0195	+ .1631
			- .3231	- .3083	- .0195	- .1631
	- .0560	+20	- .3230	+ .3081	- .0210	+ .1630
			- .3230	- .3081	- .0210	- .1630

XV-4B PHASE I

70K

DERIVATIVE	VALUE	% CHANGE	ROOTS 1 & 2		ROOTS 3 & 4	
			Real	Imag.	Real	Imag.
Z_w	- .2256	-20	- .2883	+ .2995	- .0233	+ .1596
			- .2883	- .2995	- .0233	- .1596
	- .2538	-10	- .3061	+ .3044	- .0195	+ .1616
			- .3061	- .3044	- .0195	- .1616
	- .2820	0	- .3234	+ .3087	- .0164	+ .1633
			- .3234	- .3087	- .0164	- .1633
	- .3102	+10	- .3401	+ .3123	- .0137	+ .1648
			- .3401	- .3123	- .0137	- .1648
	- .3384	+20	- .3566	+ .3152	- .0114	+ .1660
			- .3566	- .3152	- .0114	- .1660
Y_v	-0.	-100	+ .2346	+1.075	- .0494	+ 0
			+ .2346	-1.075	-1.354	+ 0
	- .120	-50	+ .1863	+1.077	- .0492	+ 0
			+ .1863	-1.077	-1.378	+ 0
	- .240	0	+ .1390	+1.076	- .0490	+ 0
			+ .1390	-1.076	-1.403	+ 0
	- .360	+50	+ .0928	-1.073	- .0488	+ 0
			+ .0928	+1.073	-1.431	+ 0
	- .480	+100	+ .0293	+1.049	- .1753	+ 0
			+ .0293	-1.049	-1.448	+ 0

XV-4B PHASE I

70K

DERIVATIVE	VALUE	% CHANGE	ROOTS 1 & 2		ROOTS 3 & 4	
			Real	Imag.	Real	Imag.
N_β	0.0	-100	+ .2488	+ .8554	- .1661	+ 0
(N_v)	(0.0)		+ .2488	- .8554	-1.506	+ 0
	+ .3155	-50	+ .1886	+ .9654	- .0996	+ 0
	(+ .002675)		+ .1886	- .9654	-1.452	+ 0
	+ .6320	0	+ .1390	+1.076	- .0490	+ 0
	(+ .00535)		+ .1390	-1.076	-1.403	+ 0
	+ .9460	+50	+ .0990	+1.184	- .0118	+ 0
	(+ .008025)		+ .0990	-1.184	-1.360	+ 0
	+1.260	+100	+ .0662	+1.289	+ .0162	+ 0
	(+ .01070)		+ .0662	-1.289	-1.323	+ 0
L_β	0.0	-100	- .2178	+ .8580	+ .1658	+ 0
	(0.0)		- .2178	- .8580	- .9044	+ 0
	-2.42	-50	- .0050	- .9648	+ 0163	+ 0
	(- .0205)		- .0050	+ .9648	-1.201	+ 0
	-4.84	0	+ .1390	+1.076	- .0490	+ 0
	(- .041)		+ .1390	-1.076	-1.403	+ 0
	-7.26	+50	+ .2333	+1.171	- .0810	+ 0
	(- .0615)		+ .2333	-1.171	-1.560	+ 0
	-9.66	+100	+ .3068	+1.251	- .0994	+ 0
	(- .082)		+ .3068	-1.251	-1.688	+ 0

XV-4B PHASE I

70K

DERIVATIVE	VALUE	% CHANGE	ROOTS 1 & 2		ROOTS 3 & 4	
			Real	Imag.	Real	Imag.
N_r	0.0	-100	+ .1603	+1.090	+ .0685	+ 0
			+ .1603	-1.090	-1.413	+ 0
	- .075	-50	+ .1492	+1.084	+ .0108	+ 0
			+ .1492	-1.084	-1.408	+ 0
	- .150	0	+ .1390	+1.076	- .0490	+ 0
			+ .1390	-1.076	-1.403	+ 0
	- .225	+50	+ .1290	+1.068	- .1115	+ 0
			+ .1298	-1.068	-1.398	+ 0
	- .300	+100	+ .1217	+1.058	- .1771	+ 0
			+ .1217	-1.058	-1.391	+ 0
L_p	0	-100	+ .3344	+1.022	- .0723	+ 0
			+ .3344	-1.022	- .9691	+ 0
	- .40	-50	+ .2290	+1.063	- .0584	+ 0
			+ .2290	-1.063	-1.173	+ 0
	- .80	0	+ .1390	+1.076	- .0490	+ 0
			+ .1390	-1.076	-1.403	+ 0
	-1.20	+50	+ .0657	+1.072	- .0422	+ 0
			+ .0657	-1.072	-1.664	+ 0
	-1.60	+100	+ .0085	+1.057	- .0371	+ 0
			+ .0085	-1.057	-1.956	+ 0

XV-4B PHASE I

100K

DERIVATIVE	VALUE	% CHANGE	ROOTS 1 & 2		ROOTS 3 & 4	
			Real	Imag.	Real	Imag.
M_u	- .000436	-50	- .4840	+ .7712	- .0220	+ .0251
			- .4840	- .7712	- .0220	- .0251
	- .000655	-25	- .4852	+ .7741	+ .0325	+ 0
			- .4052	- .7741	- .0742	+ 0
	- .000873	0	- .4863	+ .7769	+ .0594	+ 0
			- .4863	- .7769	- .0989	+ 0
	- .0011	+25	- .4874	+ .7798	+ .0795	+ 0
			- .4874	- .7798	- .1168	+ 0
	- .0013	+50	- .4884	+ .7825	+ .0957	+ 0
			- .4884	- .7825	- .1308	+ 0
M_q	- .2700	-50	- .3538	+ .7762	+ .0669	+ 0
			- .3538	- .7762	- .1014	+ 0
	- .4050	-25	- .4199	+ .7795	+ .0629	+ 0
			- .4199	- .7795	- .1001	+ 0
	- .5400	0	- .4863	+ .7769	+ .0594	+ 0
			- .4863	- .7769	- .0989	+ 0
	- .6700	+25	- .5528	+ .7684	+ .0563	+ 0
			- .5528	- .7684	- .0978	+ 0
	- .8100	+50	- .6194	+ .7537	+ .0536	+ 0
			- .6194	- .7537	- .0967	+ 0

XV-4B PHASE I

100K

DERIVATIVE	VALUE	% CHANGE	ROOTS 1 & 2		ROOTS 3 & 4	
			Real	Imag.	Real	Imag.
M_w	- .00175	-50	- .4826	+ .5605	+ .1021	+ 0
			- .4826	- .5605	- .1488	+ 0
	- .00263	-25	- .4855	+ .6774	+ .0793	+ 0
			- .4885	- .6774	- .1202	+ 0
	- .0035	0	- .4863	+ .7769	+ .0594	+ 0
			- .4863	- .7769	- .0989	+ 0
	- .00438	+25	- .4862	+ .8654	+ .0491	+ 0
			- .4862	- .8654	- .0804	+ 0
	- .00525	+50	- .4859	+ .9458	+ .0221	+ 0
			- .4859	- .9458	- .0623	+ 0
X_u	- .0448	-20	- .4861	+ .7770	+ .0636	+ 0
			- .4861	- .7770	- .0923	+ 0
	- .0504	-10	- .4862	+ .7770	+ .0615	+ 0
			- .4862	- .7770	- .0955	+ 0
	- .05600	0	- .4863	+ .7769	+ .0594	+ 0
			- .4863	- .7769	- .0989	+ 0
	- .06160	+10	- .4863	+ .7769	+ .0594	+ 0
			- .4863	- .7769	- .1023	+ 0
	- .0672	+20	- .4864	+ .7769	+ .0555	+ 0
			- .4864	- .7769	- .1058	+ 0

XV-4B PHASE I

100K

DERIVATIVE	VALUE	% CHANGE	ROOTS 1 & 2		ROOTS 3 & 4	
			Real	Imag.	Real	Imag.
N_β	0.0	-100	+ .2991	+ .8175	- .2706	+ 0
(N_v)	(0.0)		+ .2991	- .8175	-1.641	+ 0
	+ .6350	-50	+ .1816	+1.018	- .1557	+ 0
	(+ .003775)		+ .1816	-1.018	-1.521	+ 0
	+1.105	0	+ .1134	+1.170	- .0961	+ 0
	(+ .00655)		+ .1134	-1.170	-1.445	+ 0
	+1.745	+50	+ .0433	+1.370	- .0424	+ 0
	(+ .010325)		+ .0433	-1.370	-1.358	+ 0
	+2.210	+100	+ .0048	+1.509	- .0159	+ 0
	(+ .01310)		+ .0048	-1.509	-1.308	+ 0
L_β	0.0	-100	- .2536	+1.093	+ .1235	+ 0
(L_v)	(0.0)		- .2536	-1.093	- .9302	+ 0
	-3.80	-50	- .0419	+1.113	- .0157	+ 0
	(- .0225)		- .0419	-1.113	-1.215	+ 0
	-7.60	0	+ .1134	+1.170	- .0961	+ 0
	(- .045)		+ .1134	-1.170	-1.445	+ 0
	-11.40	+50	+ .2296	+1.229	- .1411	+ 0
	(- .0675)		+ .2296	-1.229	-1.632	+ 0
	-15.20	+100	+ .3227	+1.284	- .1685	+ 0
	(- .090)		+ .3227	-1.284	-1.791	+ 0

XV-4B PHASE I

100K

DERIVATIVE	VALUE	% CHANGE	ROOTS 1 & 2		ROOTS 3 & 4	
			Real	Imag.	Real	Imag.
Z_w	- .3330	-20	- .4470	+ .7716	+ .0423	+ 0
			- .4470	- .7716	- .0773	+ 0
	- .3744	-10	- .4665	+ .7746	+ .0517	+ 0
			- .4665	- .7746	- .0890	+ 0
	- .4160	0	- .4863	+ .7769	+ .0594	+ 0
			- .4863	- .7769	- .0989	+ 0
	- .4576	+10	- .5060	+ .7787	+ .0658	+ 0
			- .5060	- .7787	- .1075	+ 0
	- .4992	+20	- .5258	+ .7798	+ .0714	+ 0
			- .5258	- .7798	- .1151	+ 0
Y_v	-0	-100	+ .2173	-1.169	- .0972	+ 0
			+ .2173	+1.169	-1.396	+ 0
	- .1275	-50	+ .1649	+1.171	- .0967	+ 0
			+ .1649	-1.171	-1.419	+ 0
	- .255	0	+ .1134	+1.170	- .0961	+ 0
			+ .1134	-1.170	-1.445	+ 0
	- .3825	+50	+ .0631	+1.166	- .0956	+ 0
			+ .0631	-1.166	-1.472	+ 0
	- .510	+100	+ .0141	+1.159	- .0951	+ 0
			+ .0141	-1.159	-1.502	+ 0

XV-4B PHASE I

100K

DERIVATIVE	VALUE	% CHANGE	ROOTS 1 & 2 Real	ROOTS 1 & 2 Imag.	ROOTS 3 & 4 Real	ROOTS 3 & 4 Imag.
N_r	0.0	-100	+ .1562	+1.193	- .0684	+ 0
			+ .1562	-1.193	-1.462	+ 0
	- .115	-50	+ .1339	+1.183	- .0115	+ 0
			+ .1339	-1.183	-1.454	+ 0
	- .230	0	+ .1134	+1.170	- .0961	+ 0
			+ .1134	-1.170	-1.445	+ 0
	- .345	+50	+ .0953	+1.154	- .1875	+ 0
			+ .0953	-1.154	-1.433	+ 0
	- .460	+100	+ .0801	-1.136	- .2874	+ 0
			+ .0801	-1.136	-1.419	+ 0
L_p	0	-100	+ .2854	+1.041	- .2025	+ 0
			+ .2854	-1.041	- .8136	+ 0
	-.43	-50	+ .1935	-1.125	- .1295	+ 0
			+ .1935	+1.125	-1.137	+ 0
	- .86	0	+ .1134	+1.170	- .0961	+ 0
			+ .1134	-1.170	-1.445	+ 0
	-1.29	+50	+ .0468	+1.190	- .0766	+ 0
			+ .0468	-1.190	-1.765	+ 0
	-1.720	+100	- .0064	+1.196	- .0637	+ 0
			- .0064	-1.196	-2.106	+ 0

APPENDIX II

PHASE II

XV-4B PHASE II DERIVATIVES

70 KTS

DERIVATIVE	VALUE	% CHANGE	ROOTS 1 & 2 Real	ROOTS 1 & 2 Imag.	ROOTS 3 & 4 Real	ROOTS 3 & 4 Imag.
M_u	+ .0000872	-50	- .3510	+ .4017	- .0200	+ .1118
			- .3510	- .4017	- .0200	- .1118
	+ .0001309	-25	- .3510	+ .3996	- .0200	+ .1189
			- .3510	- .3996	- .0200	- .1189
	+ .0001745	0	- .3510	+ .3976	- .0200	+ .1256
			- .3510	- .3976	- .0200	- .1256
	+ .0002281	+25	- .3511	+ .3951	- .0200	+ .1335
			- .3511	- .3951	- .0200	- .1335
	+ .0002618	+50	- .3511	+ .3935	- .0199	+ .1382
			- .3511	- .3935	- .0199	- .1382
M_q	- .1850	-50	- .2613	+ .3867	- .0172	+ .1435
			- .2613	- .3867	- .0172	- .1435
	- .2775	-25	- .3060	+ .3954	- .0188	+ .1336
			- .3060	- .3954	- .0188	- .1336
	- .3700	0	- .3510	+ .3976	- .0200	+ .1256
			- .3510	- .3976	- .0200	- .1256
	- .4625	+25	- .3962	+ .3937	- .0211	+ .1189
			- .3962	- .3937	- .0211	- .1189
	- .5550	+50	- .4415	+ .3838	- .0220	+ .1132
			- .4415	- .3838	- .0220	- .1132

XV-4B PHASE II DERIVATIVES

70 KTS

DERIVATIVE	VALUE	% CHANGE	ROOTS 1 & 2	ROOTS 3 & 4
			Real Imag.	Real Imag.
M_w	- .00070	-50	- .3546 + .2801	- .0164 + .1231
			- .3546 - .2801	- .0164 - .1231
	- .00105	-25	- .3526 + .3436	- .0184 + .1247
			- .3526 - .3436	- .0184 - .1247
	- .00140	0	- .3510 + .3976	- .0200 + .1256
			- .3510 - .3976	- .0200 - .1256
	- .00175	+25	- .3497 + .4454	- .0213 + .1261
			- .3497 - .4454	- .0213 - .1261
	- .00210	+50	- .3487 + .4888	- .0223 + .1265
			- .3487 - .4888	- .0223 + .1265
X_u	- .0480	-20	- .3510 + .3979	- .0140 + .1263
			- .3510 - .3979	- .0140 - .1263
	- .0540	-10	- .3510 + .3977	- .0170 + .1260
			- .3510 - .3977	- .0170 - .1260
	- .0600	0	- .3510 + .3976	- .0200 + .1256
			- .3510 - .3976	- .0200 - .1256
	- .0660	+10	- .3510 + .3974	- .0230 + .1251
			- .3510 - .3974	- .0230 - .1251
	- .0720	+20	- .3510 + .3973	- .0260 + .1245
			- .3510 - .3973	- .0260 - .1245

XV-4B PHASE II DERIVATIVES

70 KTS

DERIVATIVE	VALUE	% CHANGE	ROOTS 1 & 2 Real	ROOTS 1 & 2 Imag.	ROOTS 3 & 4 Real	ROOTS 3 & 4 Imag.
Z_w	- .2496	-20	- .3188	+ .3922	- .0210	+ .1264
			- .3188	- .3922	- .0210	- .1264
	- .2808	-10	- .3349	+ .3952	- .0205	+ .1260
			- .3349	- .3952	- .0205	- .1260
	- .3120	0	- .3510	+ .3976	- .0200	+ .1256
			- .3510	- .3976	- .0200	- .1256
	- .3432	+10	- .3670	+ .3993	- .0196	+ .1252
			- .3670	- .3993	- .0196	- .1252
	- .3744	+20	- .3830	+ .4004	- .0192	+ .1248
			- .3830	- .4004	- .0192	- .1248
Y_v	0	-100	+ .1607	+1.095	- .0135	+ 0
			+ .1607	-1.095	-1.071	+ 0
	- .096	-50	+ .1204	+1.096	- .0134	+ 0
			+ .1204	-1.096	-1.087	+ 0
	- .192	0	+ .0808	+1.094	- .0133	+ 0
			+ .0808	-1.094	-1.104	+ 0
	- .285	+50	+ .0418	+1.091	- .0133	+ 0
			+ .0418	-1.091	-1.122	+ 0
	- .384	+100	+ .0036	+1.085	- .0132	+ 0
			+ .0036	-1.085	-1.141	+ 0

XV-4B PHASE II DERIVATIVES

70 KTS

DERIVATIVE	VALUE	% CHANGE	ROOTS 1 & 2		ROOTS 3 & 4	
			Real	Imag.	Real	Imag.
N_v	0	-100	- .2131	+ .8066	- .1536	+ 0
			- .2131	- .8066	-1.228	+ 0
(N_β)						
	+ .00315	-50	+ .1368	+ .9507	- .0696	+ 0
	(+ .371)		+ .1368	- .9507	-1.159	+ 0
	+ .0063	0	+ .0808	+1.094	- .0133	+ 0
	(+ .742)		+ .0808	-1.094	-1.104	+ 0
	+ .00945	+50	+ .0399	+1.231	+ .0243	+ 0
	(+1.113)		+ .0399	-1.231	-1.059	+ 0
	+ .0126	+100	+ .0094	+1.360	+ .0505	+ 0
	(+1.484)		+ .0094	-1.360	-1.025	+ 0
L_v	0	-100	- .1831	+ .9264	+ .1681	+ 0
	(0)		- .1831	- .9264	- .7573	+ 0
(L_β)						
	- .0134	-50	- .0257	+1.005	+ .0498	+ 0
	(-1.58)		- .0257	-1.005	- .9537	+ 0
	- .0268	0	+ .0808	+1.094	- .0133	+ 0
	(-3.16)		+ .0808	-1.094	-1.104	+ 0
	- .0402	+50	+ .1581	+1.177	- .0483	+ 0
	(-4.74)		+ .1581	-1.177	-1.223	+ 0
	- .0536	+100	+ .2187	+1.251	- .0698	+ 0
	(-6.32)		+ .2187	-1.251	-1.323	+ 0

XV - 4B PHASE II DERIVATIVES

70 KTS

DERIVATIVE	VALUE	% CHANGE	ROOTS 1 & 2 Real	ROOTS 1 & 2 Imag.	ROOTS 3 & 4 Real	ROOTS 3 & 4 Imag.
N_r	0	-100	+ .1182	+1.113	+ .0808	+ 0
			+ .1182	-1.113	-1.120	+ 0
	- .076	-50	+ .0992	+1.105	+ .0350	+ 0
			+ .0992	-1.105	-1.113	+ 0
	- .152	0	+ .0808	+1.094	- .0133	+ 0
			+ .0808	-1.094	-1.104	+ 0
	- .225	+50	+ .0634	+1.082	- .0649	+ 0
			+ .0634	-1.082	-1.093	+ 0
	- .304	+100	+ .0472	+1.067	- .1207	+ 0
			+ .0472	-1.067	-1.081	+ 0
L_p	0	-100	+ .2105	+1.048	- .0205	+ 0
			+ .2105	-1.048	- .7550	+ 0
	- .300	-50	+ .1422	+1.080	- .0162	+ 0
			+ .1422	-1.080	- .9233	+ 0
	- .600	0	+ .0808	+1.094	- .0133	+ 0
			+ .0808	-1.094	-1.104	+ 0
	- .900	+50	+ .0281	+1.095	- .0113	+ 0
			+ .0281	-1.095	-1.301	+ 0
	-1.20	+100	- .0153	+1.088	- .0099	+ 0
			- .0153	-1.088	-1.516	+ 0

XV-4B PHASE II

100 KTS

DERIVATIVE	VALUE	% CHANGE	ROOTS 1 & 2	ROOTS 3 & 4
			Real Imag.	Real Imag.
M_u	- .000370	-50	- .4762 + .7972	- .0258 + .1003
			- .4762 - .7972	- .0258 - .1003
	- .000555	-25	- .4769 + .7994	- .0251 + .0846
			- .4769 - .7994	- .0251 - .0846
	- .000740	0	- .4776 + .8016	- .0244 + .0654
			- .4776 - .8016	- .0244 - .0654
	- .000925	+25	- .4783 + .8037	- .0237 + .0377
			- .4783 - .8037	- .0237 - .0377
	- .00111	+50	- .4789 + .8059	- .0605 + 0
			- .4789 - .8059	+ .0144 + 0
M_q	- .2580	-50	- .3508 + .7978	- .0222 + .0714
			- .3508 - .7978	- .0222 - .0714
	- .3870	-25	- .4141 + .8023	- .0234 + .0682
			- .4141 - .8023	- .0234 - .0682
	- .5160	0	- .4776 + .8016	- .0244 + .0654
			- .4776 - .8016	- .0244 - .0654
	- .7450	+25	- .5904 + .7870	- .0261 + .0608
			- .5904 - .7870	- .0261 - .0608
	- .8740	+50	- .6541 + .7710	- .0269 + .0585
			- .6541 - .7710	- .0269 - .0585

XV-4B PHASE II

100 KTS

DERIVATIVE	VALUE	% CHANGE	ROOTS 1 & 2	ROOTS 3 & 4
			Real Imag.	Real Imag.
M_w	- .001875	-50	- .4747 + .5774	- .1042 + 0
			- .4747 - .5774	+ .0495 + 0
	- .00281	-25	- .4772 + .6981	- .0248 + .0179
			- .4772 - .6981	- .0248 - .0179
	- .00375	0	- .4776 + .8016	- .0244 + .0654
			- .4776 - .8016	- .0244 - .0654
	- .00469	+25	- .4773 + .8935	- .0247 + .0837
			- .4773 - .8935	- .0247 - .0837
	- .005625	+50	- .4768 + .9766	- .0252 + .0948
			- .4768 - .9766	- .0252 - .0948
X_u	- .0544	-20	- .4774 + .8016	- .0178 + .0675
			- .4774 - .8016	- .0178 - .0675
	- .0612	-10	- .4775 + .8016	- .0211 + .0665
			- .4775 - .8016	- .0211 - .0665
	- .0680	0	- .4776 + .8016	- .0244 + .0654
			- .4776 - .8016	- .0244 - .0654
	- .0748	+10	- .4777 + .8015	- .0277 + .0640
			- .4777 - .8015	- .0277 - .0640
	- .0816	+20	- .4777 + .8015	- .0311 + .0625
			- .4777 - .8015	- .0311 - .0625

XV-4B PHASE II

100 KTS

DERIVATIVE	VALUE	% CHANGE	ROOTS 1 & 2		ROOTS 3 & 4	
			Real	Imag.	Real	Imag.
Z_w	- .3360	-20	- .4372	+ .7966	- .0228	+ .0839
			- .4372	- .7966	- .0228	- .0839
	- .3780	-10	- .4574	+ .7994	- .0236	+ .0750
			- .4574	- .7994	- .0236	- .0750
	- .4200	0	- .4776	+ .8016	- .0244	+ .0654
			- .4776	- .8016	- .0244	- .0654
	- .4620	+10	- .4978	+ .8031	- .0252	+ .0547
			- .4978	- .8031	- .0252	- .0547
	- .5040	-20	- .5180	+ .8041	- .0260	+ .0421
			- .5180	- .8041	- .0260	- .0421
Y_v	0	-100	+ .0893	+1.314	- .0194	+ 0
			+ .0893	-1.314	-1.235	+ 0
	- .094	-50	+ .0478	+1.315	- .0192	+ 0
			+ .0478	-1.315	-1.246	+ 0
	- .188	0	+ .0066	+1.315	- .0191	+ 0
			+ .0066	-1.315	-1.257	+ 0
	- .282	+50	- .0342	+1.313	- .0190	+ 0
			- .0342	-1.313	-1.270	+ 0
	- .376	+100	- .0746	+1.309	- .0189	+ 0
			- .0746	-1.309	-1.283	+ 0

XV-4B PHASE II

100 KTS

DERIVATIVE	VALUE	% CHANGE	ROOTS 1 & 2 Real	ROOTS 1 & 2 Imag.	ROOTS 3 & 4 Real	ROOTS 3 & 4 Imag.
N_v	0	-100	+ .1778	+ .8616	- .2121	+ 0
	(0)		+ .1778	- .8616	-1.407	+ 0
(N_β)						
	+ .003665	-50	+ .0714	+1.095	- .0857	+ 0
	(+ .620)		+ .0714	-1.095	-1,320	+ 0
	+ .00733	0	+ .0066	+1.315	- .0191	+ 0
	(+1.24)		+ .0066	-1.315	-1.257	+ 0
	+ .011	+50	- .0352	+1.515	+ .0191	+ 0
	(+1.86)		- .0352	-1.515	-1.212	+ 0
	+ .0147	+100	- .0639	+1.696	+ .0435	+ 0
	(+2.48		- .0639	-1.696	-1.179	+ 0
L_v	0	-100	- .2210	+1.165	+ .1400	+ 0
	(0)		- .2210	-1.165	- .9613	+ 0
(L_β)						
	- .01625	-50	- .0914	+1.236	- .0428	+ 0
	(-2.75)		- .0914	-1.236	-1.123	+ 0
	- .0325	0	+ .0066	+1.315	- .0191	+ 0
	(-5.50)		+ .0066	-1.315	-1.257	+ 0
	- .04975	+50	+ .0828	+1.391	- .0591	+ 0
	(-8.25)		+ .0828	-1.391	-1.370	+ 0
	- .0650	+100	+ .1447	+1.463	- .0861	+ 0
	(-11.00)		+ .1447	-1.463	-1.467	+ 0

XV-4B PHASE II

100 KTS

DERIVATIVE	VALUE	% CHANGE	ROOTS 1 & 2	ROOTS 3 & 4
			Real Imag.	Real Imag.
N_r	0	-100	+ .0773 +1.339	+ .0822 + 0
			+ .0773 +1.339	-1.280 + 0
	- .110	-50	+ .0417 +1.329	+ .0329 + 0
			+ .0417 -1.329	-1.269 + 0
	- .220	0	+ .0066 +1.315	- .0191 + 0
			+ .0066 -1.315	-1.257 + 0
	- .330	+50	- .0276 +1.297	- .0751 + 0
			- .0276 -1.297	-1.234 + 0
	- .440	+100	- .0606 +1.275	- .1364 + 0
			- .0606 -1.275	-1.226 + 0
L_p	0	-100	+ .1490 +1.249	- .0386 + 0
			+ .1490 -1.249	- .6814 + 0
	- .420	-50	+ .0743 +1.297	- .0255 + 0
			+ .0743 -1.297	- .9657 + 0
	- .840	0	+ .0066 +1.315	- .0191 + 0
			+ .0066 -1.315	-1.257 + 0
	-1.260	+50	- .0489 +1.314	- .0153 + 0
			- .0489 -1.314	-1.571 + 0
	-1.68	+100	- .0910 +1.303	- .0128 + 0
			- .0910 -1.303	-1.910 + 0

XV-4B PHASE II

130 KTS

DERIVATIVE	VALUE	% CHANGE	ROOTS 1 & 2		ROOTS 3 & 4	
			Real	Imag.	Real	Imag.
M_u	- .000645	-50	- .5934	+1.171	- .0326	+ .1152
			- .5934	-1.171	- .0326	+ .1152
	- .000868	-25	- .5937	+1.172	- .0323	+ .1059
			- .5937	-1.172	- .0323	- .1059
	- .001290	0	- .5943	+1.174	- .0317	+ .0856
			- .5943	-1.174	- .0317	- .0856
	- .001612	+25	- .5948	+1.175	- .0312	+ .0661
			- .5948	-1.175	- .0312	- .0661
	- .002935	+50	- .5967	+1.181	- .1166	+ 0
			- .5967	-1.181	+ .0581	+ 0
M_q	- .3400	-50	- .4258	+1.174	- .0302	+ .0913
			- .4258	-1.174	- .0302	- .0913
	- .5100	-25	- .5100	+1.177	- .0310	+ .0883
			- .5100	-1.177	- .0310	- .0883
	- .6800	0	- .5943	+1.174	- .0317	+ .0856
			- .5943	-1.174	- .0317	- .0856
	- .8500	+25	- .6787	+1.164	- .0323	+ .0830
			- .6787	-1.164	- .0323	- .0830
	- .920	+50	- .7134	+1.159	- .0326	+ .0820
			- .7134	-1.159	- .0326	- .0820

XV-4B PHASE II

130 KTS

DERIVATIVE	VALUE	% CHANGE	ROOTS 1 & 2		ROOTS 3 & 4	
			Real	Imag.	Real	Imag.
M_w	- .00312	-50	- .5923	+ .8359	- .0978	+ 0
			- .5923	- .8359	+ .0304	+ 0
	- .00469	-25	- .5942	+1.019	- .0318	+ .0553
			- .5942	-1.019	- .0318	- .0553
	- .00625	0	- .5943	+1.174	- .0317	+ .0856
			- .5943	-1.174	- .0317	- .0856
	- .00781	+25	- .5940	+1.311	- .0320	+ .1008
			- .5940	-1.311	- .0320	- .1008
	- .00937	+50	- .5936	+1.435	- .0324	+ .1104
			- .5936	-1.435	- .0324	- .1104
X_u	- .0608	-20	- .5942	+1.174	- .0242	+ .0880
			- .5942	-1.174	- .0242	- .0880
	- .0684	-10	- .5943	+1.174	- .0261	+ .0874
			- .5943	-1.174	- .0261	- .0874
	- .0760	0	- .5943	+1.174	- .0317	+ .0856
			- .5943	-1.174	- .0317	- .0856
	- .0836	+10	- .5944	+1.174	- .0354	+ .0841
			- .5944	-1.174	- .0354	- .0841
	- .0912	+20	- .5944	+1.174	- .0392	+ .0824
			- .5944	-1.174	- .0392	- .0824

XV-4B PHASE II

130 KTS

DERIVATIVE	VALUE	% CHANGE	ROOTS 1 & 2		ROOTS 3 & 4	
			Real	Imag.	Real	Imag.
Z_w	-.3968	-20	- .5456	+1.168	- .0308	+ .1010
			- .5456	-1.168	- .0308	- .1010
	-.4464	-10	- .5700	+1.17	- .0312	+ .0935
			- .5700	-1.17	- .0312	- .0935
	-.4960	0	- .5943	+1.174	- .0317	+ .0856
			- .5943	-1.174	- .0317	- .0856
	-.5456	+10	- .6187	+1.176	- .0321	+ .0772
			- .6187	-1.176	- .0321	- .0772
	- .5952	+20	- .6430	+1.178	- .0326	+ .0682
			- .6430	-1.178	- .0326	- .0682
Y_v	0	-100	+ .0610	+1.423	- .0819	+ 0
			+ .0610	-1.423	-1.469	+ 0
	- .104	-50	+ .0140	+1.426	- .0811	+ 0
			+ .0140	-1.426	-1.480	+ 0
	- .208	0	- .0327	+1.426	- .0804	+ 0
			- .0327	-1.426	-1.491	+ 0
	- .312	+50	- .0790	+1.425	- .0797	+ 0
			- .0790	-1.425	-1.503	+ 0
	- .416	+100	- .1248	+1.422	- .0790	+ 0
			- .1248	-1.422	-1.516	+ 0

XV-4B PHASE II

130 KTS

DERIVATIVE	VALUE	% CHANGE	ROOTS 1 & 2 Real	ROOTS 1 & 2 Imag.	ROOTS 3 & 4 Real	ROOTS 3 & 4 Imag.
N_v	0	-100	+ .1479	+ .9433	- .2990	+ 0
(N_β)	(0)		+ .1479	- .9433	-1.633	+ 0
	+ .00325	-50	+ .0355	+1.192	- .1562	+ 0
	(+ .715)		+ .0355	-1.192	-1.552	+ 0
	+ .0065	0	- .0327	+1.426	- .0804	+ 0
	(+1.43)		- .0327	-1.426	-1.491	+ 0
	+ .00975	+50	- .0768	+1.639	- .0369	+ 0
	(+2.145)		- .0768	-1.639	-1.446	+ 0
	+ .0130	+100	- .1073	+1.832	- .0900	+ 0
	(+2.86)		- .1073	-1.832	-1.413	+ 0
L_v	0	-100	- .2782	+1.235	+ .1058	+ 0
(L_β)	(0)		- .2782	-1.235	-1.186	+ 0
	- .0223	-50	- .1368	+1.328	- .0089	+ 0
	(-4.90)		- .1368	-1.328	-1.354	+ 0
	- .0446	0	- .0327	+1.426	- .0804	+ 0
	(-9.80		- .0327	-1.426	-1.491	+ 0
	- .0669	+50	+ .0472	+1.519	- .1259	+ 0
	(-14.70)		+ .0472	-1.519	-1.605	+ 0
	- .0892	+100	+ .1116	+1.604	- .1565	+ 0
	(-19.60)		+ .1116	-1.604	-1.704	+ 0

XV-4B PHASE II

150 KTS

DERIVATIVE	VALUE	% CHANGE	ROOTS 1 & 2 Real	ROOTS 1 & 2 Imag.	ROOTS 3 & 4 Real	ROOTS 3 & 4 Imag.
M_w	- .00392	-50	- .6666	+1.001	- .1032	+ 0
			- .6666	-1.001	+ .0244	+ 0
	- .00590	-25	- .6688	+1.224	- .0372	+ .0613
			- .6688	-1.224	- .0372	- .0613
	- .00785	0	- .6692	+1.410	- .0368	+ .0909
			- .6692	-1.410	- .0368	- .0909
	- .00980	+25	- .6691	+1.574	- .0369	+ .1060
			- .6691	-1.574	- .0369	- .1060
	- .01077	+50	- .6690	+1.650	- .0370	+ .1112
			- .6690	-1.650	- .0370	- .1112
X_u	- .0656	-20	- .6691	+1.410	- .0287	+ .0938
			- .6691	-1.410	- .0287	- .0938
	- .0738	-10	- .6691	+1.410	- .0328	+ .0925
			- .6691	-1.410	- .0328	- .0925
	- .0820	0	- .6692	1.410	- .0368	+ .0909
			- .6692	-1.410	- .0368	- .0909
	- .0902	+10	- .6692	+1.410	- .0407	+ .0892
			- .6692	-1.410	- .0407	- .0892
	- .1084	+20	- .6693	+1.410	- .0499	+ .0844
			- .6693	-1.410	- .0499	+ .0844

XV-4B PHASE II

130 KTS

DERIVATIVE	VALUE	% CHANGE	ROOTS 1 & 2 Real	Imag.	ROOTS 3 & 4 Real	Imag.
N_r	0	-100	+ .0665	+1.461	+ .0618	+ 0
			+ .0665	-1.461	-1.521	+ 0
	- .155	-50	+ .0163	+1.447	- .0068	+ 0
			+ .0163	-1.447	-1.507	+ 0
	- .310	0	- .0327	+1.426	- .0804	+ 0
			- .0327	-1.426	-1.491	+ 0
	- .465	+50	- .0798	+1.399	- .1617	+ 0
			- .0798	-1.399	-1.471	+ 0
	- .620	+100	- .1240	+1.364	- .2545	+ 0
			- .1240	-1.364	-1.445	+ 0
L_p	0	-100	+ .1676	+1.349	- .1960	+ 0
			+ .1676	-1.349	- .6743	+ 0
	- .5500	-50	+ .0591	+1.410	- .1122	+ 0
			+ .0591	-1.410	-1.092	+ 0
	-1.10	0	- .0327	+1.426	- .0804	+ 0
			- .0327	-1.426	-1.491	+ 0
	-1.65	+50	- .1019	+1.417	- .0630	+ 0
			- .1019	-1.417	-1.921	+ 0
	-2.20	+100	- .1500	+1.397	- .0518	+ 0
			- .1500	-1.397	-2,387	+ 0

XV-4B PHASE II

150 KTS

DERIVATIVE	VALUE	% CHANGE	ROOTS 1 & 2		ROOTS 3 & 4	
			Real	Imag.	Real	Imag.
M_u	- .850000	-50	- .6688	+1.408	- .0372	+ .1207
			- .6688	-1.408	- .0372	- .1207
	- .127500	-25	- .6690	+1.409	- .0370	+ .1069
			- .6690	-1.409	- .0370	- .1069
	- .17000	0	- .6692	+1.410	- .0368	+ .0909
			- .6692	-1.410	- .0368	- .0909
	- .212500	+25	- .6694	+1.411	- .0366	+ .0716
			- .6694	-1.411	- .0366	- .0716
	- .255000	+50	- .6696	+1.412	- .0365	+ .0446
			- .6696	-1.412	- .0365	- .0446
M_q	- .3850	-50	- .4779	+1.411	- .0356	+ .0965
			- .4779	-1.411	- .0356	- .0965
	- .5785	-25	- .5740	+1.414	- .0362	+ .0936
			- .5740	-1.414	- .0362	- .0936
	- .7700	0	- .6692	+1.410	- .0368	+ .0909
			- .6692	-1.410	- .0368	- .0909
	- .9615	+25	- .7643	+1.400	- .0374	+ .0884
			- .7643	-1.400	- .0374	- .0884
	-1.155	+50	- .8605	+1.382	- .0380	+ .0860
			- .8605	-1.382	- .0380	- .0860

XV-4B PHASE II

150 KTS

DERIVATIVE	VALUE	% CHANGE	ROOTS 1 & 2 Real	ROOTS 1 & 2 Imag.	ROOTS 3 & 4 Real	ROOTS 3 & 4 Imag.
Z_w	- .4480	-20	- .6138	+1.404	- .0362	+ .1063
			- .6138	-1.404	- .0362	- .1063
	- .5040	-10	- .6415	+1.407	- .0365	+ .0988
			- .6415	-1.407	- .0365	- .0988
	- .5600	0	- .6692	+1.410	- .0368	+ .0909
			- .6692	-1.410	- .0368	- .0909
	- .6160	+10	- .6968	+1.412	- .0372	+ .0827
			- .6968	-1.412	- .0372	- .0827
	- .6720	+20	- .7245	+1.414	- .0375	+ .0738
			- .7245	-1.414	- .0375	- .0738
Y_v	0	-100	+ .0848	+1.579	- .0740	+ 0
			+ .0848	-1.579	-1.564	+ 0
	- .080	-50	- .0286	+1.582	- .0735	+ 0
			- .0286	-1.582	-1.571	+ 0
	- .160	0	- .0655	+1.583	- .0729	+ 0
			- .0655	-1.583	-1.577	+ 0
	- .240	+50	- .1022	+1.583	- .0724	+ 0
			- .1022	-1.583	-1.585	+ 0
	- .320	+100	- .1388	+1.583	- .0719	+ 0
			- .1388	-1.583	-1.592	+ 0

XV-4B PHASE II

150 KTS

DERIVATIVE	VALUE	% CHANGE	ROOTS 1 & 2		ROOTS 3 & 4	
			Real	Imag.	Real	Imag.
N_v	0	-100	+ .1426	+ .9616	- .3403	+ 0
	(0)		+ .1426	- .9616	-1.726	+ 0
(N_β)	+ .00375	-50	+.00585	+1.288	- .1553	+ 0
	(+ .95)		+.00585	-1.288	-1.638	+ 0
	+ .0075	0	- .0655	+1.583	- .0729	+ 0
	(+1.90)		- .0655	-1.583	-1.577	+ 0
	+ .01125	+50	- .1078	+1.843	- .0297	+ 0
	(+2.85)		- .1078	-1.843	-1.536	+ 0
	+ .0150	+100	- .1358	+2.075	- .0034	+ 0
	(+3.80		- .1358	-2.075	-1.506	+ 0
L_v						
(L_β)	0	-100	- .2806	+1.409	+ .0979	+ 0
	(0)		- .2806	-1.409	-1.318	+ 0
	- .0239	-50	- .1599	+1.494	- .0034	+ 0
	(-6.05)		- .1599	-1.494	-1.458	+ 0
	- .0478	0	- .0655	+1.583	- .0729	+ 0
	(-12.10)		- .0655	-1.583	-1.577	+ 0
	- .0717	+50	+ .0101	+1.669	- .1210	+ 0
	(-18.15)		+ .0101	-1.669	-1.681	+ 0
	- .0956	+100	+ .0725	+1.750	- .1553	+ 0
	(-24.20)		+ .0725	-1.750	-1.771	+ 0

XV-4B PHASE II

150 KTS

DERIVATIVE	VALUE	% CHANGE	ROOTS 1 & 2 Real	ROOTS 1 & 2 Imag.	ROOTS 3 & 4 Real	ROOTS 3 & 4 Imag.
N_r	0	-100	+ .0631	+1.622	+ .0628	+ 0
			+ .0631	-1.622	-1.610	+ 0
	- .180	-50	- .0016	+1.606	- .0027	+ 0
			- .0016	-1.606	-1.595	+ 0
	- .360	0	- .0655	+1.583	- .0729	+ 0
			- .0655	-1.583	-1.577	+ 0
	- .540	+50	- .1280	+1.552	- .1502	+ 0
			- .1280	-1.552	-1.555	+ 0
	- .720	+100	- .1881	+1.511	- .2384	+ 0
			- .1881	-1.511	- .1527	+ 0
L_p	0	-100	+ .1210	+1.497	- .2335	+ 0
			+ .1210	-1.497	- .5480	+ 0
	- .620	-50	+ .0214	+1.566	- .1075	+ 0
			+ .0214	-1.566	-1.096	+ 0
	-1.24	0	- .0655	+1.583	- .0729	+ 0
			- .0655	-1.583	-1.577	+ 0
	-1.86	+50	- .1297	+1.573	- .0555	+ 0
			- .1297	-1.573	-2.087	+ 0
	-2.48	+100	- .1728	+1.554	- .0449	+ 0
			- .1728	-1.554	-2.633	+ 0

APPENDIX III

XV-4B Inertia Characteristics for a Center of Gravity at 10% MAC

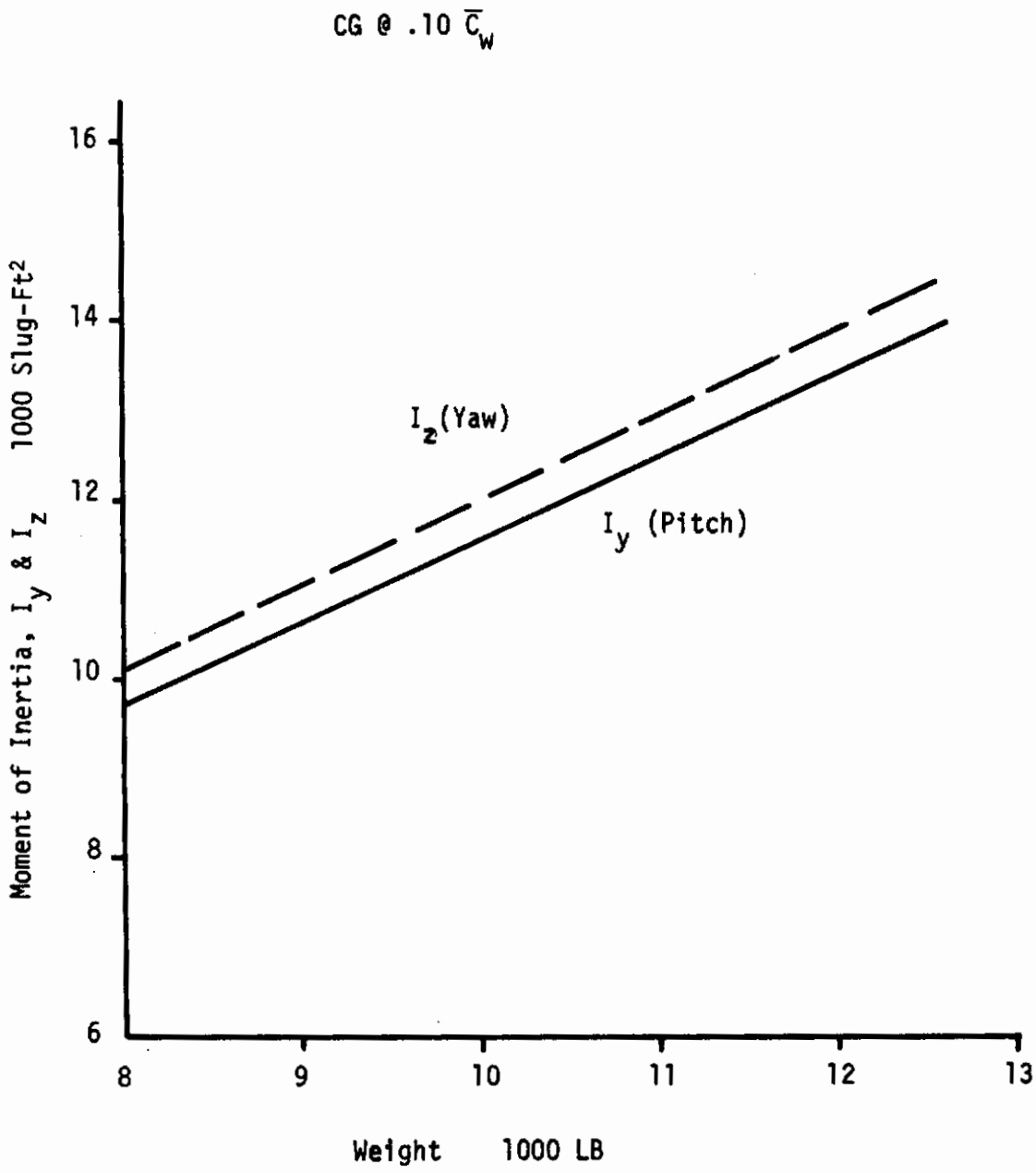

Figure 38. Pitch and Yaw Moments of Inertia

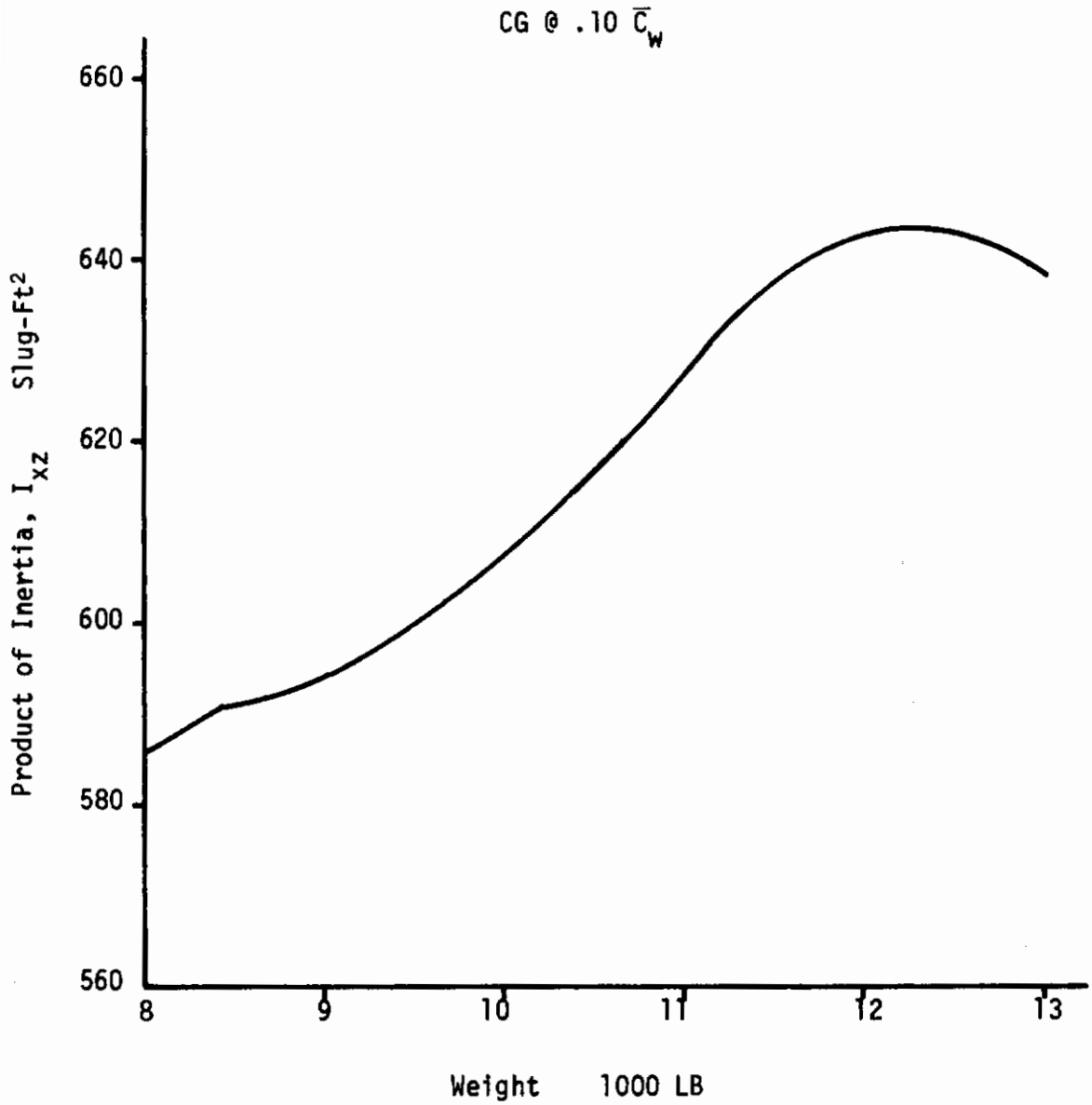

Figure 39. Products of Inertia with Respect to X and Z Axes

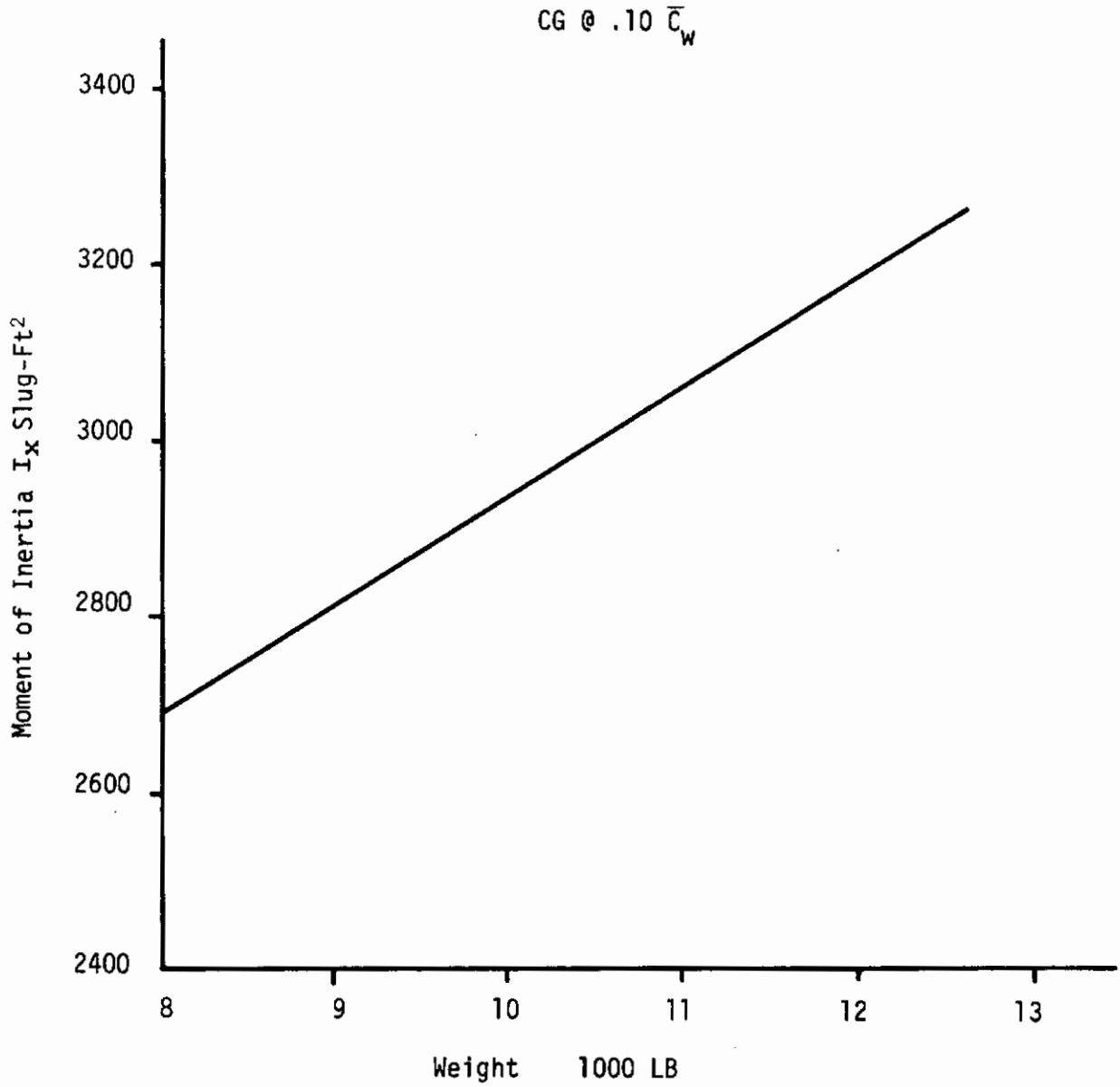

Figure 40. Moment of Inertia in Roll, I_x

REFERENCES

1. Jones, A. G., "Parameter Variation--An Insight to V/STOL Design", AIAA Paper 70-551, presented at the Atmospheric Flight Mechanics Conference, Tullhoma, Tenn., May 13-15, 1970, and printed in the Journal of Aircraft, Vol. 8, No. 8, Aug. 1971, pp. 629-633.

2. Barnes, O. G., Jr., "XV-4B, 'Hummingbird' Aerodynamic Analysis Report", May 1968, Lockheed-Georgia Co.

3. Casteel, G. R., "Aerodynamic Stability and Control Wind Tunnel Data Correlation", AFFDL-TR-71-3, North American Rockwell Corp.

4. "The Hummingbird XV-4B VTOL Research Aircraft Program", AFFDL-TR 69-75, Aug. 1969, Lockheed-Georgia Co.

5. Black, E. L. and Booth, G. C., "Correlation of Aerodynamic Stability and Control Derivatives Obtained from Flight Tests and Wind Tunnel Tests on the XC-142A Airplane", AFFDL-TR-68-167, Dec. 1968, Vought Aeronautics Div., LTV Aerospace Corp.

6. Rampy, J. M., "Important V/STOL Aircraft Stability Derivatives in Hover and Transition", FTC-TR-66-29, Oct. 1966, Air Force Flight Test Center, Edwards Air Force Base, Calif., Air Force Systems Command.

7. Parks, W. C., Swingle, R. L., and Swope, W. A., "CV-5A Aerodynamic-Propulsion Data Correlation and Characteristics Development Based on Wind Tunnel Characteristics", AVLABS TR-67-75, July 1968, Ryan Aeronautical Co., San Diego, Calif.

8. Griffin, John M., "Digital Computer Solution of Aircraft Longitudinal and Lateral-Directional Dynamic Characteristics", SEG-TR-66-52, December 1967.

UNCLASSIFIED
Security Classification

DOCUMENT CONTROL DATA - R & D

(Security classification of title, body of abstract and indexing annotation must be entered when the overall report is classified)

1. ORIGINATING ACTIVITY (Corporate author) AIR FORCE FLIGHT DYNAMICS LABORATORY WRIGHT-PATTERSON AIR FORCE BASE, OHIO	2a. REPORT SECURITY CLASSIFICATION UNCLASSIFIED 2b. GROUP

3. REPORT TITLE
A STUDY OF THE EFFECTS OF PARAMETER VARIATION ON THE FLYING QUALITIES OF THE XV-4B V/STOL AIRCRAFT

4. DESCRIPTIVE NOTES (Type of report and inclusive dates)
IN-HOUSE REPORT

5. AUTHOR(S) (First name, middle initial, last name)
ARTHUR G. JONES

6. REPORT DATE	7a. TOTAL NO. OF PAGES	7b. NO. OF REFS
MARCH 1972	134	8

8a. CONTRACT OR GRANT NO.	9a. ORIGINATOR'S REPORT NUMBER(S)
NONE b. PROJECT NO. 82190712 c. d.	AFFDL-TR-72-44 9b. OTHER REPORT NO(S) (Any other numbers that may be assigned this report) --

10. DISTRIBUTION STATEMENT
APPROVED FOR PUBLIC RELEASE; DISTRIBUTION UNLIMITED.

11. SUPPLEMENTARY NOTES	12. SPONSORING MILITARY ACTIVITY
	AIR FORCE FLIGHT DYNAMICS LABORATORY WRIGHT-PATTERSON AIR FORCE BASE, OHIO

13. ABSTRACT

The dominating influence of the propulsion system on the dynamic motion of a V/STOL aircraft operating in the hover or low-velocity flight modes has greatly increased the difficulty of developing such an aircraft to be stable and controllable during these modes. Small variations in stability derivatives caused by either changes in the propulsive system or errors in measurement or analytical prediction programs have been shown to cause significant changes in the dynamic characteristics of such aircraft. To better understand relationships, a program was performed using the Lockheed XV-4B jet-lift aircraft as a subject configuration. During this program, the magnitudes of ten of the stability derivatives used to describe the aircraft were varied individually, and the change in the roots of the linearized, uncoupled equations of motion noted. The derivatives found to have the greatest influence on the dynamic characteristics of the XV-4B at hover and low transition velocities were M_u in the longitudinal mode and L_v in the lateral-directional mode.

DD FORM 1 NOV 68 1473

UNCLASSIFIED
Security Classification

14. KEY WORDS	LINK A		LINK B		LINK C	
	ROLE	WT	ROLE	WT	ROLE	WT
(U) XV-4B; (U) STABILITY DERIVATIVES; (U) INTERFERENCE EFFECTS; (U) HANDLING QUALITIES; (U) V/STOL.						

☆U.S.Government Printing Office: 1972 — 759-086/635